

https://dspace.org/

Characterisation of the nitrile biocatalytic activity of rhodococcus Rhodochrous ATCC BAA-870

Frederick, Joni

2007-02-15T13:31:55Z
http://hdl.handle.net/10539/2016

Downloaded from a DSpace repository. https://dspace.org/

CHARACTERISATION OF THE NITRILE BIOCATALYTIC ACTIVITY OF *RHODOCOCCUS RHODOCHROUS* ATCC BAA-870

Joni Frederick

A dissertation submitted to the Faculty of Science, University of the Witwatersrand, Johannesburg, in fulfilment of the requirements for the degree of Master of Science.

Johannesburg, 2006

Declaration

I declare that this dissertation is my own, unaided work. It is being submitted for the Degree of Master of Science at the University of the Witwatersrand, Johannesburg. It has not been submitted before for any degree or examination in any other University.

_____

_____ day of _____ 2006

Abstract

A versatile nitrile-degrading bacterium was isolated through enrichment culturing of soil samples from Johannesburg, South Africa. It was identified as *Rhodococcus rhodochrous* and submitted to the ATCC culture collection as strain BAA-870. This organism was determined to be a potential biocatalyst in that it contains a two enzyme system with strong nitrile-converting activity comprising nitrile hydratase and amidase. The development of a suitable assay for measuring the activity of the enzymes of interest was explored. A pH-sensitive indicator-based assay was found to be suitable only for colorimetrically identifying highly concentrated enzymes with acid-forming activity. An *o*-phthaldialdehyde-based fluorimetric assay was found to be applicable to conversions of select compounds, but the assay could not be used to measure the activity of *Rhodoccocus rhodochrous* ATCC BAA-870. High performance liquid chromatography was the most suitable method for reliable and quantitative measurement of nitrile hydrolysis, and is applicable to monitoring activities of whole-cell and cell-free extracts. Initial analysis of six compounds, benzonitrile, benzamide, benzoic acid, hydrocinnamonitrile, 3-hydroxy-3-phenylpropionitrile and 3-hydroxy-3-phenylpropionic acid, was performed by HPLC to measure linearly the average retention area, amount and absorbance of the compounds up to 10 mM concentrations. The conversion of the substrates benzonitrile, benzamide and 3-hydroxy-3-phenylpropionitrile were further analysed with respect to time and enzyme concentration. Conversion of benzonitrile to benzamide by the nitrile hydratase was rapid and could be measured in 10 minutes. Conversion of benzamide to benzoic acid by the amidase was considered the rate-limiting step and could be followed for 90 minutes of the reaction at the concentrations tested. Conversion of 3-hydroxy-3-phenylpropionitrile was linearly measured over 20 minutes. Mass spectral analysis was used to confirm, at a structural level, relatively less volatile reactant compounds with a higher thermal stability, including benzamide, 3-hydroxy-3-phenylpropionitrile and 3-hydroxy-3-phenylpropionic acid. Protein concentration studies indicated that activity against benzonitrile was probably due to a nitrile hydratase with potent activity rather than a concentrated enzyme, since formation of benzamide from benzonitrile showed first order reaction kinetics at protein concentrations less than 0.2 mg/ml. Formation of benzoic acid from benzamide was linear up to 1.3 mg total protein and product formation from 3-hydroxy-3-phenylpropionitrile

was linear up to 1.4 mg total protein. Overlapping activities against benzonitrile and 3-hydroxy-3-phenylpropionitrile indicate that the nitrile hydratase has differing substrate specificity for the two compounds, with higher activity toward the small aromatic mononitrile, benzonitrile, than the arylaliphatic β-hydroxy nitrile, 3-hydroxy-3-phenylpropionitrile. The nitrile-converting activity of *Rhodococcus rhodochrous* ATCC BAA-870 would be suitable for biocatalysis as the conversions take place under a wide pH range, require low concentrations of enzyme and reactions are fast. Separation of nitrile-converting activities in *Rhodococcus rhodochrous* ATCC BAA-870 was undertaken using various chromatography methods to establish a simple, one-step protocol for biocatalytic enzyme preparations. HPLC was not suited to assaying nitrile-converting activity in chromatofocusing fractions, and chromatofocusing Ampholyte buffers were found to interfere with activity measurements. Gel exclusion chromatography of the soluble protein extract from *Rhodococcus rhodochrous* ATCC BAA-870 indicated the enzyme/s responsible for nitrile hydratase activity are high molecular weight proteins ranging from 40 to 700 kDa in size, while the amidase native enzyme is proposed to be roughly 17 to 25 kDa. SDS-PAGE analysis of gel exclusion and ion exchange chromatography fractions indicated nitrile converting activity in *Rhodococcus rhodochrous* ATCC BAA-870 is likely due to multimer-forming enzymes made up of 84, 56, 48 and 21 kDa subunits. It is postulated that nitrile hydratase is made up of $\alpha\beta$ and $\alpha_2\beta_2$ tetramers that may form larger enzyme aggregates. Ion exchange chromatography was used to separate nitrile hydratase with high activity against benzonitrile and 3-hydroxy-3-phenylpropionitrile from amidase activity, and showed that an additional, substrate specific nitrile hydratase may exist in the organism.

Acknowledgements

I wish to thank the Council For Scientific and Industrial Research, BioSciences unit, Modderfontein, for the opportunity to make use of their laboratories and other facilities, as well as for the financial assistance provided during the project. In particular I want to thank Dr Dean Brady for his supervision, constant support and encouragement throughout the project. I thank the National Research Foundation and the University of the Witwatersrand for the financial assistance and post-graduate merit award, respectively. I also thank Professor Heini Dirr for his supervision and magnetic passion for Biochemistry.

Since thanking “all who were involved” means nothing to anyone, I wish to thank the following people for influencing me, supporting me, encouraging me, assisting me, or simply giving me a laugh, and in some cases, all of the above during this trying time: Dad, Mom, Bonnie, John, Macky, Varsha, Nosisa, Mamosa, Henry, Fritha, Neeresh, Clinton, Thandeka, Mapitso, Justin, Nasreen, Dan, Nichole and Carlo, Sheryl, Chien-Teng, Kelly, Loren, Stoyan, Harris, Kgama, Stephen, Paul, 5fm and Highveld stereo, The Pig, 33 High Street, Boland, Boland Bank, and most of all, myself.

Table of Contents

Declaration....i
Abstract....ii
Acknowledgements....iv
Table of Contents....v
List of Figures....viii
List of Tables....xii
List of Abbreviations....xiii
1 Introduction....1
1.1 Nitrile Hydrolysing Enzymes: Comparison of General Structure and Enzymology…2
1.1.1 Nitrilase....2
1.1.2 Nitrile Hydratase....4
1.2 Nitrilase (EC 3.5.5.1)....5
1.3 Nitrile Hydratase (EC 4.2.1.84)....6
1.4 Amidase (EC 3.5.1.4)....9
1.5 Nitrile biotransformation, biosynthesis and bioremediation....10
1.6 Nitrile Hydrolysis Activity Assays....14
1.6.1 The Ninhydrin Assay....14
1.6.2 Nesslerization....14
1.6.3 The Berthelot Method....15
1.6.4 A Fourier Transform Infrared Method....15
1.6.5 A Colorimetric pH Method....15
1.6.6 Fluorimetric Methods....16
1.7 *Rhodococcus rhodochrous* as the chosen biocatalyst....16
1.8 Objectives and potential applications of the research....20
2 Materials and Methods....22
2.1 Materials....22
2.1.1 Chemicals....22
2.1.2 Nitrile Stocks....22
2.1.3 Commercial Nitrilases....22

2.1.4 Organism and Media....22
2.1.5 Column Chromatography....23
2.2 Methods....24
2.2.1 *Rhodococcus rhodochrous* ATCC BAA-870....24
2.2.2 Assays for Measuring Nitrilase/ Nitrile Hydratase Activity....26
2.2.3 Assay Development: High Performance Liquid Chromatography....29
2.2.4 Column Chromatography....35
2.2.5 Polyacrylamide Gel Electrophoresis....36
3 Results....38
3.1 *Rhodococcus rhodochrous* ATCC BAA-870 Characteristics....38
3.1.1 *Rhodococcus rhodochrous* Growth Curves in Different Media....38
3.1.2 Dry Cell Weight Determination....40
3.1.3 Observations of *Rhodococcus rhodochrous* growth patterns....40
3.1.4 Microscope Observations of the life cycle of *Rhodococcus rhodochrous*....41
3.1.5 *Rhodococcus rhodochrous* Cell Disruption Study....42
3.2 Towards Establishing an Activity Assay for Nitrilase and/or Nitrile Hydratase....44
3.2.1 Colorimetric Method....44
3.2.2 Fluorescence-based OPA Assay and Comparison to HPLC Method....44
3.2.3 High Performance Liquid Chromatography....45
3.3 HPLC Assay Method Development....46
3.3.1 Standard Curves....49
3.3.2 LC-Mass Spectral Analysis of the Standards Used in This Study....53
3.3.3 Different Buffer Types....58
3.3.4 pH Activity Profiles....61
3.3.5 Time Course Activity Study....62
3.3.6 Protein Concentration Effects....68
3.4 Column Chromatography....73
3.4.1 Chromatofocusing....74
3.4.2 Gel Exclusion Chromatography....75
3.4.3 Ion Exchange....85
4 Discussion....93
4.1 Characteristics of the chosen biocatalyst, *Rhodococcus rhodochrous*....93
4.2 Towards Establishing an Activity Assay for Nitrile Hydratase....94
4.3 High Performance Liquid Chromatography and Mass Spectrometry....97

4.3.1 Different Buffer Types....99
4.3.2 pH Profiles....100
4.3.3 Time Course Activity Study....102
4.3.4 Protein Concentration Effects....103
4.4 Column Chromatography....105
4.4.1 Chromatofocusing....105
4.4.2 Gel Exclusion....107
4.4.3 Ion Exchange....109
4.5 General Discussion....111
4.6 Conclusion....113
5 Appendix....115
5.1 Standard Curves....115
5.2 Chromatography....117
5.3 Nitrile Hydratase Theoretical pI....120
5.4 Mass Spectra....121
5.5 Structures....125
6 References....130

List of Figures

Figure 1: Nitrile hydrolysis catalysed by one of two distinct pathways.....1
Figure 2: The four reaction types carried out by members of the nitrilase superfamily.....3
Figure 3: A reaction mechanism for a nitrilase reaction requiring a covalent enzyme intermediate.....5
Figure 4: Ribbon representation of photoactivated iron-containing nitrile hydratase from Rhodococcus sp. R312 prepared from Protein Data Bank entry 1AHJ.....7
Figure 5: Iron coordination at the active site proposed for nitrile hydratase and a possible reaction mechanism involving a coordinated hydroxyl group.....8
Figure 6: Alkaline and acid hydrolysis of nitriles.....11
Figure 7: Schematic addition of cyanide to a molecule providing an additional carbon and nitrogen for subsequent conversion to other functional groups.....12
Figure 8: Schematic representation of the method used for colorimetric identification of nitrilase or nitrile hydratase activity.....27
Figure 9: Three-dimensional contour map of absorbance with wavelength and elution time for benzonitrile as acquired by the photodiode array detector in HPLC.....30
Figure 10: Two-dimensional chromatograph of a 5 mM benzonitrile sample showing absorbance over time at 224.1 nm.....30
Figure 11: Growth curve of *Rhodococcus rhodochrous* in minimal media measured at 600 and 660 nm. 39
Figure 12: Growth curve of *Rhodococcus rhodochrous* in rich media measured at 600 and 660 nm.....39
Figure 13: Close-up detail of the fanning formation developed by aged Rhodococcus rhodochrous culture on tryptone soya agar streak plates.....40
Figure 14: Germinating Rhodococcus rhodochrous ATCC BAA-870 cells in minimal media.....41
Figure 15: Rhodococcus rhodochrous ATCC BAA-870 in advanced stages of growth showing two distinct cell morphologies.....41
Figure 16: Amount of benzoic acid formed from benzonitrile in post-extraction reactions of samples sonicated for increasing lengths of time.....42

Figure 17: Micrographs of *Rhodococcus rhodochrous* sonicated for increasing time periods. 43
Figure 18: Average integrated area of benzonitrile, benzamide, benzoic acid, hydrocinnamonitrile, 3-hydroxy-3-phenylpropionitrile and 3-hydroxy-3-phenylpropionic acid with increasing concentration....50
Figure 19: Average absorbance of benzonitrile, benzamide, benzoic acid, hydrocinnamonitrile, 3-hydroxy-3-phenylpropionitrile and 3-hydroxy-3-phenylpropionic acid with increasing concentration....52
Figure 20: Mass spectra of 3-hydroxy-3-phenylpropionic acid and 3-hydroxy-3-phenylpropinitrile standards....55
Figure 21: Chromatographs of 3-hydroxy-3-phenylpropionic acid and 3-hydroxy-3-phenylpropionitrile standards....56
Figure 22: Benzonitrile conversion to benzoic acid in ten different buffer systems....58
Figure 23: Relative conversion of 3-hydroxy-3-phenylpropionitrile to product in ten different buffer types....59
Figure 24: Relative levels of hydrocinnamonitrile measured in ten different buffer types by HPLC....60
Figure 25: Amount of benzoic acid formed from benzonitrile at different pH's....62
Figure 26: Conversion of 5 mM benzonitrile to benzamide and benzoic acid over three hours....63
Figure 27: Conversion of 5 mM benzamide over three hours....64
Figure 28: Formation of benzoic acid from benzamide over time....65
Figure 29: Conversion of 5 mM 3-hydroxy-3-phenylpropionitrile over three hours....66
Figure 30: Conversion of 5 mM 3-hydroxy-3-phenylpropionitrile over a twenty minute reaction....67
Figure 31: Conversion of 5 mM benzonitrile over a ten minute time reaction, excluding time zero....67
Figure 32: Formation of benzoic acid from benzonitrile with increasing protein concentration....68
Figure 33: Formation of benzoic acid from benzamide with increasing protein concentration....69
Figure 34: Amount of benzamide and benzoic acid formed from benzonitrile with increasing protein concentration....70

Figure 35: Average integrated area of benzoic acid formation from benzamide over a 25 minute reaction with increasing protein concentration. 72
Figure 36: Average integrated area of product formed from 3-hydroxy-3-phenylpropionitrile over a 25 minute reaction. 73
Figure 37: Polybuffer Exchanger 94 Chromatofocusing elution profile of the soluble protein fraction from *Rhodococcus rhodochrous* grown in minimal media. 75
Figure 38: 10% SDS-PAGE of supernatant prepared from *Rhodococcus rhodochrous* grown in defined minimal media containing benzonitrile as inducer. 76
Figure 39: Protein elution from Sephacryl S-200 during gel exclusion of a cell free protein mix from *Rhodococcus rhodochrous*. 77
Figure 40: Nitrile hydrolytic activity profile of fractions from Sephacryl S-200 gel exclusion of a cell free protein mix from *Rhodococcus rhodochrous* showing residual substrate after reaction. 78
Figure 41: 12% SDS-PAGE of Sephacryl S-200 size exclusion chromatography fractions. 79
Figure 42: Sephacryl S-200 gel exclusion protein elution profile of *Rhodococcus rhodochrous* supernatant treated with polyethylenimine. 80
Figure 43: Conversion of benzonitrile to product in Sephacryl S-200 gel exclusion fractions showing total amount of product formation. 81
Figure 44: Conversion of benzamide to benzoic acid in Sephacryl S-200 eluted fractions. 81
Figure 45: Conversion of 3-hydroxy-3-phenylpropionitrile to product in Sephacryl S-200 eluted fractions. 82
Figure 46: Conversion of benzonitrile, benzamide and 3-hydroxy-3-phenylpropionitrile in Sephacryl S-200 eluted fractions. 83
Figure 47: Wavelength scans of a coloured Sephacryl S-200 eluted gel exclusion fraction compared to other fractions. 85
Figure 48: Protein elution profile from Toyopearl SuperQ 650M during ion exchange chromatography of supernatant from *Rhodococcus rhodochrous*. 86
Figure 49: Conversion of benzonitrile to benzamide and benzoic acid in Toyopearl SuperQ 650M ion exchange eluted fractions. 87
Figure 50: Conversion of benzamide to benzoic acid in Toyopearl SuperQ 650M ion exchange eluted fractions. 87

Figure 51: Conversion of 3-hydroxy-3-phenylpropionitrile to product in Toyopearl SuperQ 650M ion exchange eluted fractions. 88
Figure 52: Amount of benzonitrile, benzamide and 3-hydroxy-3-phenylpropionitrile remaining in Toyopearl SuperQ 650M ion exchange eluted fractions. 89
Figure 53: 10% SDS-PAGE of Toyopearl SuperQ 650M ion exchange eluted fractions. 90
Figure 54: Toyopearl Super-Q 650M ion exchange chromatography of supernatant from *Rhodococcus rhodochrous* eluted with a 500 mM NaCl gradient. 91
Figure 55: Amount of benzamide formed from benzonitrile, and conversion of 3-hydroxy-3-phenylpropionitrile in Toyopearl SuperQ 650M ion exchange eluted fractions. 92
Figure 56: NH4Cl Standard curve. 115
Figure 57: Sample BioRad protein concentration determination standard curve. 115
Figure 58: Standard curve of 10% SDS-PAGE size markers. 116
Figure 59: Sephacryl S-200 gel exclusion standard curve. 116
Figure 60: Sephacryl S-200 gel exclusion standard elution profile. 117
Figure 61: Sephacryl S-200 gel exclusion selectivity curve. 118
Figure 62: Benzamide mass spectrum. 121
Figure 63: Mass spectrum breakdown for benzamide showing the mass/charge ratio of possible peak components. 122
Figure 64: Mass spectrum breakdown for 3-hydroxy-3-phenylpropionitrile showing the mass/charge ratio of identified peak components. 122
Figure 65: 3-Hydroxy-3-phenylpropionitrile mass spectrum. 123
Figure 66: 3-Hydroxy-3-phenylpropionic acid mass spectrum. 124
Figure 67: Mass spectrum breakdown for 3-hydroxy-3-phenylpropionic acid showing the mass/charge ratio of identified peak components. 124

List of Tables

Table 1: Relative growth of some *Rhodococcus rhodochrous* strains on different sole nitrogen sources.....18

Table 2: Percentage substrate conversion of selected commercial nitrilases and biocatalysts 18

Table 3: The ten different buffer types used in this study and their composition.....33

Table 4: Relative activities of various commercial nitrilase enzymes and *Rhodococcus rhodochrous* whole cells reacted with benzonitrile.....46

Table 5: Name, structure and retention time of compounds used in this study.....48

Table 6: Linear regression equations and R^2 values for standard curves of the average integrated areas of increasing concentrations of various standard compounds...49

Table 7: Linear regression equations and R^2 values for standard curves of absorbance with increasing concentration for various compounds.....51

Table 8: Apparent molecular weight of the proteins within each Sephacryl S-200 gel exclusion fraction as estimated by comparison of the ratio of elution volume/void volume of Blue Dextran to that of molecular weight standards…119

Table 9: Theoretical pI values of different nitrile hydratase enzymes from Rhodococcal and Pseudomonad species.....120

Table 10: Table of compounds and structures referred to in this study.....125

List of Abbreviations

A	absorbance
ACN	acetonitrile
BSA	bovine serum albumin
BTB	bromothymol blue
DTT	dithiothreitol
EDTA	ethylene diamine tetraacetic acid
EPR	electron paramagnetic resonance
ENDOR	electron nuclear double resonance
EXAFS	extended x-ray absorption fine structure
Fhit	fragile histidine triad protein
H-NHase	high molecular mass nitrile hydratase
HPLC	high performance liquid chromatography
K_{av}	partition coefficient
kDa	kilodaltons
L-NHase	low molecular mass nitrile hydratase
M	molar
M_r	relative molecular mass
NHase	nitrile hydratase
Nit	nitrilase
NitFhit	nitrilase-fragile histidine triad fusion protein
NO	nitric oxide
OD	optical density
OPA	*o*-phthaldialdehyde
PDA	photo diode array
rev./min	revolutions per minute
RP-HPLC	reversed-phase high performance liquid chromatography
SDS	sodium dodecyl sulphate
SDS-PAGE	sodium dodecyl sulphate polyacrylamide gel electrophoresis
TEMED	N,N,N'N'-tetramethylethylenediamine
TFA	trifluoroacetic acid

Tris	Tris(hydroxymethyl)-aminomethane
TSA	tryptone soya agar
TSB	tryptone soya broth
UV	ultraviolet
V_e	elution volume
V_o	void volume
V_t	total column volume

The IUPAC-IUBMB one letter codes are used for amino acids.

Chapter 1

1 Introduction

Nitrilases and nitrile hydratases are attracting increasing attention in the field of biotransformation and biocatalysis. Their ability to produce a carboxylic acid from a corresponding nitrile, with nitrile hydratase producing an amide as an intermediate, has provided great potential for the use of these enzymes as nitrile catalysts functioning under relatively mild reaction conditions. One of the most well-known commercial examples of nitrile bioconversion is that of the manufacture of acrylamide from acrylonitrile [1]. This application of nitrile hydratase for the synthesis of acrylamide started in 1985, and Mitsubishi Rayon now produces over 30,000 tons of acrylamide every year. This was the first bioconversion process to be successfully applied to the petrochemical industry and implemented for the industrial production of a commodity chemical. Most nitrile bioconversions are still achieved through whole-cell treatment of substrates using industrially useful microbial strains such as *Rhodococcus rhodochrous*.

Hydration of nitriles in plants and microbes may be catalysed by one of two distinct pathways (Figure 1). Aliphatic nitriles are converted to amides by nitrile hydratases and then hydrolysed by amidases to carboxylic acids. Aromatic nitriles, on the other hand, are metabolised to the corresponding acid in a single-step reaction by nitrilases. Exceptions to this include the nitrile hydratases of a *Rhodococcus* sp. [2] and *Bacillus smithii* SCJ05-1 [3], and the nitrilase of *Rhodococcus rhodochrous* K22 [4], which are capable of hydrolysing both aliphatic and aromatic nitriles.

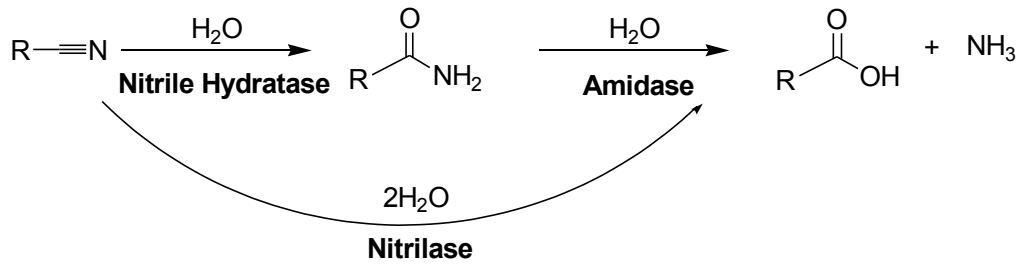


Figure 1: Nitrile hydrolysis catalysed by one of two distinct pathways.

It is usual for the expression of nitrile hydratase and amidase enzymes to be associated in the same organism. Indeed, the structural genes are adjacent on the same operon and are under the control of the same activator protein. The nitrile hydratase (NHase) operon consists of six genes, *nhr2*, *nhr1*, *ami*, *nha1*, *nha2* and *nha3*, that encode NHase regulator 2, NHase regulator 1, amidase, NHase α subunit, NHase β subunit and NHase activator, respectively [5]. Expression of nitrilase, however, is separate from NHase and amidase expression in the same organism, and can be selectively affected without affecting the expression of nitrile hydratase and amidase genes (and *vice versa*). The amount of each enzyme produced by an organism can be increased by addition of an inducer such as propionitrile to the fermentation medium [6].

Although several nitrile-hydrolysing enzymes have been isolated from natural sources, these enzymes were generally too unstable for commercial use in the isolated state, and most applications of these enzymes has consequently been as whole-cell biocatalysts. However, applying whole cell biocatalysts can present disadvantages in that some small aliphatic nitriles, and those with hydroxy and amino groups, can be utilized by the organism itself as carbon sources [7]. Also, the decreased yield of amides obtained when whole cell systems are used can be avoided when using purified enzymes since they are not utilized by the organism. Despite the large number of nitrilases and nitrile hydratases that have been purified there is a scarcity of suitable and/or well-characterised commercial nitrile-converting biocatalysts. Purified enzymes are the biocatalysts of choice for specific hydrolysis of nitriles containing other hydrolysable groups, and for the production of amides without carboxylic acid contamination.

1.1 Nitrile Hydrolysing Enzymes: Comparison of General Structure and Enzymology

1.1.1 Nitrilase

Nitrilase enzymes form part of a superfamily of thiol enzymes that are found in all animals, plants, fungi and bacteria [8]. Figure 2 shows the four types of reactions carried out by the nitrilase superfamily branches. Some organisms may have multiple nitrilases from more

than one of the thirteen superfamily branches, and have been classified according to sequence similarity and domain presence [8, 9].

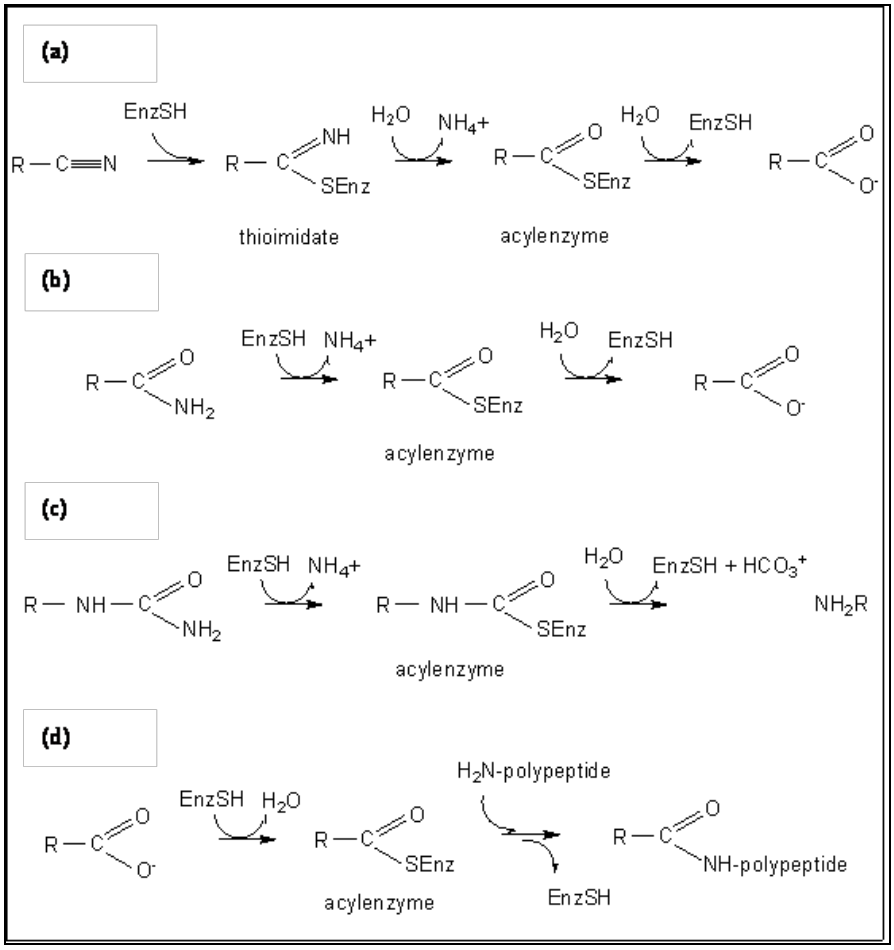


Figure 2: The four reaction types carried out by members of the nitrilase superfamily.

On the basis of sequence similarity and the presence of additional domains, the superfamily is classified into 13 branches, nine of which have known or deduced reaction specificity. **(a)** The nitrilase reaction is carried out by branch 1 enzymes. In plants, this includes the production of indole-3-acetic acid from indole-3-acetonitrile. **(b)** The amidase reaction is performed by branch 2-4 amidase enzymes and the nitrilase-related domains of branch 7 and 8 enzymes which are proposed to be glutamine-specific amidases. Amidase reactions are the most frequently observed activities in the nitrilase superfamily. **(c)** The carbamylase reaction is carried out by branch 5 and 6 enzymes and is a special case of amidase reaction. **(d)** The reverse amidase reaction in which a phospholipid fatty acid is transferred to a polypeptide amino terminus is performed by branch 9 N-acyltransferases. The polypeptide amino-terminal acceptor usually contains a diacylglyceride-modified cysteine (not shown). All nitrilase-related reactions are thought to proceed through acylenzyme intermediates. The reaction scheme was redrawn from Pace and Brenner (2001) [9].

Nitrilases are usually homooligomers, and very infrequently monomers, and do not contain metal cofactors. The structures of other members of the superfamily, *N*-carbamyl-D-amino acid amidohydrolase from *Agrobacterium* and worm NitFhit, branch 6 and 10 enzymes respectively, were independently shown to consist of a tetramer of compact α-β-β-α sandwiches in which two sheets of six β-strands form layers between pairs of α-helices. The superfamily likely utilizes a novel glutamic acid, lysine and cysteine catalytic triad [8]. Both the lysine and glutamic acid residues have been shown to be catalytically essential by construction of stable, inactive mutants with K134N and E59Q substitutions, respectively [10]. *Rhodococcus* nitrilase characterisation has indicated the protein is a thiol enzyme that proceeds via a covalent intermediate [11], and mutagenesis has identified the cysteine nucleophile [12], as well as confirmed the essentiality of the corresponding cysteine residue in other nitrilase superfamily branches [8, 13].

The nitrilase superfamily enzymes serve diverse roles in nature, including synthesis of hormones and other signalling molecules, vitamin and coenzyme metabolism, protein post-translational modification, as well as roles in the detoxification of small molecules [14, 15]. There is significant amino acid sequence similarity between bacterial and plant nitrilases [16].

1.1.2 Nitrile Hydratase

Although they are involved in hydrolysis of the nitrile bond, the nitrile hydratases are not members of the nitrilase superfamily, and hence have no structural or mechanistic similarity. All characterised bacterial nitrile hydratases are composed of two kinds of subunits assembled into heterooligomers (mostly dimers or tetramers, with a few larger molecules containing up to 20 subunits). Nitrile hydratases typically form αβ or $\alpha_2\beta_2$ functional proteins with the catalytic centre at the α-β subunit interface. Nitrile hydratase contain a metal ion at the active site. Bacterial nitrile hydratases usually contain Fe^{3+} and/or Co^{3+} [17] whilst the *Myrrothecium verrucaria* fungus has been shown to contain Zn^{2+} [18].

The microbial strain that has been the most exploited for its activity by industry, *Rhodococcus rhodochrous* J1, produces both a high molecular mass (H-NHase) [19] and lower molecular mass (L-NHase) nitrile hydratase [20, 21]. The enzymes are each

composed of two subunits, α and β, with the α subunit differing in size from the β, and both subunits of H-NHase differing from that of L-NHase. H-NHase is overproduced in this strain (as more than 50% of the soluble protein fraction) when urea is used as an inducer in the culturing medium.

1.2 Nitrilase (EC 3.5.5.1)

Nitrilase enzymes catalyse the direct hydrolysis of aliphatic and aromatic nitriles into the corresponding carboxylic acid and ammonia (Equation 1).

$$\mathbf{R\text{-}CN + 2H_2O \rightarrow R\text{-}COOH + NH_3} \qquad \textbf{Equation 1.}$$

Nitrilases are widely distributed in plants, where they catalyse the conversion of indole-3-acetonitrile into the plant hormone indole-3-acetic acid. They are also found in fungi and bacteria that can metabolise nitrile-containing herbicides. The cDNA for a number of nitrilases has been obtained, and a comparative amino acid sequence analysis reveals the presence of a conserved cysteine residue that is essential for catalytic activity [22, 23]. The function of the conserved cysteine may be to act as a nucleophile in analogy to the bound water molecule used for catalysis in the metal-containing nitrile hydratases. The formation of an enzyme-bound intermediate upon the release of ammonia, and the subsequent hydrolysis of this intermediate to restore the cysteine residue, could account for the difference in reaction products from the two distinct types of nitrile-metabolizing enzymes. The nitrilase reaction mechanism (Figure 3) probably involves a nucleophilic attack on the nitrile carbon atom by a sulfhydryl (thiol) group of a cysteine residue with a concomitant protonation of nitrogen to form a tetrahedral thiomidate intermediate. Hydrolysis of the covalent thiomidate complex and protonation of the nitrogen atom then occurs, and this nitrogen is lost as ammonia [11, 24].

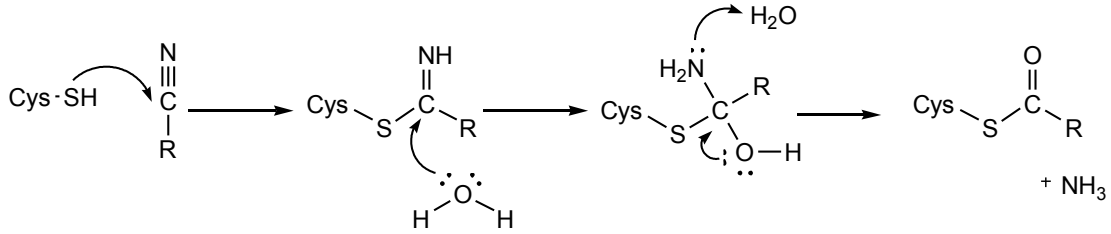


Figure 3: A reaction mechanism for a nitrilase reaction requiring a covalent enzyme intermediate.

Recently, nitrilase (*nit*) genes have been described as fusion proteins with the nucleotide-binding protein fragile histidine triad (Fhit). Fhit, an enzyme known to be crucial in apoptosis, is encoded as a fusion protein with Nit in invertebrates, and in mice *Nit1* and *Fhit* genes have almost identical expression profiles. The naturally occurring fusion protein, NitFhit (nitrilase-fragile histidine triad fusion protein) has recently had its crystallographic structure solved by Pace *et al*. [25]. The fusion of the two enzymes is proposed to imply a functional, but as yet unknown, link of two separate pathways.

A nitrilase isolated from *Rhodococcus rhodochrous* ATCC 39484 is reportedly converted to an active form by subunit association when incubated with substrate [26] or when in the presence of higher concentrations of enzyme, salt or organic solvent [27]. These conditions may result in a hydrophobic effect that changes the conformation of the enzyme in such a way so as to expose hydrophobic sites which enable subunit assembly and hence enzyme activation.

1.3 Nitrile Hydratase (EC 4.2.1.84)

Nitrile hydratases (NHases) catalyse the direct hydrolytic conversion of aromatic and aliphatic nitriles into the corresponding amide (Equation 2).

$$\mathbf{R\text{-}CN + 2H_2O \rightarrow R\text{-}CONH_2} \qquad \textbf{(Equation 2)}$$

These enzymes are widely distributed in bacteria, plants and fungi. The industrial and commercial uses of these enzymes have been demonstrated by the annual production of over 30 000 tons of acrylamide from acrylonitrile in bioreactors [1], as well as the production of the plant hormone indole-3-acetic acid from indole-3-acetonitrile.

Both cobalt- and iron-containing forms of the nitrile hydratases are known. The properties of metal-containing NHases have been reviewed in detail [28] and the catalytic mechanism is likely similar for all. An iron-containing NHase isolated from *Rhodococcus* sp. N-774 has been characterised by biochemical and genetic methods, and shown to be an $(\alpha\beta)_2$ dimer. The α and β subunits, as calculated from their nucleotide sequences, are roughly 22 870 and 23 850 Da, respectively.

The α subunit of NHase has the primary amino acid sequence motif Cys-X-X-Cys-X-Cys. The observed amino acid motif and iron stoichiometry is comparable to the motif that provides two of the four cysteine ligands in the rubredoxin iron site, suggesting that the active site resides in the α subunit. It has been shown, through separation of the two subunits, that iron is present in the α subunit but not the β subunit [29]. Various NHase crystal structures have been obtained, including the apoenzyme of cobalt-containing nitrile hydratase [30], a thermophilic *Bacillus smithii* nitrile hydratase [31], and nitrile hydratase complexed with nitric oxide [32] or cyclohexyl isocyanide [33]. All protein ligands to the iron in ferric NHase are provided by the α subunit, and there is one iron atom per αβ unit. The crystal structure of photoactivated iron-containing nitrile hydratase from *Rhodococcus* sp. R312 [34] was determined to 2.65 Å resolution by Huang *et al*. (1997) and is shown in Figure 4.

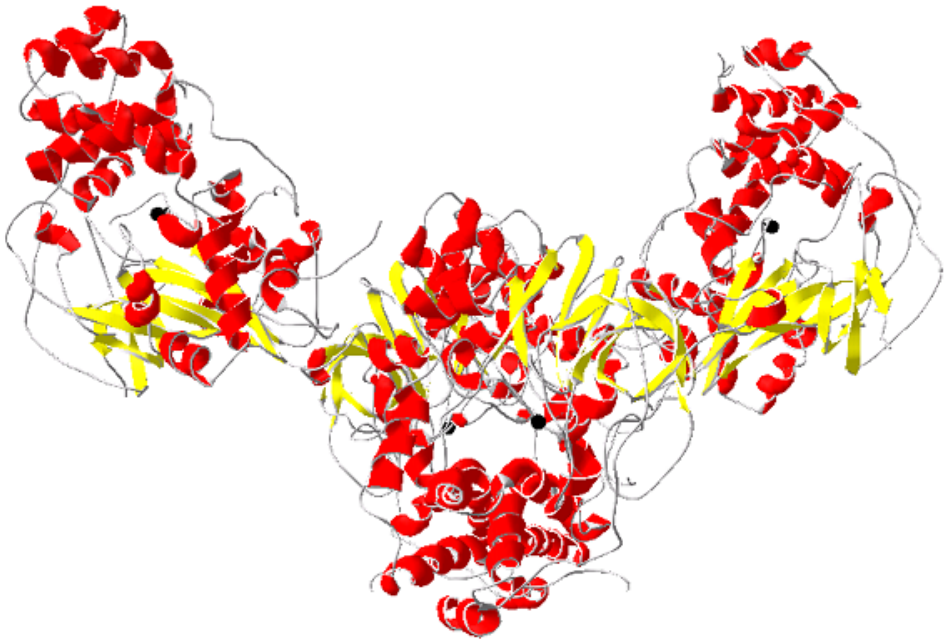


Figure 4: Ribbon representation of photoactivated iron-containing nitrile hydratase from *Rhodococcus* sp. R312 prepared from Protein Data Bank entry 1AHJ.

The enzyme is shown as a homotetramer made up of the αβ asymmetric unit. The iron metal centre (Fe^{3+}) is located at the central cavity at the interface between two subunits and is indicated by black spheres. The image was modelled on the protein data bank entry by Huang *et al*. (1997) [34] using Swiss-PdbViewer version 3.7 by Berman *et al*. (2000) [35].

Resonance Raman spectroscopy [36, 37], EPR (electron paramagnetic resonance) [38], ENDOR (electron nuclear double resonance) [39, 40] and EXAFS (extended X-ray

absorption fine structure) [37, 41] studies have been used to propose a structural model for the ferric active site shown in Figure 5. It is proposed to have an octahedral coordination geometry consisting of two cysteine thiol ligands in *cis* configuration, three histidine nitrogen ligands in *mer* configuration, and one solvent-exchangeable hydroxide ligand. This configuration is considered to be relatively rare in a biological molecule [29].

Chemical synthesis of carboxylic acids from nitriles proceeds at elevated temperature and pH. The feasible reaction mechanism for NHase shown in Figure 5 involves attack of the metal-bound hydroxide on the nitrile group, which gives rise to an unstable amide tautomer coordinated to the metal active site (Figure 5B). Rearrangement of the amide and subsequent dissociation of the product implies there is a transient formation of a five-coordinate iron site upon transfer of the bound hydroxide (Figure 5C). Re-coordination of a solvent-derived hydroxide completes the catalytic cycle and accounts for the products observed from NHases. A possible alternate mechanism in which the bound intermediate is activated for attack by a solvent molecule, is also shown.

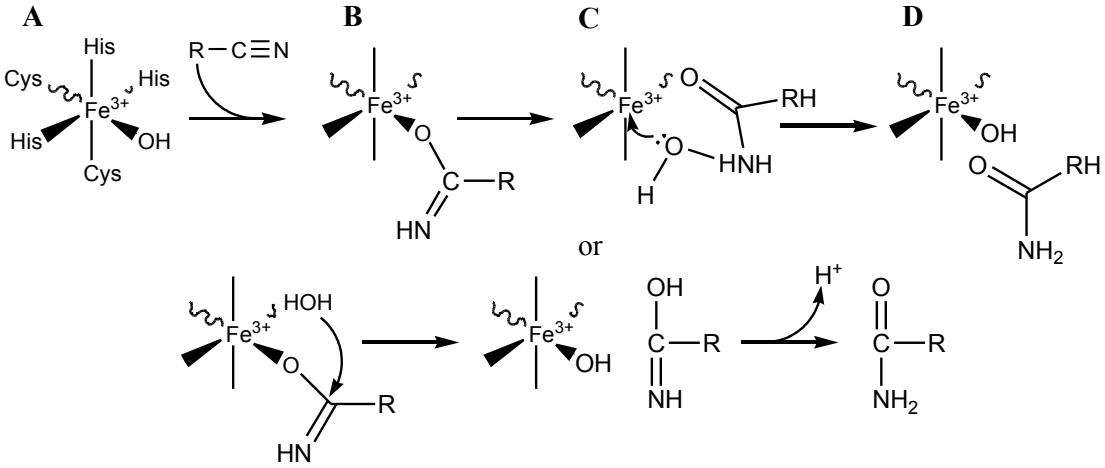


Figure 5: Iron coordination at the active site proposed for nitrile hydratase and a possible reaction mechanism involving a coordinated hydroxyl group.

The mechanism for nitrile hydration was proposed on the basis of EXAFS and EPR studies and two X-ray crystal structures, and redrawn from Shearer *et al*. (2002) and Nagashima *et al*. (1998) [42, 43].

Purified NHase may be obtained as a mixture of 'low pH' and 'high pH' forms. Low pH forms are catalytically active while the high pH form needs to be activated. This activation can be accomplished through photolysis [44]. Resonance Raman spectroscopy studies have

shown that low- and high-pH forms have extensive differences in hydrogen bonding [36]. NHase, therefore, possesses unique intrinsic activity traits in the presence of light in that it can undergo photo-reactivation when irradiated with visible light after aerobic incubation in the dark. Endo and colleagues [45] have proposed a biochemical mechanism for this photoreactivity. Light irradiation of an iron complex (chromophore) in the β-subunit of the enzyme induces a conformational change of the subunit. Inactive NHase has a non-heme iron (III) centre to which an endogenous nitric oxide (NO) molecule is bound. Upon photo-reactivation, the NO is released and the activity of the enzyme recovered. It has been suggested through the use of Fourier-transform infrared difference spectroscopy [45] that irradiation causes a conformational change in the β subunit, and a subsequent breakage of the Fe-N bond. This results in photo-dissociation of the endogenous NO molecule from the NHase catalytic centre. Further studies of photo-activation of NHase is required to define the structure of the enzyme fully, since the mechanism of photoactivation is still poorly understood and reports are generally conflicting [36, 41, 44, 46-48]. Photoregulation and NO-addition both allow points of control of NHase activity, and afford potential in the use of the enzyme in biocatalysis.

Interestingly, it has been repeatedly reported that nitrile hydratase is generally induced by amides (the reaction product) rather than the nitrile (substrate) in microorganisms that metabolise nitriles [1, 20]. This may mean that a low level constitutive expression of NHase may occur, allowing for formation of amide from nitrile, thereby causing induction.

1.4 Amidase (EC 3.5.1.4)

Amidases catalyse the hydrolysis of amides to free carboxylic acids and ammonia (Equation 3) and are involved in nitrogen metabolism in both prokaryotic and eukaryotic organisms [49].

$$\mathbf{R\text{-}CONH_2 + 2H_2O \rightarrow R\text{-}COOH + NH_3} \qquad \textbf{(Equation 3)}$$

Amidases display huge differences in substrate-specificity and characteristics. Some are specific for aromatic amides [50] while others are specific for aliphatic amides [51] or amides of α- or ω-amino acids [52]. The majority of the nitrilase superfamily consists of

various amidase branches [8, 9]. However, there are many amidases that are unrelated to the nitrilase superfamily by virtue of their sequence similarities, including thiol proteases [53], triad hydrolases [54] and amidase signature enzymes [55].

The branch two enzymes are generally aliphatic amidases, and comprise a small group of nearly identical proteins found mainly in *Bacillus*, *Brevibacteria*, *Helicobacteria* and *Pseudomonas* [9]. They hydrolyse substrates such as the carboxamide sidechains of glutamine and asparagines using the conserved cysteine found in the nitrilase superfamily. The *Pseudomonas* amidase now has a predicted three-dimensional structure [10]. While branch two amidases hydrolyse small-molecule substrates, the branch three enzymes convert tertiary amino acid residues to secondary residues [8] and are generally described as amino-terminal amidases. Typically, bacterial nitrile hydratases are co-expressed with an amidase. Nitrile hydratase and amidase structural genes are co-transcribed in *Brevibacterium* R312 [56] and *Pseudomonas chlororaphis* B23 [57]. It is therefore likely that the branch two enzymes are those mostly involved in nitrile biocatalysis.

Amidases are being increasingly used in the biotechnology arena for production and/or conversion of valuable intermediates. For example, immobilized penicillin acylase (amidase) (E.C. 3.5.1.11) is widely used in the production of 6-aminopenicillanic acid from penicillin [58]. *Klebsiella oxytoca* contains an (*R*)-specific amidase, and converts (*R*,*S*)-amide to (*R*)-acid while the (*S*)-amide remains unconverted [59]. This enantiomeric reaction has been developed for large-scale biotransformation by Lonza [60].

1.5 Nitrile biotransformation, biosynthesis and bioremediation

Nitrile compounds (R-C≡N) are widespread in nature where they are mainly present as cyanoglycosides, cyanolipids, ricinine and phenylacetonitrile produced by plants [61]. Nitriles are also important and versatile intermediates in organic synthesis and used extensively in industry for the production of polymers and chemicals. For example, nylon-6,6 polymers and polyacrylonitrile (a plastics and acrylic fibre precursor) are produced from adiponitrile and acrylonitrile, respectively. Nitriles are also used as solvents, extractants, pharmaceuticals, feedstock, drug intermediates (chiral synthons), and pesticides, as well as in organic synthesis of amines, amides, amidines, esters, carboxylic

acids, aldehydes, ketones and heterocyclic compounds. Applications of nitrile-hydrolysing enzymes include production of amides and acids such as acrylamide, nicotinic acid and lactic acid from their corresponding nitriles [62], and the conversion of α–aminonitriles to optically active amino acids [63]. Enantioselective hydrolysis of α-hydroxynitriles (cyanohydrins) [64] and the production of optically active 2-arylpropionic acids, ibuprofen [65] and naproxen [66, 67] have also been achieved using nitrile-converting biocatalysts.

Nitriles contain the cyanide group (-CN) and used to be referred to as cyanides. Most small nitriles are soluble in water, but their solubility decreases with longer chain lengths or inclusion of aromatic structures. For this reason, most reaction mixtures incorporate up to 5% (v/v) methanol as a co-solvent. Nitriles can be made by one of several routes, including the dehydration of amides, or addition of hydrogen cyanide to carbonyl groups (aldehydes and ketones). Traditionally, acid or alkaline hydrolysis of nitriles is used to form the corresponding amide or acid from a nitrile (Figure 6). Chemical transformations of nitriles require relatively severe conditions and often generate toxic by-products [68-70].

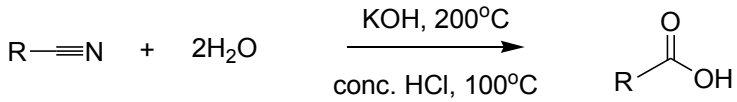


Figure 6: Alkaline and acid hydrolysis of nitriles.

Nitriles can be hydrolysed to carboxylic acids, partially hydrolysed to amides, reduced to primary amines (Figure 7), or selectively unconverted by regio-specific catalysts where there are multiple nitrile groups on one molecule.

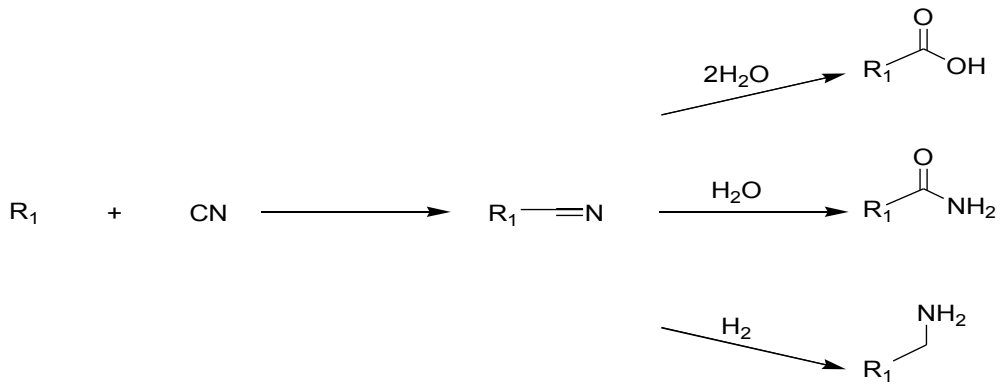


Figure 7: Schematic addition of cyanide to a molecule providing an additional carbon and nitrogen for subsequent conversion to other functional groups.

In synthetic chemistry, nitriles are important sources (as precursors) of amides and carboxylic acids via hydrolysis. A wide range of nitriles are substrates for nitrilases and NHases. The enzyme-catalysed hydrolysis of nitriles has advantages over the traditional organic synthesis route in many ways: The reaction proceeds under relatively mild conditions (neutral pH and room temperature), and often with regio-, chemo- and stereoselectivity [69]. Chemoselective hydrolysis of cyano functional groups, without any effect on other functional groups such as esters, can also be enzymatically achieved [71].

The study of nitrile metabolism revolves around three major viewpoints, namely biotransformation, biosynthesis and bioremediation. The application of these processes in industry is becoming increasingly useful. Production of acrylamide from acrylonitrile is an ongoing, commercially successful, biotransformation using NHase [1], as is the production of nicotinic acid from 3-cyanopyridine using nitrilase [24]. Biosynthesis of the plant hormone indole-3-acetic acid from indole-3-acetonitrile is another useful nitrile-converting activity that has found a footing in industry [22]. The remediation of highly toxic nitrile-containing wastes and the metabolism of nitrile-containing herbicides have proven useful in environmental management [60]. Synthetic fibre production results in large amounts of propionitrile as waste, and this was successfully converted by cells of *Rhodococcus erythropolis* to ammonium propionate which is useful as a feed supplement [72].

The enzymatic synthesis of enantiopure carboxylic acids using nitrilases reached another major milestone when Yamamato and co-workers produced (*R*)-mandelic acid from mandelonitrile using *Alcaligenes faecalis* whole cells [73]. However, due to the limited availability and stability of nitrilase enzymes, work on enantiopure compounds did not progress much during the 1990's. Recent developments in the technologies used to improve enzymes, such as directed evolution techniques, have greatly influenced the use of nitrilase in applied biocatalysis. One such example is that of the newly engineered papain nitrile hydratase for use as a biocatalyst by Dufour and co-workers [74].

Papain, a cysteine protease, was successfully converted into an enzyme with nitrile hydratase activity through protein engineering. This was achieved by replacing Gln^{19} in the oxyanion hole of papain with a glutamic acid residue. The nitrile substrate forms a covalent thiomidate adduct with the active site thiol group of the enzyme. The Glu^{19} residue participates in the acid-catalysed hydrolysis of the thiomidate to an amide by providing a

proton to form a more reactive protonated thiomidate. The hydrolysis of nitrile substrates therefore proceeds in a stepwise manner. First, the nitrile is hydrolysed to the corresponding amide. Since the Q19E mutant protein retains most of the natural amidase activity of natural papain, the amide is then further hydrolysed in the second step to the corresponding carboxylic acid. This mutant enzyme is considered a nitrilase in overall function, since it possesses both nitrile hydratase and amidase activities. The mutant papain is stable, active in organic solvents and at low pH, and is specific for peptide-based substrates. To illustrate the uses of this engineered protein, the mutant enzyme has since been used to synthesise amidrazones (that serve as intermediates in the synthesis of key components of biologically active molecules) with a more than 4000-fold increase in rate of production over the wild-type activity, and with a much higher level of purity [75].

Due to the hydrophobic nature of most nitriles, organic solvents are usually added to the reaction medium during nitrile-conversion by nitrilases and serves to enhance the bioavailability of the substrate. However, complete solubilisation of the substrate is not necessary for enzymatic conversion. Moreover, some solvent systems significantly enhance the enantioselectivity of certain enzymes. For example, hexane and acetone improved the enantioselectivity of the asymmetrization of 3-arylglutaronitriles [76]. Unfortunately, many of these nitrile-hydrolysing enzymes cannot be used in the presence of organic solvents, especially at high concentrations, which hampers their applicability to situations where the organonitrile substrate is very poorly soluble in water. Water-miscible solvents such as methanol and ethanol have been shown to be suitable cosolvents for purified enzyme only in concentrations of up to 20% (v/v), above which inactivation occurs. However, a purified NHase from *Rhodococcus equi* displayed activity in the presence of high concentrations of water-immiscible hydrocarbons, for example up to 90% (v/v) isooctane [77]. Purified high molecular mass NHase from *Rhodococcus rhodochrous* is unusually stable, retaining 89 – 100% of its original activity in alcohols, and showing appreciable activities in 50% (v/v) ethylene glycol, dimethyl sulfoxide and acetone [76]. This enzyme may be unusually tolerant to organic solvents due to its complex quaternary structure, the holoenzyme being composed of 20 subunits [76].

1.6 Nitrile Hydrolysis Activity Assays

The current methods for measuring or estimating nitrile hydrolyzing activity are limited and most of them have many disadvantages. There is a need to explore and develop more appropriate assaying procedures for nitrile activity. Most of the methods currently used rely on measurement of the ammonia formed from nitrile hydrolysis.

1.6.1 The Ninhydrin Assay

The ninhydrin method, which detects α-amino acids colorimetrically, is now an uncommon and old-fashioned method used to measure nitrile hydrolysis. Hydrolysis of an α-amino nitrile gives an α-amino acid which is reacted with ninhydrin reagent. The originally yellow ninhydrin reagent forms a purple anion that is colorimetrically measured at 570 nm. The assay is limited, however, to the type of nitrile hydrolysis being detected, and is non-specific for the type of α-amino acid produced.

1.6.2 Nesslerization

Nesslerization refers to the determination of ammonia using the Nessler method. Addition of Nessler reagent to a solution containing ammonia produces an orange-brown colour after development for a certain amount of time. This colour is read spectrophotometrically between 400 and 425 nm. Unfortunately, the assay is interfered with by several inorganic ions and some organic solvents, and the sensitivity of the method is very low (with accuracy only between 0.4 – 5.0 mg ammonia/L) [78]. Calcium and magnesium ions for example, can cause cloudiness of the reagent. Nesslerization is a common method for determination of nitrile hydrolysing activity, and is used to measure quantitatively the concentration of ammonia produced by the reaction. Most nitrogen in bacteria is assimilated and released in the form of ammonia, and this method would not necessarily only measure ammonia produced from nitrile hydrolysis when whole cell samples are used.

1.6.3 The Berthelot Method

The Berthelot method for measuring nitrile-hydrolysing activity is also referred to as the phenol/hypochlorite method. Ammonia liberated from nitrile hydrolysis is quantified colorimetrically at 640 nm after reaction with phenol/hypochlorite reagent. The procedure requires heating of the test solution at 90 °C for 30 min or 100 °C for 5 min. Heating is disadvantageous since vaporization of toxic phenols can occur. Also, insoluble MnO_2 (used as a catalyst) is formed, which interferes with the spectrophotometric determination. It is reportedly sensitive in the range of 20-200 μM NH_4Cl and at least 2 hours are required for development of a stable fluorochrome [79]. There are several disadvantages to this method other than the use of corrosive reagents, including the requirement for large samples due to the low sensitivity of the assay.

1.6.4 A Fourier Transform Infrared Method

Nitrilase-catalysed reactions have been monitored in real-time using a silicone probe with Fourier-transform IR technology [80]. A major drawback to an assay of this nature is the lack of availability of such an instrument and probe in most biological laboratories. Another problem is that the method is again insensitive. However, the technique may provide kinetic data for nitrile hydrolysis under certain conditions, such as high nitrile concentrations.

1.6.5 A Colorimetric pH Method

Kaul *et al*. (2004) have described measurement of nitrilase activity in several microorganisms using a pH-sensitive indicator-based colorimetric assay [81]. Reaction mixtures consisted of bromothymol blue (BTB) as indicator, mandelonitrile as substrate, and whole cell culture as the source of enzyme. The colour change (green to yellow) could be monitored over two hours. This method is of limited applicability due to poor sensitivity, and the possibility of false reactions due to the generation of metabolic acids by the microorganism (this is particularly true of yeasts).

1.6.6 Fluorimetric Methods

Banerjee *et al*. (2003) described a fluorimetric assay method for the measurement of nitrilase activity, in which 3-cyanopyridine was hydrolysed to nicotinic acid using *Rhodococcus rhodochrous* [82]. The ammonia liberated in the reaction is reacted with a buffered OPA (*o*-phthaldialdehyde) solution containing 2-mercaptoethanol and allowed to form a fluorescent isoindole derivative. The fluorescence intensity of the resultant fluorochrome is measured using excitation and emission wavelengths of 412 and 467 nm, respectively. Unknown concentrations of ammonia are determined from a standard curve constructed using known concentrations of NH_4Cl. A unit of nitrile-hydrolysing activity was defined as the amount able to release 1 μmol of NH_3/ min per mg of cells. Their study showed that this fluorescence method was more sensitive (2.5 – 1000 μM NH_4Cl) than previously used methods as summarised above [82].

Mana and Spohn [83] reported a method for determination of NH_4^+ ions using fluorimetric flow-injection analysis based on the same principle of isoindole derivative formation. However, the reported linearity range (0.05 – 100 μM NH_4Cl) differed substantially from that stated by Banerjee *et al*. (2.5 – 1000 μM NH_4Cl) [82]. Although the sensitivity of the OPA-based method used by Banerjee *et al*. (2003) is reportedly high, it has been suggested by Goddard and Reymond (2004) that only very potent enzymes can be detected using this method [84]. This is due to the fact that signal of the fluorescent isoindole chromophore requires very high concentrations of substrate (100 mM) in order to be detectable.

1.7 *Rhodococcus rhodochrous* as the chosen biocatalyst

Rhodococcal nitrilases and nitrile hydratases are the best characterised of the nitrile-degrading enzymes. By virtue of their ability to degrade a wide variety of nitrile compounds they have found many uses in industry, and applications of their activity have afforded useful industrial processes. *Rhodococcus* sp. R312 and *Rhodococcus erythropolis* NCIMB 11540 whole cells, for example, were used to transform β-amino nitriles to β-amino amides/acids [85], which have important pharmacological functions due to their antibiotic [86-88], antifungal [89, 90] and cytotoxic [91] properties. *Rhodococcus equi* A4 is an efficient biocatalyst for chemoselective and diastereoselective transformations [92].

Although many Pseudomonal nitrile-metabolising enzymes have been studied, they generally have narrower substrate ranges than the Rhodococcal enzymes [93, 94].

Nitrile converting enzymes are found in Rhodococcus bacteria from geographically diverse locations, including shallow marine sediments [95], deep-sea sediments [96] and various soil types, including garden soil [66, 97, 98], subtropical rain forest soil [99], mangrove mud [99] and contaminated river bank soil and sludges [100, 101]. The suitability of the organism to diverse habitats accounts for the numerous types of nitrile metabolising enzymes found within the species, including enzymes with wide pH and temperature profiles from mesophilic and thermophilic organisms [102, 103]. The majority of Rhodococcal nitrilases, nitrile hydratases and amidases referred to in literature are inducible enzymes [12, 16, 81, 102, 104, 105].

The previously demonstrated broad nitrile substrate profile of *Rhodococcus rhodochrous* ATCC BAA-870 by Brady *et al*. (2004), and its ability to be cultured using different nitriles as the sole nitrogen source have made the organism a good target for further investigation [106]. The relative growth of the organisms isolated from culturing on various nitrile nitrogen sources is summarised in Table 1, while the relative activities of various biocatalysts against different nitriles is summarised in Table 2. *Rhodococcus rhodochrous* ATCC BAA-870 was cultured using 3-hydroxy-3-phenylpropionitrile as the sole nitrogen source and was found to grow on 13 of the 17 growth substrates (Table 1). Of these, the organism showed good or exceptionally good growth on at least 11 compounds. Its ability to utilise benzamide, adipamide and acetoxy-phenylacetamide as sole nitrogen sources suggested it contained amidase activity. *Rhodococcus rhodochrous* ATCC BAA-870 converted 100% of benzonitrile, chlorobenzonitrile and naproxen nitrile, and displayed fair activity towards phenylglycinonitrile, 1,2-cyanonitrile, 3-hydroxy-3-phenylpropionitrile and benzylnitrile (Table 2). Both aliphatic and aromatic nitriles could be utilised by the organism and its applications as a biocatalyst would therefore be favourably versatile.

Table 1: Relative growth of some *Rhodococcus rhodochrous* strains on different sole nitrogen sources

	Substrate																
	Acrylonitrile	Adipamide	Adiponitrile	Acetoxyphenyl-propionitrile	Acetoxyphenyl-acetamide	α-Methylbenzyl-cyanide	Benzylidene malononitrile	Benzonitrile	Benzamide	4-Cyanopyridine	Diamino-malenonitrile	Fumaronitrile	Isobutyronitrile	Malononitrile	Phenylglycinonitrile	Propionitrile	Propionamide
Biocatalyst																	
Rhodococcus 1	4	4	4	1	3	1	0	1	5	1	1	1	4	2	2	4	5
Rhodococcus 2	4	4	3	4	2	0	0	0	4	0	1	0	4	2	1	3	5
Rhodococcus 3	4	4	3	5	0	3	0	2	4	2	0	0	5	3	5	3	5
Rhodococcus 4 (ATCC BAA-870)	5	5	4	3	4	0	0	1	5	1	0	0	5	4	4	5	5
Rhodococcus 5	0	0	4	0	0	0	0	0	0	0	0	0	0	0	4	4	0

Growth of the organism on each substrate is designated by 5 – exceptional, 4 – strong, 3 – good, 2 – fair, 1 – poor, and 0 – no growth. Screening of organisms was performed on minimal medium agar plates containing 5 mM of each substrate as the sole nitrogen source. Plates were incubated at 30 °C and the growth observed. Table adapted from results obtained by Brady *et al*. (2004) [106].

Table 2: Percentage substrate conversion of selected commercial nitrilases and biocatalysts

	% Conversion															
	O-Acetoxyphenyl-acetonitrile	Benzylnitrile	α-Methylbenzyl-cyanide	2-Phenyl-glycinonitrile	Mandelonitrile	3-Hydroxy-3-phenylpropionitrile	2-Phenyl-butyronitrile	Benzonitrile	N-Phenyl-glycinonitrile	1,2-Cyanonitrile	Chlorobenzonitrile	p-Tolunitrile	3,4-Dimethoxy-benzonitrile	3-Phenyl-propionitrile	Naproxen nitrile	Phenylglycinonitrile
Biocatalyst																
BioCatalytics Nit-1001	0	16	0	0	0	0	1	55	100	2	75	4	0	100	0	0
BioCatalytics Nit-1004	ND	87	0	0	1	0	0	ND	9	3	ND	19	2	31	ND	ND
BioCatalytics Nit-1005	0	78	0	0	0	0	0	100	100	48	100	100	100	100	0	0
BioCatalytics Nit-1006	100	100	0	14	41	0	0	100	7	3	85	0	0	0	0	100
P. fluorescens Nitrilase	ND	97	21	89	64	0	1	ND	0	14	ND	0	0	ND	ND	ND
Rhodococcus ATCC BAA-870	9	14	1	1	2	24	3	100	5	33	100	5	5	6	100	18
Rhodococcus ABFGs	ND	22	0	0	1	2	0	ND	30	0	ND	16	3	ND	ND	ND
Rhodococcus MAWA (C6)	ND	100	46	11	6	76	3	ND	2	32	ND	100	44	ND	ND	ND
Rhodococcus NOVO SP361	ND	102	15	4	2	30	11	ND	41	19	ND	32	24	ND	ND	ND
Pseudomonas alcaligenes 1	0	ND	ND	ND	ND	ND	ND	0	ND	ND	0	ND	ND	ND	0	7
Microbacterium 1	0	ND	ND	ND	ND	ND	ND	0	ND	ND	0	ND	ND	ND	40	9
Alcaligenes faecalis 1	0	ND	ND	ND	ND	ND	ND	0	ND	ND	0	ND	ND	ND	2	12

Conversion of each substrate is a percentage conversion. ND – not determined. Reactions were analysed using a Phenomenex Luna C18 column (from Separations) and a Hewlett Packard Series 1100 Chromatograph with a Photo Diode Array detector (PDA). Gradient elution of compounds was done according to the method developed by N. Wilde (2001, personal communication) and modified by G. Kupi (2003, personal communication), using a 1 ml/min flow rate, 5 µl injection volume, and 20 minute run time. Table compiled from results obtained by Brady *et al*. (2004) [106].

1.8 Objectives and potential applications of the research

Nitrile-converting enzymes are versatile biocatalysts and their applications are becoming increasingly recognised for the production of several pharmaceutically important compounds and fine chemicals. Although useful, they are generally not commercially available and are extremely limited in variety. The scarcity of suitable and/or well-characterised nitrile-converting biocatalysts has left a huge gap in the market for development of the enzymes as a product available for specific reactions, or even as a broad kit of enzymes with many purposes. Chemical industries make extensive use of nitrile compounds for manufacturing a variety of polymers and other chemicals, and the potential for nitrile-converting biocatalysts in these processes is great. Biocatalysis is a much 'greener' approach to synthesis or treatment of compounds since enzymes work under milder conditions and are non-destructive. By virtue of their capability to eliminate highly toxic nitriles, nitrile-degrading enzymes also play a significant role in protecting the environment.

The search for nitrile-hydrolysing enzymes with unique and improved properties, such as higher activity and stability, for use in commercial processes is ongoing. The current research may ultimately afford a new, efficient nitrile-converting biocatalyst that will add to the rapidly expanding field of biotechnology, whether as a whole cell application for selective activity or a partially purified enzyme preparation. Viral protease inhibitors have been synthesized using β-hydroxynitriles as intermediates in the synthetic pathway, and therefore exploration of the activity profile of *Rhodococcus rhodochrous* enzymes against β-substituted nitriles may yield potential novel routes or intermediates for biotransformations under milder conditions.

The biocatalyst studied herein is a bacteria isolated from South African soil. This brings the opportunity to apply an indigenous biocatalyst to processes that are of use in this country. The useful nitrile-metabolising activity of *Rhodococcus rhodochrous* ATCC BAA-870 is explored herein. The development of appropriate activity assaying methods was investigated for the purpose of finding assays specific enough for identifying nitrile hydrolysing activity in both whole cell extracts and purified enzyme reactions. A nitrile-hydrolysing assay with easily-identifiable colour change would be of use in the discovery

of new enzyme sources, and could be applied to high-throughput screening of microbes or enzymes with certain substrate specificities. The existing high performance liquid chromatography assay for identifying nitrile hydrolysis is investigated and optimised for the activity found within the studied organism. Buffer type and pH, and the influence of time and protein concentration on nitrile hydrolysis is investigated with the aim of assaying nitrile-converting activity with suitable parameters. In this study, enzyme separation strategies are also investigated. An enzyme preparation with industrial use need not necessarily be pure, but rather be one where specific activities can be easily separated in a one-step process. The potential biocatalyst, *Rhodococcus rhodochrous* ATCC BAA-870, displayed two types of activity in previous studies. This study aims to investigate the nitrile-metabolising activities of the organism, namely that due to the nitrile hydratase/amidase enzyme system. Assays for measuring this activity will be explored and further developed, and strategies for the one-step separation of the enzyme activities using chromatographic techniques will be investigated.

Chapter 2

2 Materials and Methods

2.1 Materials

2.1.1 Chemicals

All chemicals, unless otherwise stated, were purchased from Sigma Aldrich. Precision Plus protein standards and BioRad Protein Concentration Determination Reagent were obtained from BioRad.

2.1.2 Nitrile Stocks

Nitriles, and the products thereof, were made up as 100 mM stock solutions in methanol. The compounds 3-hydroxy-3-phenylpropionitrile and 3-hydroxy-4-phenylvaleronitrile were synthesized by R. Pieterson and M. Molefe (CSIR, BioSciences).

2.1.3 Commercial Nitrilases

Broad-range purified Nitrilases-1001, -1005 and -1006 (catalogue numbers NIT-101, NIT-105 and NIT-106, respectively) were obtained from Biocatalytics Inc. (USA). Purified nitrilases from *Pseudomonas fluorescens*, *Rhodococcus rhodochrous* and *Arabidopsis thaliana* (recombinant from *Escherichia coli*) were purchased from Fluka/ Sigma Aldrich.

2.1.4 Organism and Media

Rhodococcus rhodochrous ATCC BAA-870 was isolated from soil and characterised based on morphological and substrate-usage profiling at the Onderstepoort Veterinary Institute, South African Agricultural Research Council. The 16S rRNA was sequenced by the University of Cape Town. Lyophilised stores of the organism cultured in defined medium were available as part of an internal culture collection at CSIR Biosciences (South Africa).

Tryptone soya broth was obtained from Anatech (Scharlau Chemie, S.A. Barcelona). Its formula in g/L was: casein peptone, 17.0, soya peptone, 3.0, sodium chloride, 5.0, dipotassium phosphate, 2.5, and dextrose, 2.5. The approximate pH of the media was 7.3. Minimal medium consisted of a defined salt medium (4.97 g/L $NaHPO_4$, 0.2 g/L KH_2PO_4, 0.05 g/L $CaCl_2.2H_2O$, 0.09 g/L $FeSO_4.7H_2O$ and 0.02 g/L $MgSO_4$) containing 1.2 g/L glucose, 1 ml/L trace element solution (0.2 g/L $ZnSO_4.5H_2O$, 0.4 g/L $CuSO_4.5H_2O$, 0.004 g/L $CoSO_4.7H_2O$, 50 g/L trisodium citric acid and 0.4 g/L $MnSO_4.H_2O$) and 20 mM benzonitrile as inducer [97].

2.1.5 Column Chromatography

Gel exclusion protein standards were purchased from BioRad. Sephacryl S-200 gel exclusion media with a fractionation range in relative molecular mass (M_r) of 5 x 10^3 – 2.5 x 10^5 was obtained from Bio-Rad/Amersham Biosciences. Blue Dextran 2 000 was from Pharmacia, Uppsala, Sweden. Polybuffer 74 and Polybuffer Exchanger 94 were purchased from Amersham Biosciences. TOYOPEARL Super-Q 650M ion exchange media was from TOSOH Bioscience.

2.2 Methods

2.2.1 *Rhodococcus rhodochrous* ATCC BAA-870

2.2.1.1 Routine Maintenance of *Rhodococcus rhodochrous* Cultures

Rhodococcus rhodochrous ATCC BAA-870 was originally isolated from soil samples by Brady *et al*. (CSIR) using the enrichment method of Layh *et al*. (1997) [97]. Prior to growth on defined medium agar plates, the cultures were enriched in nutrient agar. Isolate biomass was stored as lyophilised powder at -80 °C, and regenerated by addition of a small amount of sample to tryptone soya broth. The culture was grown at 30 °C with shaking at 200 rev./min for 24 hours. Streak plates were made of the culture and incubated at 30 °C for observation. The inoculum was diluted 1:100 into fresh tryptone soya broth. Streak plates were stored at 4 °C until further culturing was necessary.

2.2.1.2 Observations of *Rhodococcus rhodochrous* Growth

Routine streak plates from both liquid broth culture and other streak plates were made of the organism. Plates were incubated at 30 °C and kept for different periods. A Sony Cybershot digital camera was used to take photographs of various streak plates at different stages of growth.

2.2.1.3 Microscope Observations of the Life Cycle of *Rhodococcus rhodochrous*

Microscope slides of samples of *Rhodococcus rhodochrous* ATCC BAA-870 at various stages of growth were prepared by smearing a bacterial colony with a drop of distilled water or using a drop of culture directly on a slide. Slides were viewed under high power using an Olympus BX40 microscope equipped with a Sony 3CCD colour video camera/ CCD-iris. Samples included culture grown in minimal media for different time periods, as well as on rich medium (tryptone soya agar) plates for up to two weeks. The stages of growth were then compared.

2.2.1.4 *Rhodococcus rhodochrous* Growth Curves in Different Media

Tryptone soya broth was selected as the rich media of choice since the organism was observed to grow well on tryptone soya agar. Defined minimal medium had benzonitrile added to a concentration of 20 mM to induce production of nitrile hydrolysing enzymes during growth. An overnight inoculum of *Rhodococcus rhodochrous* ATCC BAA-870 was diluted 1:100 in tryptone soya agar for rich medium studies or defined medium for minimal media studies and flasks incubated at 30 °C with shaking at 200 rev./min. Aliquots of the culture were taken at hourly intervals from duplicate flasks and the optical densities measured at 600 and 660 nm using a DU 800 Spectrophotometer.

2.2.1.5 Dry Cell Weight Determination

Eppendorf tubes (2 ml) were labelled and placed in a 105 °C drying oven for 24 hours with their lids open. Tubes were then placed in a desiccator for an hour to cool, and the mass of each recorded. Samples of *Rhodococcus rhodochrous* ATCC BAA-870 culture were pipetted in 2 ml volumes into the Eppendorf tubes and centrifuged at 13 000 *g* for 5 min in a standard microcentrifuge. The supernatant was discarded and the pellet washed with 2 ml distilled water, 2 ml 0.1 M HCl and 2 ml distilled water again. The pellet was then placed in a 105 °C drying oven for 24 hours with their lids open. Tubes were then cooled and dried in a desiccator for one hour. Each tube was weighed and the average dry cell weight calculated.

2.2.1.6 Cell Disruption Study

Rhodococcus rhodochrous ATCC BAA-870 grown in 200 ml minimal media for approximately 28 hours at 30 °C with shaking was harvested by centrifugation at 8 000 x *g* for 15 minutes at 4 °C. Pellets were resuspended with, and washed twice in 50 mM phosphate buffer, pH 7.4. After re-centrifugation, pellets were resuspended as an approximately 1 g/ml whole cell broth, and aliquoted into 2 ml volumes. Lysate volumes were sonicated using a Vibra Cell™ sonicator from Sonics & Materials Inc. (Danbury, Conneticut, U.S.A.) for a total of up to six minutes (30 s on, 30 s off), sampled at one minute intervals. Microscope slides of samples of *Rhodococcus rhodochrous* at different stages of sonication were prepared by adding 100 µl of sonicated broth to a drop of distilled water. Slides were viewed under high power using an Olympus BX40 microscope

equipped with a Sony 3CCD colour video camera/ CCD-iris. Volumes of lysate were tested for activity against benzonitrile and measured using high performance liquid chromatography (HPLC) as described below in section 2.2.3.

2.2.1.7 BioRad Protein Concentration Determination Assays

Dye reagent was prepared by adding one part dye reagent to 4 parts distilled water and filtered through Whatman® number 1 filter paper to remove particulates. Bovine serum albumin (BSA) standards in the range 0.2 – 0.9 mg/ml were prepared in duplicate, and 100 µl of each added to 5 ml dye reagent. After vortexing, standards were incubated at room temperature for a minimum of 5 minutes. The absorbance at 595 nm was read using a Beckman Coultier DU 800 Spectrophotometer and a standard curve constructed (see Appendix). The sample of unknown concentration (100 µl) was added to 5 ml dye reagent and treated in the same manner. If required, dilutions of the unknown sample were prepared until the absorbance reading fell within the linear range of the standard curve.

2.2.1.8 Preparation and Storage of *Rhodococcus rhodochrous* Supernatant

Rhodococcus rhodochrous was cultivated in 2 L shake flasks containing 400 ml defined minimal media at 30 °C with shaking at 200 rev./min. After growth for 28 – 30 hours, cells were harvested by centrifugation at 8 000 x *g* at 4 °C for 30 minutes, and washed twice with 50 mM potassium phosphate buffer, pH 7.4. Cells were stored at -20 °C as approximately 1 mg/ml suspensions in 20 mM potassium phosphate buffer, pH 7.4. To prepare supernatant, cell suspensions were thawed on ice before sonicating for a total of five minutes. Lysate was centrifuged at 8 000 x *g* for 30 minutes at 4 °C and the supernatant collected.

2.2.2 Assays for Measuring Nitrilase/ Nitrile Hydratase Activity

2.2.2.1 Colorimetric Method

A pH-sensitive indicator-based assay based on experiments done by Kaul *et al*. (2004) [81] was used to identify nitrilase and nitrile hydratase activity first in solution using cuvettes, and secondly in agarose plate wells (Figure 8). An attempt to establish an easily detectable assay for locating nitrilase activity on a native PAGE gel was undertaken. The assay

involved using bromothymol blue as indicator for detecting a drop in pH on formation of the corresponding acid from a nitrile.

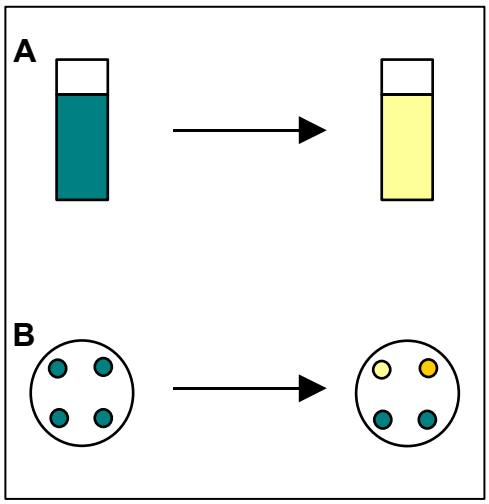


Figure 8: Schematic representation of the method used for colorimetric identification of nitrilase or nitrile hydratase activity.

Blue colour represents solutions containing 0.05% (v/v) bromothymol blue and 2 mM benzonitrile in 0.01 M potassium phosphate buffer, pH 7.2, with either commercial nitrile standards (1 mg/ml) or whole cell culture. pH-induced colour change is shown in yellow. Colour change was monitored over 2 hours. (A) Cuvettes containing 2 ml final reaction volumes showed colour changes using both 0.05 and 0.01% (v/v) BTB indicator concentrations. (B) Only wells containing 10 and 20 µl of commercial 1 mg/ml nitrilase exhibited yellowing of BTB-containing agarose with increasing intensity respectively. Control reactions containing no enzyme showed no colour change.

The buffering capacity of potassium phosphate buffer at pH 7.2 was tested using phenylglycinonitrile, benzonitrile and chlorobenzonitrile. Each substrate was added to the buffer to a final concentration of 2 mM and the pH tested. Substrates were only used if the pH of the final reaction mix was approximately 7.2. Agar plates (15 g/L) were made in 0.01 M potassium phosphate buffer, pH 7.2, and benzonitrile (2 mM) and 0.01 or 0.005% (v/v) bromothymol blue added after autoclaving. Wells were punched into the plates using a 2 ml disposable syringe. Increasing volumes of commercial Nitrilase 1005 (1 mg/ml) was added to the wells and incubated at 30 °C. One well on each plate was used as an enzyme-negative control. SDS-PAGE gels of commercial nitrilase enzymes were overlayed onto bromothymol blue-containing agar plates, and incubated overnight at 30 °C in order to test whether the acid-forming activity of the enzymes could be colorimetrically measured using an overlay method.

2.2.2.2 Fluorimetric Method for Determining Nitrilase Activity

A method based on formation of a fluorescent isoindole derivative from ammonia produced during nitrilase activity was developed by Banerjee *et al*. (2003) [82]. Ammonia released during the reaction reacts further with a buffered alcoholic *o*-phthaldialdehyde solution, and the fluorescent derivative formed can be measured using excitation and emission wavelengths of 412 and 467 nm, respectively. The method was reported by the authors to be rapid and sensitive in the range of 100 to 1000 μM substrate concentration. A buffered OPA/2-mercaptoethanol reagent was made by combining 4.5 ml of each of solution A (75 mM OPA in ethanol) and B (72 mM 2-mercaptoethanol in ethanol) with 91 ml 0.2 M phosphate buffer, pH 7.4. All solutions were filtered using a Cameo 25SS PES 0.22 μm filter (Osmonics). Increasing concentrations of NH_4Cl were reacted with buffered alcoholic OPA reagent in order to construct a standard curve for unknown ammonia concentration determination. Fluorescent isoindole derivatives were allowed to develop by incubation at room temperature for 20 minutes prior to measurement. A PerkinElmer LS 55 Spectrometer was used to measure the intensity of emission at 467 nm when excited at 412 nm, using a 2.5 nm slit width and a scan speed of 200 nm/min. Standard curves were generated using potassium phosphate, sodium phosphate and Tris buffers. Whole cell *Rhodococcus rhodochrous* culture and commercial nitrilase enzymes (Nitrilase 1001, 1005 and 1006) were used as enzyme sources in the reactions. Substrates tested included phenylpropionitrile, benzonitrile, chlorobenzonitrile, phenylglycinonitrile, mandelonitrile, naproxen nitrile, fumaronitrile and malononitrile. Reactions consisted of 5 mM substrate, 0.2 ml cell suspension or supernatant and 175 mM phosphate buffer, pH 7, to a final volume of 2 ml. Reactions were incubated at 50 °C for 20 minutes and stopped by the addition of 2 ml HCl. After centrifugation at 5 000 x *g* for 10 minutes, 100 μl of each reaction was added to 3 ml OPA/2-mercaptoethanol reagent and developed for 20 minutes at room temperature. Assay troubleshooting included lowering the reaction temperature to 30 °C and increasing the incubation time to 2 hours in order to make the assay more sensitive.

A modified method of the above assay was attempted to spot bands in polyacrylamide gel electrophoresis (PAGE) gels with ammonia-forming activity. Commercial nitrilase samples were prepared and run in duplicate non-denaturing PAGE gels. One gel was equilibrated with 100 mM phosphate buffer, pH 7, using slow shaking at 25 °C for further testing using

OPA while the other gel was Coomassie stained (Section 2.2.5). After equilibration, the first gel was immersed in 17.5 ml 100 mM phosphate buffer, pH 7, to which 0.5 ml of 1 M benzonitrile was added. The gel in the reaction mixture was incubated for 20 min at 30 °C with slow shaking. OPA/2-mercaptoethanol reagent (9 ml) was then added and the gel left to develop at room temperature for 20 min. The gel was viewed under a UV lamp.

2.2.3 Assay Development: High Performance Liquid Chromatography

2.2.3.1 RP-HPLC Method Set

All samples, unless otherwise indicated, were run according to the following reversed-phase HPLC (RP-HPLC) method using a Waters 2690 Separations Module HPLC with 996 Photodiode Array Detector. The column used was a 100 x 4.6 mm Chromolith Performance SpeedROD RP–18e (Merck, Germany, cat # 1.02129.0001).

Injection volume: 20 µl

Run Time: 10 minutes

Column Temperature: 28.0 °C

Flow rate: 0.5 ml/min

Isocratic elution: 6% $TFA_{(aq)}$: 40% ACN

Degasser: on

Data were acquired with the PDA (with a 200 to 300 nm wavelength range) that generated 3D data (Figure 9). A plot of absorbance versus wavelength indicates the maximum absorbance values of multiple wavelength maxima (Figure 10). Integration and data analysis was done using Millennium[32] Version 3.05.01 (© 1998 Waters Corporation) software. The instrument was primed, and the column equilibrated for at least 2 hours before each run.

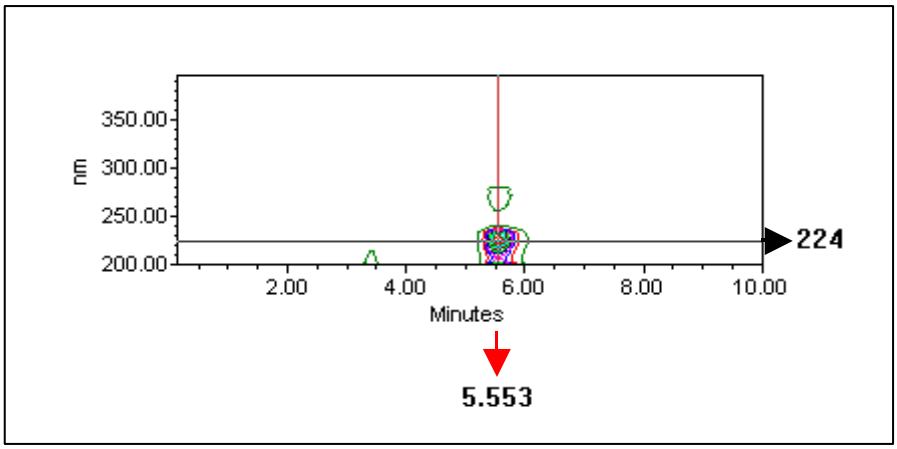


Figure 9: Three-dimensional contour map of absorbance with wavelength and elution time for benzonitrile as acquired by the photodiode array detector in HPLC.

The optimum absorbance and concentration is defined by the highest contour density. A 5 mM sample of benzonitrile prepared in eluent, was isocratically eluted using 40% acetonitrile: 6% aqueous trifluoracetic acid. Arrows indicate the retention time and absorbance maximum at which data is extracted.

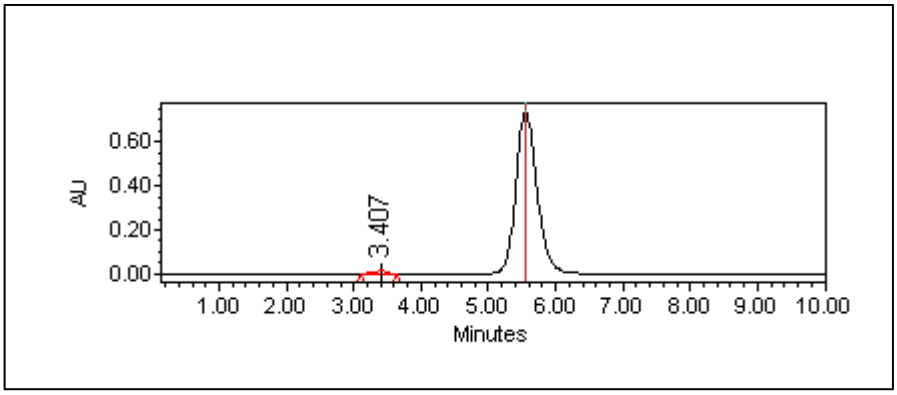


Figure 10: Two-dimensional chromatograph of a 5 mM benzonitrile sample showing absorbance over time at 224.1 nm.

Data were extracted from the three-dimensional contour map at the absorbance maximum of benzonitrile (224.1 nm). The sample was eluted isocratically using 40% acetonitrile: 6% aqueous trifluoracetic acid.

2.2.3.2 Qualitative HPLC Tests

Purified nitrilases from *Pseudomonas fluorescens*, *Rhodococcus rhodochrous* and *Arabidopsis thaliana* (recombinant from *Escherichia coli*) and nitrilases NIT-1001, -1005 and -1006 were tested against benzamide, benzoic acid and benzonitrile by HPLC as a measure of activity. Each nitrilase (750 µl of a 1 mg/ml stock) was added to 675 µl of a 50

mM phosphate buffer, pH 7.4, and 75 µl of substrate (substrate final concentration 5 mM). The final reaction volume was 1.5 ml. Standards were made by omitting enzyme from the reaction. Reactions were incubated at 30 °C for 2 hours with shaking (200 rev./min), after which they were centrifuged at 3 000 x *g* for 5 min. A 200 µl aliquot of each was filtered through a Cameo 25SS PES 0.22 µm filter (from Osmonics) and transferred into a 2 ml HPLC vial containing 800 µl acidic stop eluent (equal parts acetonitrile and aqueous 0.1% (v/v) TFA).

2.2.3.3 Comparison of the Fluorimetric Method and HPLC for Measuring Activity

Rhodococcus rhodochrous ATCC BAA-870 cells grown in minimal media for 48 hours were harvested by centrifugation at 8 000 x *g* for 15 min. Cells were washed twice in 50 mM phosphate buffer, pH 7.4, containing 20 mM dithiothreitol (DTT), and suspended in 200 µl of the same buffer. The reaction was initiated by addition of 0.05 ml 1 M benzonitrile and 1.75 ml 50 mM phosphate buffer, pH 7.4, containing 20 mM DTT, and incubated for 20 min at 30 °C with shaking (200 rev./min). The reaction was stopped by addition of 2 ml of 0.1 M HCl and the mixture centrifuged at 5 000 x *g* for 10 min. The supernatant was used for determining enzyme activity.

For reactions measured using fluorimetry, 1.5 ml buffered OPA solution was added to 0.5 ml supernatant. The generation of the fluorochrome was allowed to develop for 20 min in the dark at room temperature. Fluorescence intensity was measured using excitation and emission wavelengths of 412 and 467 nm, respectively, using a PerkinElmer LS 55 Spectrometer with a 2.5 nm slit width and a scan speed of 200 nm/min.

For reactions measured using RP-HPLC, 100 µl of supernatant or control sample was mixed with 450 µl of each of 0.1% (v/v) aqueous trifluoracetic acid (TFA) and acetonitrile (ACN), and capped in 2 ml HPLC vials. Control samples included 100 mM solutions of benzonitrile, benzamide and benzoic acid that were prepared in the same manner except no cells or enzyme was added. Also, the enzyme Nit-1005 was used as a further control based on its successful conversion of benzonitrile to benzoic acid in previous HPLC results. All samples were done in quadruplicate. HPLC results were obtained using the Waters

Integrity™ System with photodiode array detector, using a flow rate of 0.5 ml/min, 20 µl injection volume and 20 min sample run time. The column was isocratically eluted using 60% acetonitrile and 4% aqueous TFA, and the compounds monitored between 200 and 400 nm.

2.2.3.4 Standard Curves

Concentration standard curves were constructed for benzonitrile, benzamide, benzoic acid, hydrocinnamonitrile, 3-hydroxy-3-phenylpropionitrile and 3-hydroxy-3-phenylpropionic acid. Samples of each were made up in the concentration range 0 to 10 mM in 1 mM intervals from 100 mM stock solutions in methanol. After thorough mixing, 100 µl of each concentration was pipetted in triplicate into 2 ml HPLC vials containing 900 µl acidic stop eluent and filtered through a Cameo 25SS PES 0.22 µm filter. Samples were run according to the set method for nitrile analysis. Integrated peaks were measured as a function of integration area and absorbance to check linearity of the absorbance detector with concentration.

2.2.3.5 Commercial Nitrilase Enzyme Reactions

Nitrile substrate (5 mM) dissolved in methanol was added to 50 mM KH_2PO_4 buffer, pH 7.4. Enzyme dilutions (750 µl) were added to a final volume of 1.5 ml to initiate the reaction, and incubated at 30 °C for 2 hours with agitation. Controls were prepared in the same manner except no enzyme was added to the reaction mix. An aliquot (100 µl) of the reaction mixture was added to 900 µl of acidic stop eluent to a final volume of 1 ml. The reaction was centrifuged at 13 000 x *g* for 5 mins, and sealed in a 2 ml HPLC vial for analysis.

2.2.3.6 LC-Mass Spectral Analysis

Coupled HPLC and mass spectral analysis was performed using the Waters Integrity™ System with photodiode array detector and Thermabeam™ mass detector, using the set method for nitrile hydrolysis. Mass Spectral results of standards were compared to internal library spectra from the Millennium[32] Version 3.05.01 (© 1998 Waters Corporation) software. Mass spectral sampling parameters for nitrile analysis were changed to a 20 µl

injection volume and 30 min total sample run time. Initial elution was 0.2 ml/min of 0.1% (v/v) formic acid for 15 min, followed by 2 min of a 0.3 ml/min 50% methanol:50% acetonitrile elution, 5 min of 0.1% (v/v) formic acid at 0.25 ml/min, and lastly 8 min of 0.1% (v/v) formic acid at 0.2 ml/min. The column temperature was set at 40 °C. Where reaction products had been identified, HPLC UV/VIS was often used without the coupled MS detector.

2.2.3.7 The Effect of Different Buffer Types on Relative Activity

A series of ten different buffer types were made up, including Polybuffer 74 containing 5 mM DTT (pH 4, 5, 6 and 7.4), 100 mM and 50 mM potassium phosphate buffers (pH 7.4), 25 mM imidazole buffer pH 7.4, and 50 mM potassium phosphate buffers containing either 10 mM DTT, 10 mM ethylene diamine tetraacetic acid (EDTA) or 10 mM DTT and 10 mM EDTA, pH 7.4 (Table 3). Each reaction contained 975 µl of buffer, 75 µl of a 100 mM benzonitrile or hydrocinnamonitrile stock and 450 µl *Rhodococcus rhodochrous* supernatant to a final volume of 1.5 ml. Reactions were incubated at 30 °C for 2 hours with shaking at 200 rev./min and stopped by addition of one part reaction to nine parts acidic stop eluent. Samples were analysed by HPLC.

Table 3: The ten different buffer types used in this study and their composition

Buffer Number	Buffer Composition
1	Polybuffer 74* containing 5 mM DTT, pH 7.4
2	Polybuffer 74* containing 5 mM DTT, pH 6
3	Polybuffer 74* containing 5 mM DTT, pH 5
4	Polybuffer 74* containing 5 mM DTT, pH 4
5	100 mM KH_2PO_4, pH 7.4
6	50 mM KH_2PO_4, pH 7.4
7	25 mM Imidazole, pH 7.4
8	50 mM KH_2PO_4 containing 10 mM EDTA, pH 7.4
9	50 mM KH_2PO_4 containing 10 mM DTT, pH 7.4
10	50 mM KH_2PO_4 containing 10 mM DTT and 10 mM EDTA, pH 7.4

* Polybuffer 74 1:8 dilution, prepared as per chromatofocusing elution conditions.

2.2.3.8 Testing the Effect of pH on Relative Activity

Universal buffer (300 mM acetic acid, 300 mM NaH_2PO_4, 300 mM Tris) was diluted two times to a working 1 X solution and the pH adjusted in unit increments from pH 4 to ten. Each reaction contained 975 µl universal buffer, 75 µl of a 100 mM benzonitrile or hydrocinnamonitrile stock and 450 µl *Rhodococcus rhodochrous* supernatant to a final volume of 1.5 ml. Samples were reacted at 30 °C for 2 hours with shaking at 200 rev./min and stopped by addition of one part reaction to nine parts acidic stop eluent. Samples were centrifuged at 13 000 x *g*, added to 2 ml HPLC vials and analysed by HPLC.

2.2.3.9 Determining Product Formation Over Time

Cell-free protein extract (1.8 ml) was mixed with 3.9 ml of a 50 mM potassium phosphate buffer, pH 7.4, in reaction tubes set at 30 °C with stirring in a temperature-controlled reaction carousel with magnetic stirrer from Radley's Discovery Technologies. Mixes were allowed to equilibrate for ten minutes before substrate addition, using a Hamilton syringe. Substrate consisted of 5 mM benzonitrile, benzamide or 3-hydroxy-3-phenylpropionitrile added at time zero to give a total reaction volume of 6 ml. At sampling times the reaction tube was thoroughly mixed, and 100 µl immediately withdrawn using a Hamilton syringe and added to 900 µl acidic stop eluent. After centrifugation at 13 000 x *g*, the 1 ml reaction was transferred to a 2 ml sampling vial. Reactions were performed in triplicate and analysed by HPLC.

2.2.3.10 Testing the Effect of Protein Concentration on Activity

Supernatant from *Rhodococcus rhodochrous* of known protein concentration was added to 5 mM of benzonitrile, benzamide or 3-hydroxy-3-phenylpropionitrile in 50 mM potassium phosphate buffer, pH 7.4, to a total reaction volume of 1.5 ml. Total protein concentration in each reaction ranged from 0 to 1.86 mg/ml. Reactions were incubated at 30 °C with shaking at 200 rev./min for 10, 25 or 30 min when reacted with benzonitrile, benzamide and 3-hydroxy-3-phenylpropionitrile respectively. Reaction sample volumes (100 µl) were added to 900 µl acidic stop eluent. After centrifugation at 13 000 x *g*, the 1 ml reaction was transferred to a 2 ml sampling vial. Reactions were performed in triplicate and analysed by HPLC.

2.2.4 Column Chromatography

2.2.4.1 Chromatofocusing of the Soluble Protein Fraction of *Rhodococcus rhodochrous*

After packing, the PBE 94 column was equilibrated with 0.025 M imidazole buffer, pH 7.4, containing 5 mM DTT. The equilibration buffer was set 0.4 pH units higher than the start pH. Elution buffer containing 5 mM DTT was prepared by diluting commercial Polybuffer 74 1:8 with distilled water, and subsequently pH-adjusted with HCl. All buffers used in the process were degassed extensively to avoid fluctuations in the pH gradient caused by bicarbonate ions. Protein elution was tracked by monitoring absorbance at 280 nm. The pH of each fraction was measured using a pH 211 Microprocessor pH Meter (HANNA Instruments. Fractions (750 µl of each) were tested against certain substrates by reaction with 5 mM benzonitrile, hydrocinnamonitrile, (*R*)-mandelonitrile, 2-phenylglycinonitrile, 3-hydroxy-3-phenylpropionitrile, or 3-hydroxy-4-phenylvaleronitrile for 2 hours at 30 °C with shaking. Samples were analysed by HPLC as described above.

2.2.4.2 Gel Exclusion Chromatography

The gel exclusion column was equilibrated using 100 mM potassium phosphate buffer, pH 7.4, containing 0.02% (w/v) sodium azide. Supernatant from *Rhodococcus rhodochrous* was filtered using a DIAFLO® ultrafiltration membrane from AMICON Corporation (Ireland) prior to loading. Gel exclusion standards of M_r 670 000 (bovine thyroglobulin), 158 000 (bovine gamma globulin), 44 000 (chicken ovalbumin), 17 000 (horse myoglobin) and 1 350 (vitamin B-12) were used to create a size-exclusion standard curve. A gel exclusion selectivity curve was created for the column according to the protocol laid out in the Gel Filtration Principles and Methods Handbook by Amersham Biosciences (Uppsala, Sweden). The column void volume (V_o) was determined from the elution of Blue Dextran (2 000 kDa), and molecular mass estimated by comparison of its elution volume/void volume to those of the standards. Standards and unknowns were eluted using a flow rate of 0.7 ml/min and the A_{280} monitored and recorded using a chart recorder set at 2 mm/ml. Eluted fractions were tested for biocatalytic activity by adding 1.425 ml of each fraction to 75 µl benzonitrile, benzamide or 3-hydroxy-3-phenylpropionitrile. Reactions with benzonitrile were incubated for 15 minutes while reactions with benzamide and 3-hydroxy-

3-phenylpropionitrile were incubated for 30 minutes. Reactions were performed at 30 °C with shaking and analysed by HPLC.

2.2.4.3 Ion Exchange Chromatography

The Toyopearl Super-Q 650M ion exchange column was equilibrated using 20 mM Tris buffer, pH 8. Supernatant from *Rhodococcus rhodochrous* was buffer exchanged into 20 mM Tris buffer, pH 8, and 4.9 ml of a 10 mg/ml sample loaded onto the column. After sample loading, the absorbance at 280 nm of each fraction was monitored until all unbound proteins were eluted. Bound proteins were eluted using a 500 mM NaCl gradient over 42 ml. Eluted fractions were tested for biocatalytic activity by adding a volume (450 µl) of fraction to 75 µl 5 mM benzonitrile, benzamide or 3-hydroxy-3-phenylpropionitrile in 975 µl 20 mM Tris buffer, pH 8, to a final volume of 1.5 ml. Reactions were incubated at 30 °C with shaking for 30 minutes when reacting benzamide and 3-hydroxy-3-phenylpropionitrile, and 15 minutes when reacting benzonitrile. Samples were analysed by HPLC.

2.2.5 Polyacrylamide Gel Electrophoresis

2.2.5.1 SDS-PAGE

SDS-PAGE was done according to the discontinuous method of Laemmli (1970) using a BioRad mini-protean gel system [107]. Proteins were separated using a stacking gel consisting of 4% (m/v) acrylamide/bis-acrylamide solution, 0.126 M Tris-HCl, pH 6.8, distilled water, 0.1% (m/v) SDS, 0.05% (m/v) ammonium persulphate and 0.1% (v/v) TEMED, and a separating gel consisting of 10% (m/v) acrylamide/bis-acrylamide solution, 0.375 M Tris-HCl, pH 8.8, distilled water, 0.1% (m/v) SDS, 0.05% (m/v) ammonium persulphate and 0.1% (v/v) TEMED. Samples were run alongside a protein molecular weight marker (from BioRad) containing the protein standards of relative molecular mass 250 000, 150 000, 100 000, 75 000, 50 000, 37 000, 25 000, 20 000, 15 000 and 10 000. Protein samples were incubated with protein loading buffer consisting of 0.125 M Tris-HCl, 4% (w/v) SDS, 20% (v/v) glycerol, 5% (v/v) β-mercaptoethanol and 0.02% (w/v) bromophenol blue, pH 6.8, for 5 min at 95 °C prior to loading, and gels were run at 150 V. Running buffer consisted of 0.025 M Tris, 0.192 M glycine and 0.1% (w/v) SDS, pH 8.3.

Gels were stained using 0.025% (w/v) Coomassie Brilliant Blue R250, 40% (v/v) methanol and 7% (v/v) acetic acid staining solution and destained in a 7% (v/v) acetic acid, 5% (v/v) methanol destain solution.

2.2.5.2 Non-Denaturing PAGE

Non-denaturing PAGE was done according to a modified method of Laemmli [107] whereby SDS and reducing agents were omitted from the buffer and gel systems.

Chapter 3

3 Results

3.1 *Rhodococcus rhodochrous* ATCC BAA-870 Characteristics

Identification of an appropriate nitrilase-containing microbe was undertaken based on previous activity screens using various nitriles [106]. Substrate profiles were compiled by Brady *et al*. (2006) and a suitable biocatalyst for this study chosen on the basis of their results [108]. The organism, *Rhodococcus rhodochrous* ATCC BAA-870, was thoroughly investigated, and growth parameters and characteristics of the organism were tested in order to further study its activity and potential use as a bioconversion tool.

3.1.1 *Rhodococcus rhodochrous* Growth Curves in Different Media

Several nitrilases are known to be strongly induced by the addition of nitrile to culturing media [109]. The growth curves of *Rhodococcus rhodochrous* in rich media (tryptone soya broth) and a minimal defined media where benzonitrile was used as the nitrogen source were measured and compared (Figure 11 and Figure 12).

Growth of *Rhodococcus rhodochrous* in tryptone soya broth follows a shallow sigmoidal growth curve. The log phase of growth in rich medium occurs at an optical density of approximately 1.2 at 600 and 660 nm. The log phase of growth in minimal medium occurs at an optical density of approximately 0.8 (measured at both 600 and 660 nm). The cell doubling time is roughly 28 hours in minimal media and 4-8 hours in rich media.

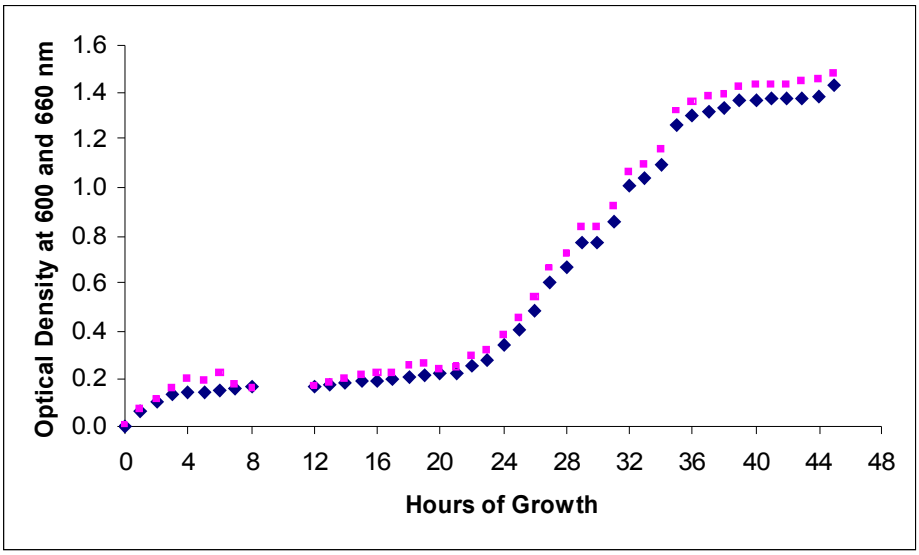


Figure 11: Growth curve of *Rhodococcus rhodochrous* in minimal media measured at 600 and 660 nm.

Optical density measurements of 50 ml shake flask cultures grown at 30 °C with shaking at 200 rev./min were performed in duplicate in separate experiments. The culture was grown in defined media containing 20 mM benzonitrile as inducer. The O.D. at 660 nm (■) and at 600 nm (■) was measured.

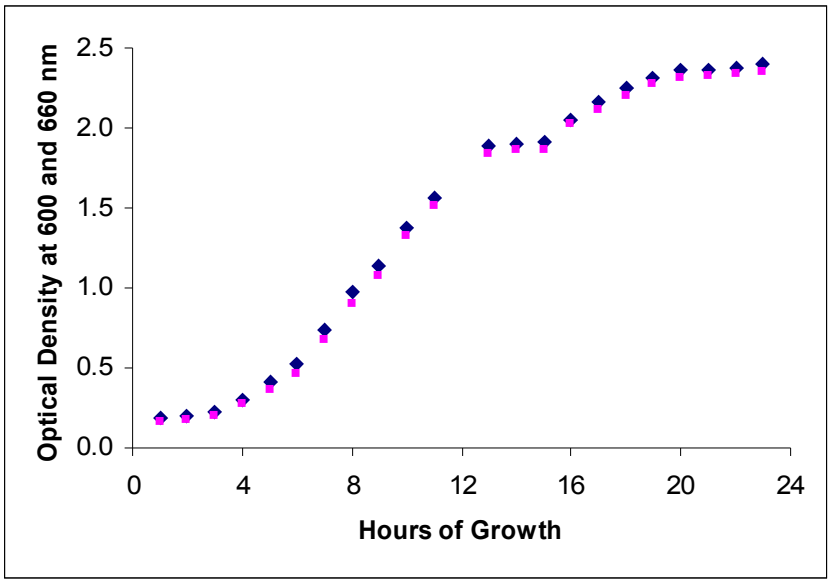


Figure 12: Growth curve of *Rhodococcus rhodochrous* in rich media measured at 600 and 660 nm.

Optical density measurements of 50 ml cultures grown in tryptone soya broth in shake flasks at 30 °C with shaking at 200 rev./min were performed in duplicate in separate experiments. The O.D. at 660 nm (■) and at 600 nm (■) was measured.

3.1.2 Dry Cell Weight Determination

The expected mass of *Rhodococcus rhodochrous* cells obtainable from batches of media was used to estimate the volume needed for bulking up of biomass used in further studies. The average dry cell weight of *Rhodococcus rhodochrous* grown in minimal media was 0.9 to 1.5 g per litre of culture.

3.1.3 Observations of *Rhodococcus rhodochrous* growth patterns

The rose-coloured appearance of *Rhodococcus rhodochrous* culture was clearly visible in liquid and on solid media. Orange to red colonies were formed on tryptone soya agar and became rough in appearance as the culture aged. *Rhodococcus rhodochrous* ATCC BAA-870 was found to grow favourably in rich medium agar plates. Tryptone soya agar was used for routine plating to check purity of cultures at each step of inoculation. A distinctive morphological feature of the organism's growth was its ability to form branches that fragment into rods and cocci. Mycelial growth became visible on the agar substrate after 1 week of growth at 30 °C. The rose colour deepened and colonies became extensively flared and spread out as the age of growth increased (Figure 13).

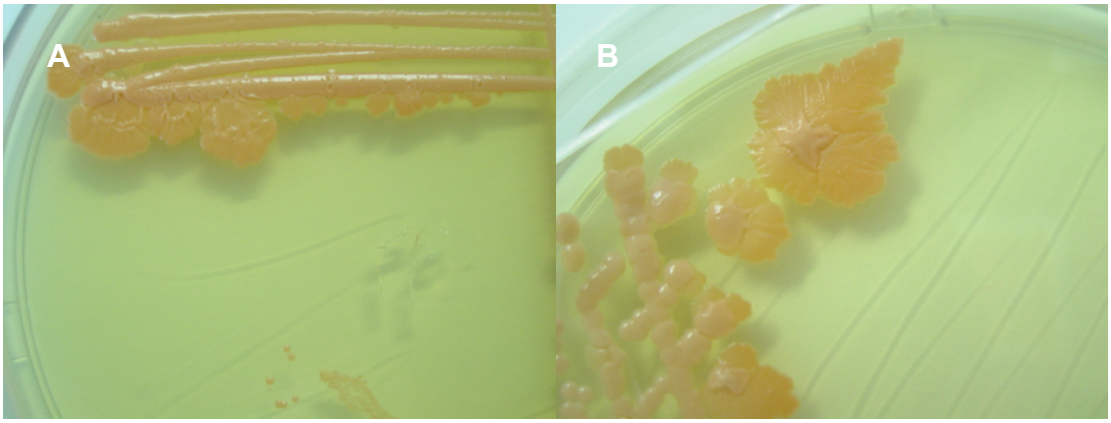


Figure 13: Close-up detail of the fanning formation developed by aged *Rhodococcus rhodochrous* culture on tryptone soya agar streak plates.

Fan formations are seen developing at the edge of a streak (A) and from a single colony (B). *Rhodococcus rhodochrous* was streaked onto tryptone soya agar plates and grown at 30 °C for more than 1 week.

3.1.4 Microscope Observations of the life cycle of *Rhodococcus rhodochrous*

Microscope photographs of *Rhodococcus rhodochrous* ATCC BAA-870 culture at different stages of growth were taken (Figure 14 and Figure 15).

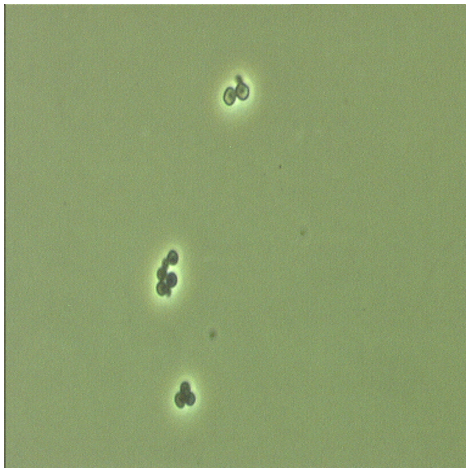


Figure 14: Germinating *Rhodococcus rhodochrous* ATCC BAA-870 cells in minimal media.

Rhodococcus rhodochrous cocci in minimal media is shown at high power resolution. Branching of the cocci cells during germination is just becoming evident. The image was taken with an Olympus BX40 microscope equipped with Sony 3CCD colour video camera/ CCD-iris at high power resolution.

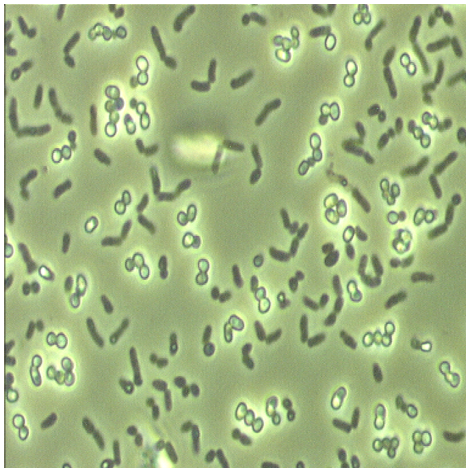


Figure 15: *Rhodococcus rhodochrous* ATCC BAA-870 in advanced stages of growth showing two distinct cell morphologies.

Rhodococcus rhodochrous grown on tryptone soya agar at 30 °C for two weeks. Both rods and cocci are now evident. The image was taken with an Olympus BX40 microscope equipped with Sony 3CCD colour video camera/ CCD-iris at high power resolution. The culture is pure as confirmed by streak plate analysis.

The cell morphology of *Rhodococcus rhodochrous* changes over time, with young cultures showing only one cell type (cocci) that progressively branch to form rod-shaped cells in mature cultures. The life-cycle growth of *Rhodococcus rhodochrous* follows an interesting elementary branching-rod-coccus morphogenetic sequence. Germinating cocci give rise to branching filaments (Figure 14), which then undergo fragmentation into rods and cocci to complete the growth cycle (Figure 15).

3.1.5 *Rhodococcus rhodochrous* Cell Disruption Study

The optimal cell disruption time was determined for *Rhodococcus rhodochrous*. The optimum total cell disruption time at which benzonitrile conversion was seen was 5 minutes (Figure 16).

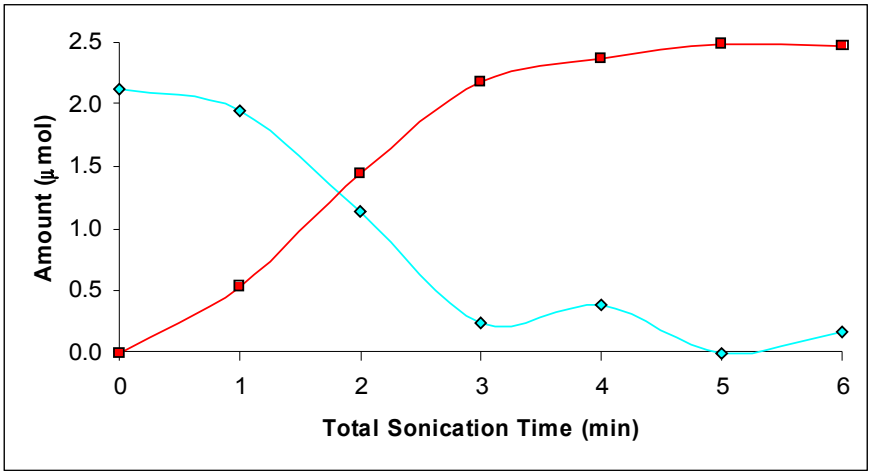


Figure 16: Amount of benzoic acid formed from benzonitrile in post-extraction reactions of samples sonicated for increasing lengths of time.

After centrifugation, samples were reacted with 5 mM benzonitrile for 2 hours with shaking (200 rev./min) at 30 °C. Reduction of benzonitrile substrate (◇) and formation of benzoic acid product (■) was monitored by HPLC. All benzonitrile was converted to product at a total sonication time of 5 minutes.

Micrographs (Figure 17) were taken to observe the breaking of cells, and qualitative HPLC data were used to determine whether optimal activity release coincided with optimal protein release.

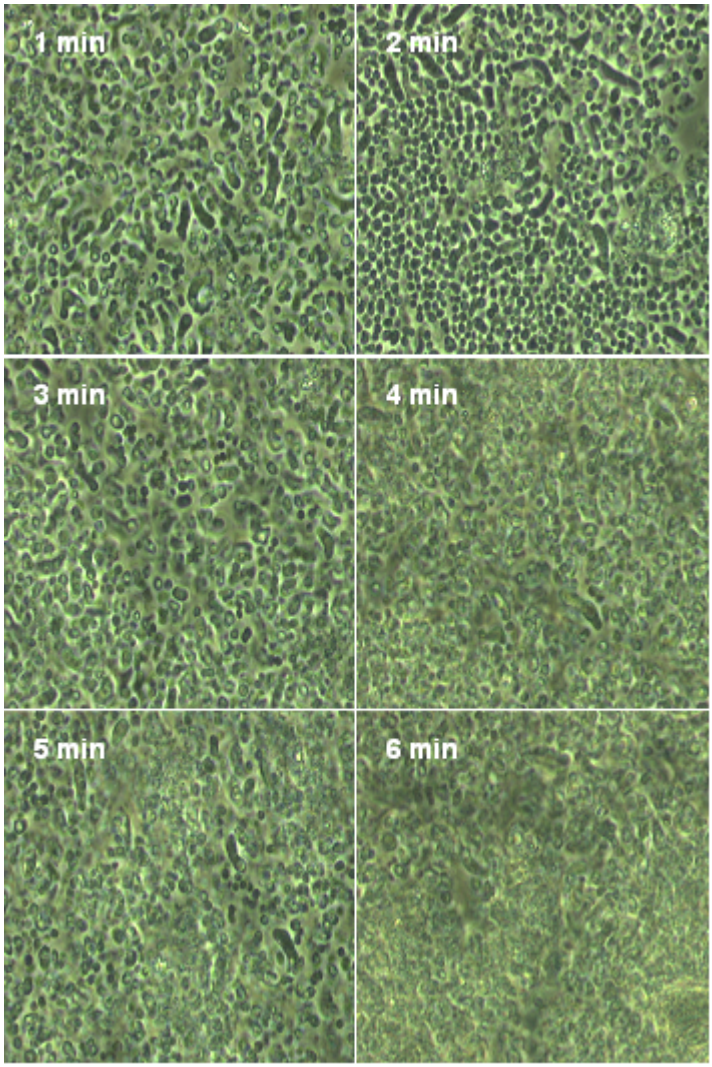


Figure 17: Micrographs of *Rhodococcus rhodochrous* sonicated for increasing time periods.

The labelled time periods on each micrograph indicate total sonication times for each sample. Cell disruption is noticeable as the sonication time is increased and distinct cell morphology is lost. The micrographs were taken of samples with the same dilution.

3.2 Towards Establishing an Activity Assay for Nitrilase and/or Nitrile Hydratase

3.2.1 Colorimetric Method

Both 0.1 and 0.01 M potassium phosphate buffer, pH 7.2, could be used to note colour change when using 2 mM benzonitrile and chlorobenzonitrile. BTB at 0.05% (v/v) was concentrated enough to indicate a colour change but at 0.01% (v/v) was more sensitive since the colour change was more noticeable. Active commercial enzymes had to be concentrated (at least 1 mg/ml in solution or a minimum of 10 mg purified enzyme) in order to note colour change. A more concentrated sample resulted in a more intense colour change to yellow. This assay was not sensitive enough to detect small concentrations of, or perhaps less active forms of enzyme. A colour change was noted when Nit-1005 was tested in agar plate wells and cuvettes, but activity could not be detected using the overlay method.

3.2.2 Fluorescence-based OPA Assay and Comparison to HPLC Method

After unsuccessful attempts at establishing colorimetric activity assays for the enzymes of interest based on electrophoretic separation of the enzymes and changes in pH on reaction, a more sensitive fluorimetric assay was tested. The assay was originally developed by Banerjee *et al*. (2003) [82], but some modifications were made after positive results were found to be unattainable when using their protocol on this material. While they could achieve linear standard ammonia fluorescence up to concentrations of 1000 μM, this study indicated fluorescence intensity was only linear up to 100 μM (Appendix 5.1, Figure 56). Troubleshooting included changing the buffers used in the assay (neither use of Tris buffer nor sodium phosphate buffer improved results) and incubating the development step at a lower temperature to avoid possible denaturation of enzyme.

When commercial nitrilases Nit 1001, 1005 and 1006 were tested against benzonitrile and phenylpropionitrile, no positive results were observed. All substrates tested against whole

cells of *Rhodococcus rhodochrous* yielded fluorescence intensity values of zero and hence no measurable activity was detected.

A modification of the OPA method was used to "spot" ammonia-forming activity on polyacrylamide gels, but did not prove useful (results not shown). Non-denaturing gels of commercial nitrilase enzymes incubated with OPA reagent did not show any fluorescent bands when viewed under UV light, although acid-forming activity was previously noted for these enzymes [106].

Since qualitative HPLC data were previously used to test the substrate selectivity of commercial nitrilases and whole cell *Rhodococcus rhodochrous*, HPLC reactions were performed using the same volumes and incubation times as used in the OPA assay, but this time assayed by HPLC to test whether the assays differed in sensitivity. The result was that the conversion of substrates could be accurately quantitatively measured by HPLC, while results obtained with the fluorimetric method proved to be unreliable or unreproducible.

3.2.3 High Performance Liquid Chromatography

HPLC is the most common method for measuring nitrile-hydrolysing activity, and is specifically preferred when measuring the enantiomeric excess of enantiomeric products formed from nitriles [6, 110-112]. HPLC was previously used by Brady *et al*. (2004) and was found to be an appropriate method for identifying nitrilase activity in whole cell bacterial samples [106]. Given the unsuccessful attempts at the previous methods of measuring activity, HPLC was explored as a more accurate means of assaying nitrilase activity in *Rhodococcus rhodochrous*. Commercial purified nitrilases from *Pseudomonas fluorescens*, *Rhodococcus rhodochrous* and *Arabidopsis thaliana* and purified nitrilases NIT-1001, -1005 and -1006 were tested by HPLC using the substrates benzamide, benzoic acid and benzonitrile, and their relative activities compared.

Table 4 shows the relative activities of commercial purified nitrilases against benzonitrile measured by HPLC. Reactions containing only buffer and substrate were used as controls. None of the commercial nitrilases tested used benzamide as a substrate, confirming no amidase activity was present. Benzoic acid was not converted indicating the reverse reaction was not possible with the enzymes tested. Nit-1005 converted 100% of

benzonitrile to benzoic acid while only residual activity was noted when using Nit-1001 and the nitrilase from *A. thaliana*. The *P. fluorescens* nitrilase was not active against benzonitrile.

Table 4: Relative activities of various commercial nitrilase enzymes and *Rhodococcus rhodochrous* whole cells reacted with benzonitrile

Enzyme	Relative Activity against Benzonitrile
NIT-1001 (BioCatalytics)	+/-
NIT-1005 (BioCatalytics)	+++
NIT-1006 (BioCatalytics)	+
Rhodococcus rhodochrous (Fluka)	+
Pseudomonas fluorescens (Fluka)	-
Arabidopsis thaliana (Fluka)	+/-
Rhodococcus rhodochrous ATCC BAA-870 whole cells	+++

Each nitrilase (750 µl of a 1 mg/ml stock) was added to 675 µl of a 50 mM phosphate buffer, pH 7.4, and 5 mM benzonitrile to a final reaction volume of 1.5 ml. Triplicate reactions were incubated at 30 °C for 2 hours with shaking (200 rev./min), and centrifuged at 3 000 x *g* for 5 min. A 200 µl aliquot of each was filtered through a 0.22 µm filter and transferred into a 2 ml HPLC vial containing 800 µl acidic stop eluent. Samples were analysed by HPLC. Relative activity is defined by +++: all substrate converted, +: some substrate converted, +/-: very little conversion, and -: no conversion.

HPLC was successfully used to measure the nitrile-hydrolysing activity of various enzyme sources, whether whole cell suspensions of *Rhodococcus rhodochrous* or purified enzymes were used. The development of the assay used for HPLC analysis was further investigated.

3.3 HPLC Assay Method Development

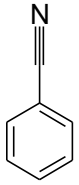
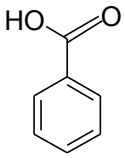
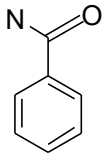
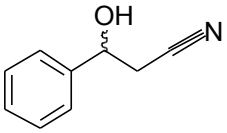
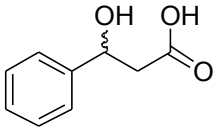
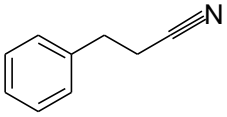
Since *Rhodococcus rhodochrous* favoured benzonitrile as a substrate, the aromatic nitrile and its corresponding amide and acid were used as controls in all further HPLC analyses. The β-hydroxy nitrile, 3-hydroxy-3-phenylpropionitrile and its corresponding acid, 3-hydroxy-3-phenylpropionic acid, were also used since the activity against this nitrile was of particular interest. Hydrocinnamonitrile was chosen as a useful measure of substrate-specificity comparison since the substrate has the same aliphatic chain length as 3-hydroxy-3-phenylpropionitrile, but lacks the hydroxyl group at the beta position.

The corresponding acid elutes earlier than the nitrile, while the amide has the shortest elution time (Table 5).

Hydrocinnamonitrile has at least a 1.65 minute longer elution time than 3-hydroxy-3-phenylpropionitrile, attributed to a structural difference of a single hydroxy group. The β-phenyl-substituted rings have much lower absorbance maximum values than the α-phenyl structures. All compounds, however, could be measured reproducibly. Average retention times for the compounds were reproducible with negligible deviation between samples.

The absorbance wavelength maxima of benzonitrile, benzamide, benzoic acid, hydrocinnamonitrile and 3-hydroxy-3-phenylpropionitrile were suitably different and therefore easily differentiated. However, 3-hydroxy-3-phenylpropionic acid and 3-hydroxy-3-phenylpropionitrile shared the same absorbance maximum. Their retention times, however, were different, and the acid predictably eluted before the nitrile. The corresponding amide product produced from 3-hydroxy-3-phenylpropionitrile by the organism in the current study has an average retention time of 3.5 ± 0.01 min (27 samples).

Table 5: Name, structure and retention time of compounds used in this study.

Compound	Structure	Absorbance wavelength (nm)	Average retention time (min) ± S.D.	Average amount in each 1.5 ml reaction (µ mol) ± S.D.
Benzonitrile		224.1	5.55 ± 0.02 (30 samples)	8 ± 0.3 (30 reactions)
Benzoic acid		228.8	4.37 ± 0.01 (30 samples)	6 ± 0.2 (30 reactions)
Benzamide		226.4	3.81 ± 0.01 (30 samples)	5.7 ± 0.1 (30 reactions)
3-Hydroxy-3-phenylpropionitrile		206.5	4.15 ± 0.004 (30 samples)	10.8 ± 0.3 (30 reactions)
3-Hydroxy-3-phenylpropionic acid		206.5	3.78 ± 0.004 (30 samples)	8.2 ± 0.2 (30 reactions)
Hydrocinnamonitrile		205.3	5.80 ± 0.01 (30 samples)	9.2 ± 0.1 (30 reactions)

Compounds were prepared as 5 mM samples in methanol and 100 µl added to 900 µl acidic eluent in 2 ml HPLC vials. A Waters 2690 Separations Module HPLC with 996 Photodiode Array Detector was used to analyse the samples. Compounds were eluted isocratically over 10 minutes from a Chromolith SpeedRod column at a flow rate of 0.5 ml/min using 40% acetonitrile:60% aqueous 0.1% (v/v) trifluoracetic acid.

3.3.1 Standard Curves

The correlation between the average integrated area of retention peaks of the standards used with increasing concentration was tested by HPLC by preparing standards of different concentrations (in the range 0 to 10 mM). The colours representing each standard were kept constant throughout the study and are outlined in Table 6. The linearity of retention area, amount and absorbance of each compound with increasing concentration was tested to ensure the concentrations used fell within an acceptable range, and also to establish the most appropriate parameters for measuring nitrile-converting activity.

Table 6: Linear regression equations and R^2 values for standard curves of the average integrated areas of increasing concentrations of various standard compounds.

Compound	Colour in Figures	Linear Regression Equation	R^2 Value	Linear Regression Equation with zero intercept	R^2 Value
Benzonitrile	Light blue	$y = 3 \times 10^6x - 905961$	0.9978	$y = 3 \times 10^6x$	0.9958
Benzoic acid	Red	$y = 2 \times 10^6x - 5798$	0.9998	$y = 2 \times 10^6x$	0.9998
Benzamide	Dark blue	$y = 2 \times 10^6x - 52285$	0.9999	$y = 2 \times 10^6x$	0.9999
3-Hydroxy-3-phenylpropionitrile	Orange	$y = 2 \times 10^6x + 123253$	0.9998	$y = 2 \times 10^6x$	0.9997
3-Hydroxy-3-phenylpropionic acid	Pink	$y = 2 \times 10^6x - 245084$	0.9995	$y = 2 \times 10^6x$	0.9989
Hydro-cinnamonitrile	Green	$y = 2 \times 10^6x - 120389$	0.9997	$y = 2 \times 10^6x$	0.9996

Linear regression equations and corresponding R^2 values were obtained from triplicate analysis of the retention areas of each compound from 0 – 10 mM by HPLC.

The linear regression equations and R^2 values of standard curves with a zero intercept were compared to standard curves where the lines were not forced through zero and the R^2 values found to be similar. The only standard with a positive y-intercept is 3-hydroxy-3-phenylpropionitrile, and therefore also the only standard which may be overestimated when extrapolating its amount from retention time. However, the values at which the standard curves cut the y-axis were all smaller than the average standard deviations between integrated areas. The standard curves of average integrated area versus

concentration are plotted in Figure 18 with zero intercepts (see Table 6 for linear equations).

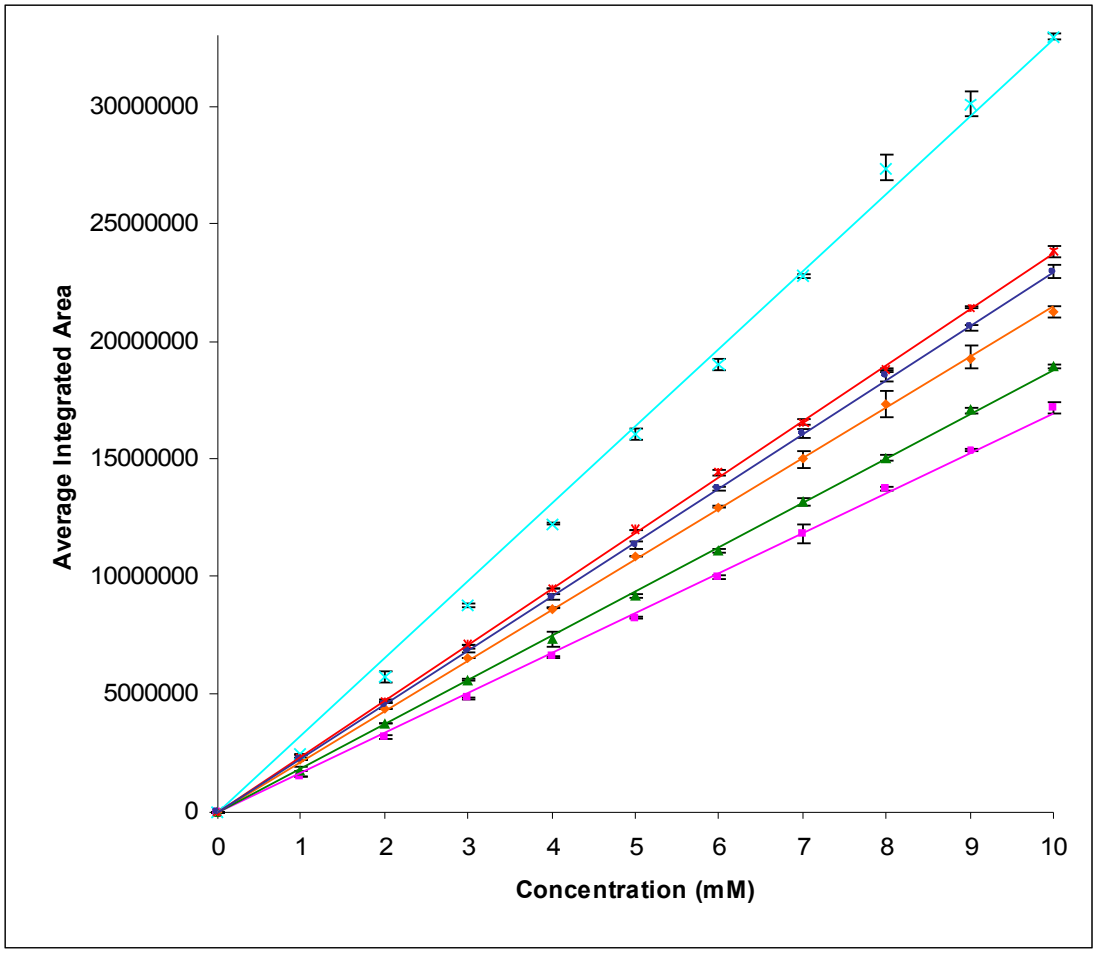


Figure 18: Average integrated area of benzonitrile, benzamide, benzoic acid, hydrocinnamonitrile, 3-hydroxy-3-phenylpropionitrile and 3-hydroxy-3-phenylpropionic acid with increasing concentration.

Standard curves for benzonitrile (■), benzamide (■), benzoic acid (■), hydrocinnamonitrile (■), 3-hydroxy-3-phenylpropionitrile (■) and 3-hydroxy-3-phenylpropionic acid (■) were constructed by measuring the integrated area of retention peaks of each substance by HPLC. Samples were analysed in triplicate and the average ± the standard deviation between samples plotted as a function of increasing concentration.

The average integrated area of each standard was plotted as a function of the amount (in µ mol) present in each 1.5 ml reaction to ensure there was good correlation between the retention area and amount of each compound. The linear regression equations obtained from the standard curves in Figure 18 were used to calculate the actual amount of standard

in each sample. The R^2 values are all close to one and show a strong correlation between retention peak integrated area and the amount or concentration used for each standard.

The absorbance of retention peaks of each standard was plotted as a function of increasing concentration and compared to the above standard curves (Figure 19). The R^2 values of linear regression equations fitted to the data points were similar for all plots, and measuring absorbance with increasing concentration by HPLC was also found to be reproducible (Table 7).

Table 7: Linear regression equations and R^2 values for standard curves of absorbance with increasing concentration for various compounds.

Compound	Colour in Figures	Linear Regression Equation	R^2 Value	Linear Regression Equation with zero intercept	R^2 Value
Benzonitrile	Light blue	y = 0.156x - 0.0338	0.9981	y = 0.1512x	0.9968
Benzoic acid	Red	y = 0.141x + 0.0047	0.9998	y = 0.1416x	0.9998
Benzamide	Dark blue	$y = 0.1379x - 3 \times 10^{-5}$	0.9999	y = 0.1379x	0.9999
3-Hydroxy-3-phenylpropionitrile	Orange	y = 0.1167x + 0.0128	0.9967	y = 0.1185x	0.9963
3-Hydroxy-3-phenylpropionic acid	Pink	y = 0.1021x - 0.0039	0.9999	y = 0.1015x	0.9999
Hydrocinnamonitrile	Green	y = 0.078x + 0.0003	0.9998	y = 0.0781x	0.9998

Linear regression equations and corresponding R^2 values were obtained from triplicate analysis of the retention areas of each compound from 0 – 10 mM by HPLC. Retention areas were converted to amounts using the concentration standard curve equations for each compound.

Linear concentration standard curves could be constructed as a function of retention area, amount or absorbance for all six compounds tested. 3-Hydroxy-3-phenylpropionitrile had greater standard deviation between the 10 mM absorbance readings than at lower concentrations (Figure 19). When plotted including the 10 mM point, however, the linear regression equation is y = 0.1185x with an R^2 value of 0.9963. Both R^2 values are, however, similar. Standard deviation values in most cases are too small to be noted in the figures.

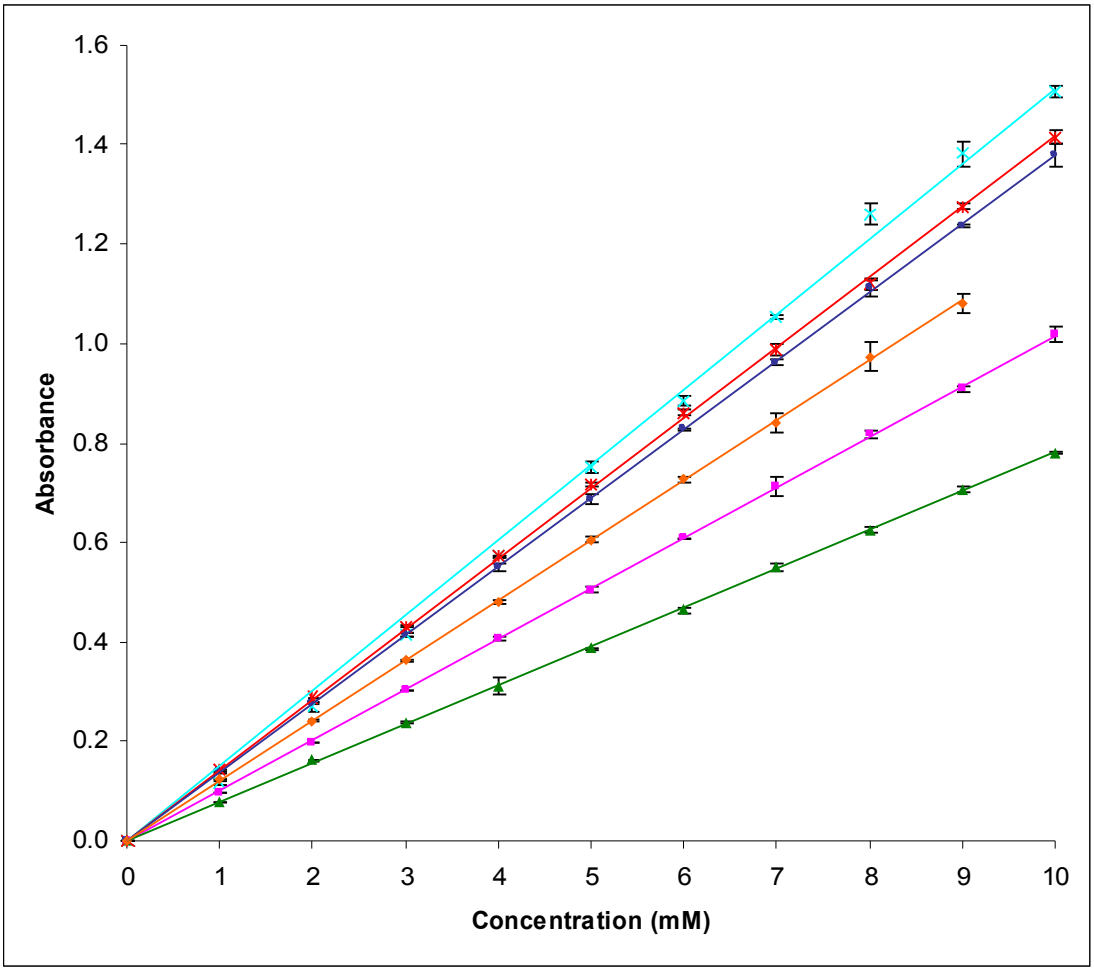


Figure 19: Average absorbance of benzonitrile, benzamide, benzoic acid, hydrocinnamonitrile, 3-hydroxy-3-phenylpropionitrile and 3-hydroxy-3-phenylpropionic acid with increasing concentration.

Standard curves for benzonitrile (■), benzamide (■), benzoic acid (■), hydrocinnamonitrile (■), 3-hydroxy-3-phenylpropionitrile (■) and 3-hydroxy-3-phenylpropionic acid (■) were constructed by measuring the average absorbance maximum of retention peaks of each substance by HPLC. Samples were analysed in triplicate and the average ± the standard deviation plotted as a function of increasing concentration. Absorbance values for hydrocinnamonitrile were extracted at 205.3 nm, and 3-hydroxy-3-phenylpropionitrile and 3-hydroxy-3-phenylpropionic acid absorbance values were extracted at 206.5 nm. Absorbance values for benzoic acid, benzamide and benzonitrile were obtained by data extraction at 228.8, 226.4 and 224.1 nm, respectively. Refer to Table 7 for compound identification.

The wavelength maxima at which each standard's data were extracted when processing HPLC data were monitored with increasing concentration to check that the compounds were stable at all the concentrations tested. Only the wavelength maximum of benzamide

was affected at higher concentrations, and it dropped from 226.4 nm to 225.2 nm when the concentration was 7 mM and higher (data not shown). The wavelength maxima of benzonitrile, benzoic acid, 3-hydroxy-3-phenylpropionitrile, 3-hydroxy-3-phenylpropionic acid and hydrocinnamonitrile remained constant at all concentrations tested.

3.3.2 LC-Mass Spectral Analysis of the Standards Used in This Study

HPLC could be used to reliably measure elution of benzonitrile, benzamide and benzoic acid. Although the elution of hydrocinnamonitrile, 3-hydroxy-3-phenylpropionitrile and 3-hydroxy-3-phenylpropionic acid could be reliably measured and displayed different elution times, the absorbance maxima of the three compounds were very similar. This was only a problem in the identification of the product formed from 3-hydroxy-3-phenylpropionitrile since only the corresponding acid was available as a standard for comparison. The acid and nitrile share the same absorbance maximum but differ in their HPLC elution times (with the nitrile eluting last). The initial product formed from 3-hydroxy-3-phenylpropionitrile by *Rhodococcus rhodochrous* ATCC BAA-870 was presumed to be the corresponding amide since previous studies showed that inhibiting the reaction at the amidase level still resulted in disappearance of substrate, while the appearance of 3-hydroxy-3-phenylpropionic acid was hindered. Also, the intermediate product formed from 3-hydroxy-3-phenylpropionitrile before the corresponding acid was formed had the earliest retention time compared to the nitrile and acid. However, mass spectral analysis was used to confirm the structure of the amide since analysis by HPLC of compounds with absorbance maxima close to 200 nm was not considered reliable since many HPLC solvents absorb at or near 200 nm.

Mass spectral results for standard benzamide (Appendix 5.4), 3-hydroxy-3-phenylpropionitrile and 3-hydroxy-3-phenylpropionic acid (Figure 20 and Figure 21) coincided with spectra from the internal Millenium spectra library, and with spectra from the Spectral Database for Organic Compounds SDBS (available at http://www.aist.go.jp/RIODB/SDBS/cgi-bin/direct_frame_top.cgi). Since 3-hydroxy-3-phenylpropionitrile was synthesized in-house, its structure was confirmed, and its corresponding acid tested. Reactions in which conversion against 3-hydroxy-3-phenylpropionitrile took place were also tested in order to identify the product formed. The molecular mass of benzoic acid (122 $g.mol^{-1}$) and benzamide (121 $g.mol^{-1}$) are similar, and

both compounds were too volatile to be measured with accuracy. Benzonitrile and benzoic acid gave poor mass spectral results that could not be improved by increasing the compound concentration. The gas phase volatility of these compounds and susceptibility to thermal degradation is too high for good mass spectral results. Benzamide was not as volatile as benzonitrile and benzoic acid since its mass spectrum could be improved and the compound matched with 98% certainty to the internal standard by increasing the concentration (Appendix 5.4). Hydrocinnamonitrile was also not suited to measurement by mass spectrometry. Again, mass spectra for the standard compound were poor and were not improved by increasing its concentration. Although hydrocinnamonitrile has a longer aliphatic nitrile group than benzonitrile, it did not necessarily impact on the stability of the compound.

The amide product formed from 3-hydroxy-3-phenylpropionitrile in bioconversion reactions could not be analysed using mass spectrometry. It is assumed the volatility and concentration of the compound may be factors in its measurement. However, 3-hydroxy-3-phenylpropionitrile and 3-hydroxy-3-phenylpropionic acid standards could be measured to reasonable degree of certainty using mass spectrometry (see Appendix 5.3, Figure 65 and Figure 66 for the mass spectrum peak break down). Reactions against 3-hydroxy-3-phenylpropionitrile are reported as a decrease in substrate or as total product formation owing to the relative inaccuracy of measuring the amide by HPLC. Gas chromatography may be a better alternative to mass spectrometry when attempting product identification and measuring smaller, more volatile nitriles. Although the retention times for 3-hydroxy-3-phenylpropionitrile and 3-hydroxy-3-phenylpropionic acid are similar (Figure 21), the acid elutes earlier than the nitrile.

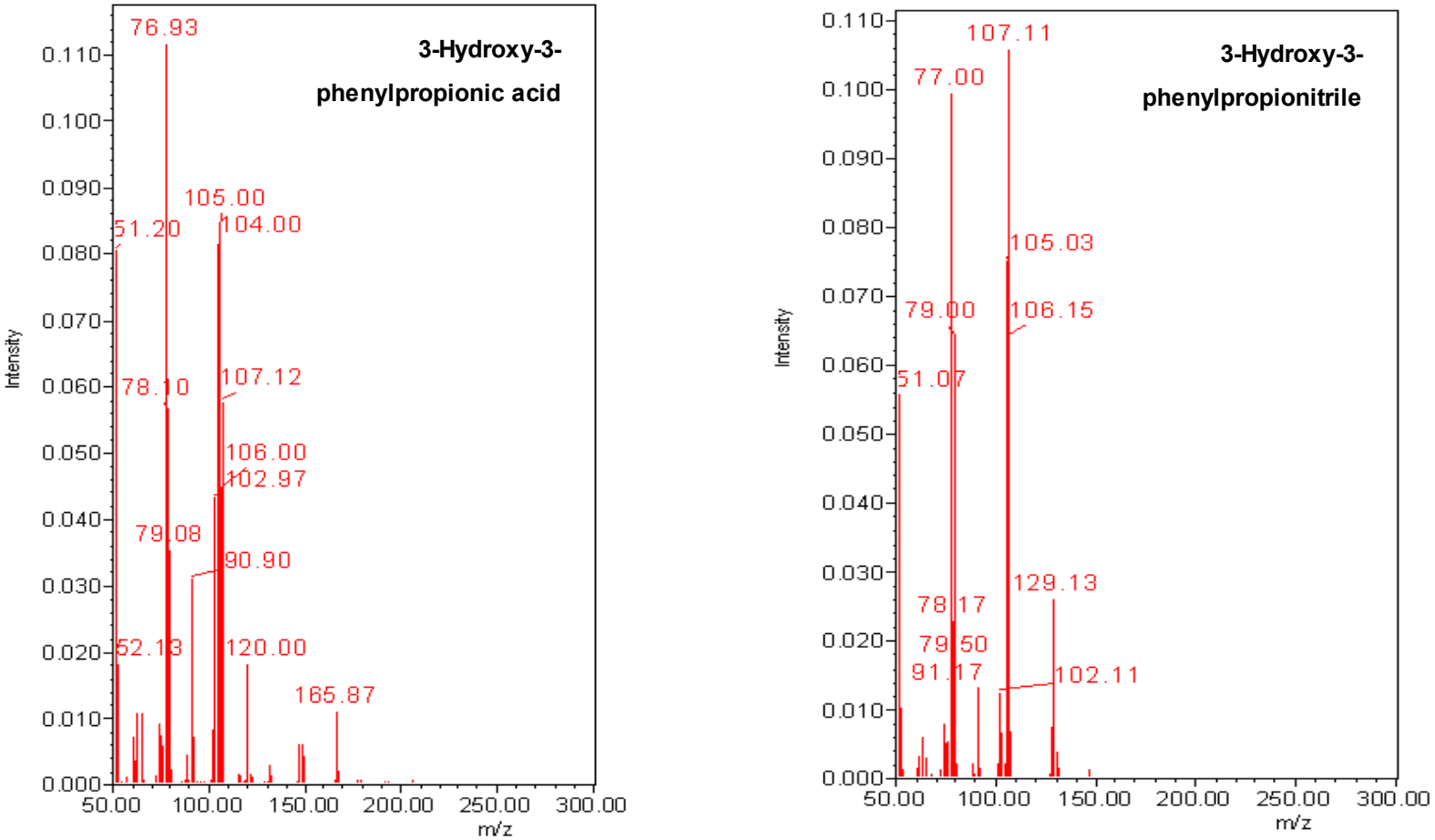


Figure 20: Mass spectra of 3-hydroxy-3-phenylpropionic acid and 3-hydroxy-3-phenylpropinitrile standards.

Mass spectral results were obtained using the Waters Integrity™ System with photodiode array detector and Thermabeam™ mass detector, using a flow rate of 0.5 ml/min, 20 µl injection volume and a 30 min run time. Initial elution was 0.2 ml/min 0.1% (v/v) formic acid for the first 15 min, followed by 2 min of a 0.3 ml/min 50% methanol:50% acetonitrile elution, 5 min of a 0.25 ml/min 0.1% (v/v) formic acid and lastly 8 min of 0.1% (v/v) formic acid at 0.2 ml/min.

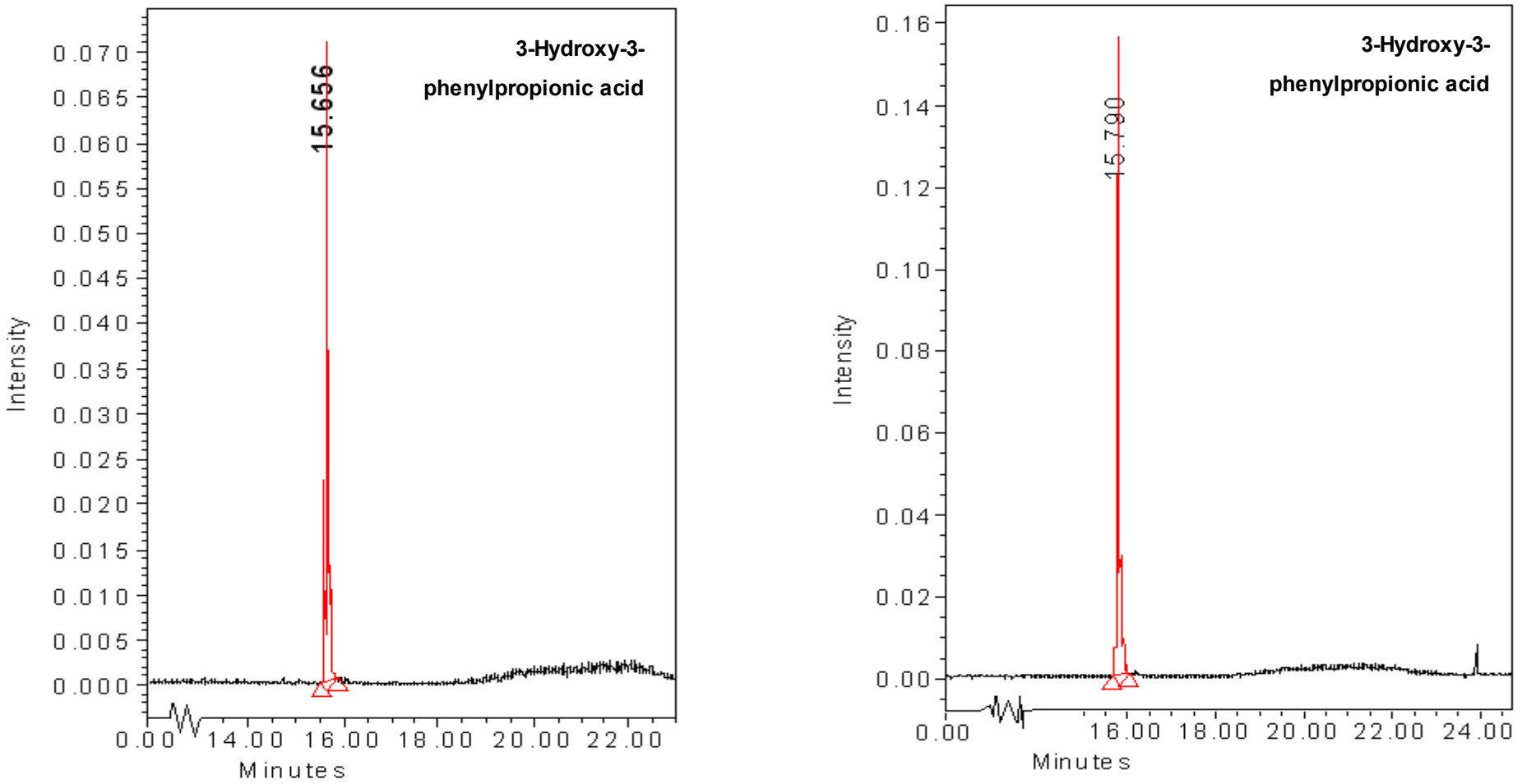


Figure 21: Chromatographs of 3-hydroxy-3-phenylpropionic acid and 3-hydroxy-3-phenylpropionitrile standards.

Chromatographs were obtained using the Waters Integrity™ System with photodiode array detector and Thermabeam™ mass detector, using a flow rate of 0.5 ml/min, 20 µl injection volume and a 30 min run time. Initial elution was 0.2 ml/min 0.1% (v/v) formic acid for the first 15 min, followed by 2 min of a 0.3 ml/min 50% methanol:50% acetonitrile elution, 5 min of a 0.25 ml/min 0.1% (v/v) formic acid and lastly 8 min of 0.1% (v/v) formic acid at 0.2 ml/min.

3.3.3 Different Buffer Types

The relative activity against benzonitrile contained in supernatant of *Rhodococcus rhodochrous* was tested in ten different buffer types (listed in Table 3). Polybuffer 74 was tested in the pH range 4 to 7.4 in order to test whether the activity against benzonitrile was affected by the buffer system used during chromatofocusing, and to test the efficacy of HPLC as an assaying method when using different buffers.

Figure 22 shows the average integrated area of benzonitrile remaining after reaction in each different buffer type and its conversion to benzoic acid. The effect of pH on activity against benzonitrile is shown by reaction in buffers 1 - 4, with the least product formation occurring at pH 4. The total amount of substrate and product was underestimated in buffer 7 (containing imidazole) whereas for all other buffers the total amount was relatively similar. Imidazole appears to greatly reduce the measurable amounts of benzonitrile and benzoic acid.

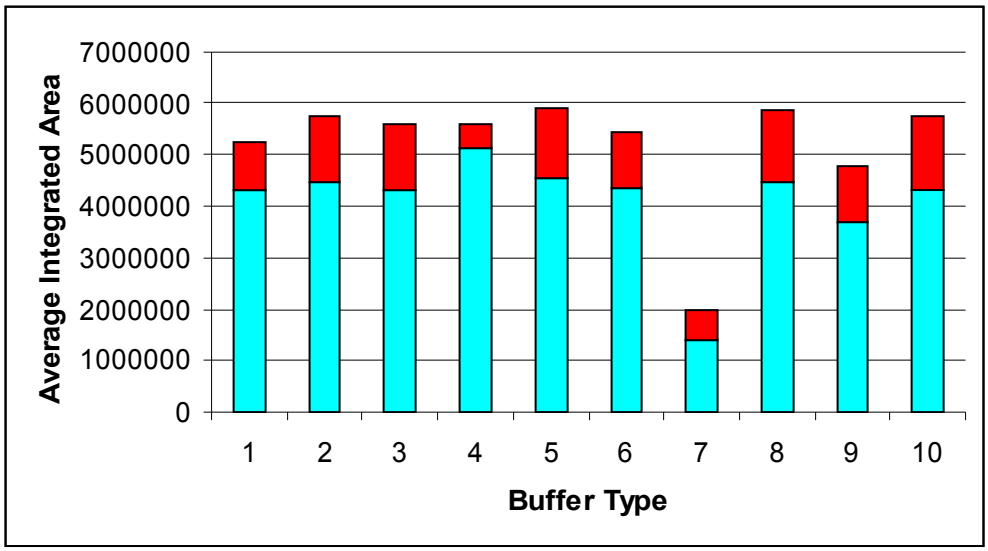


Figure 22: Benzonitrile conversion to benzoic acid in ten different buffer systems.

Rhodococcus rhodochrous supernatant was reacted with 50 mM benzonitrile (□) for 2 hrs at 30 °C with shaking (200 rev./min). Conversion of benzonitrile to benzoic acid (■) was measured in triplicate by HPLC.

The least conversion of benzonitrile to benzoic acid occurs in buffer 4 (Polybuffer 74 containing 5 mM DTT, pH 4). Although most of the benzonitrile present in samples reacted with buffer 7 has disappeared, the amount of product (benzoic acid) formed is not

necessarily more than in other buffer types. Buffer 7, containing imidazole, is therefore a problematic buffer when analysing reactions by HPLC, as it underestimates the signal produced by benzonitrile and benzoic acid. The buffer in which most benzoic acid has been produced is buffer 10 (50 mM KH_2PO_4 containing 10 mM DTT and 10 mM EDTA, pH 7.4). The addition of 10 mM EDTA has increased the amount of benzoic acid formed compared to buffer 6 where neither DTT, nor EDTA, was present. The addition of 10 mM DTT to 50 mM KH_2PO_4 on its own does not increase the amount of benzoic acid formed more than the addition of 10 mM EDTA only to the standard buffer. Slightly more benzoic acid is formed from benzonitrile in 100 mM phosphate buffer than in 50 mM phosphate buffer. Addition of EDTA to buffers 8 and 10 appears to enhance benzoic acid formation compared to DTT alone in buffer 9.

The conversion of 3-hydroxy-3-phenylpropionitrile in each buffer type was also tested. Buffer controls containing no substrate were run in conjunction with the samples tested (data not shown). The imidazole in the 25 mM imidazole buffer, pH 7.4, was shown to have the same wavelength maximum as 3-hydroxy-3-phenylpropionitrile, and therefore the amount of product in buffer 7 is over estimated (Figure 23). Buffer 7 is therefore problematic when analysing 3-hydroxy-3-phenylpropionitrile conversion by HPLC.

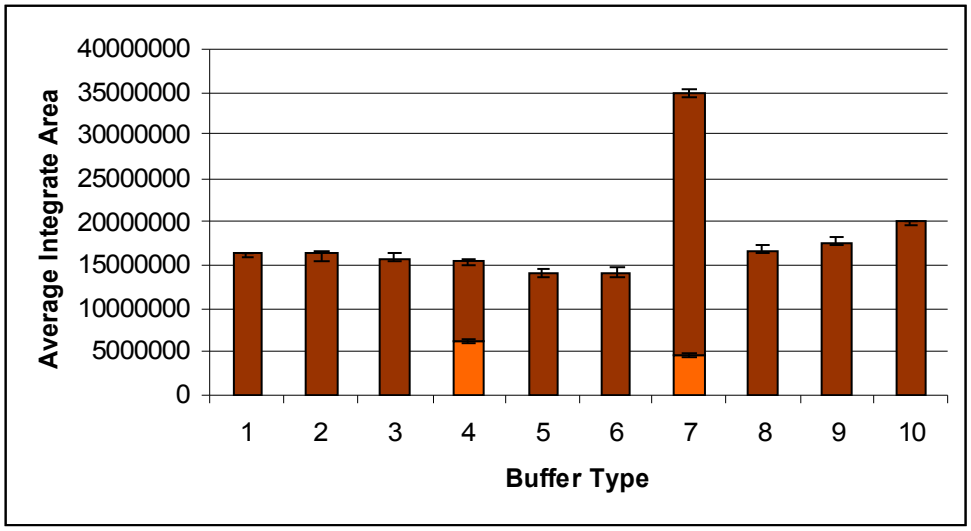


Figure 23: Relative conversion of 3-hydroxy-3-phenylpropionitrile to product in ten different buffer types.

Rhodococcus rhodochrous supernatant was reacted with 20 mM 3-hydroxy-3-phenylpropionitrile (▮) for 2 hrs at 30 °C with shaking (200 rev./min). The amount of substrate remaining and product produced (▮) was measured in triplicate by HPLC.

In buffer 4, conversion of 3-hydroxy-3-phenylpropionitrile was incomplete (Figure 23). Activity of the 3-hydroxy-3-phenylpropionitrile-converting enzyme is therefore reduced at pH 4.

Since it was previously established that *Rhodococcus rhodochrous* supernatant displayed no activity against hydrocinnamonitrile, the substrate was tested using the different buffer types to check for anomalous results arising from different buffers when measured by HPLC (Figure 24). The amount of hydrocinnamonitrile remains approximately constant in most buffer types and was only seen to drop in buffer four (Polybuffer 74 containing 5 mM DTT, pH 4) and buffer nine (50 mM KH_2PO_4 containing 10 mM DTT, pH 7.4). However, although it appears that hydrocinnamonitrile has been utilised, no product was detected in these HPLC reactions. Control reactions containing only hydrocinnamonitrile and buffer did not show disappearance of the nitrile (data not shown), and therefore it is unlikely the compound was heat-degraded during the reaction. Although the amount of hydrocinnamonitrile dropped in buffer four, the total amount of substrate and apparent product remained constant in all buffers.

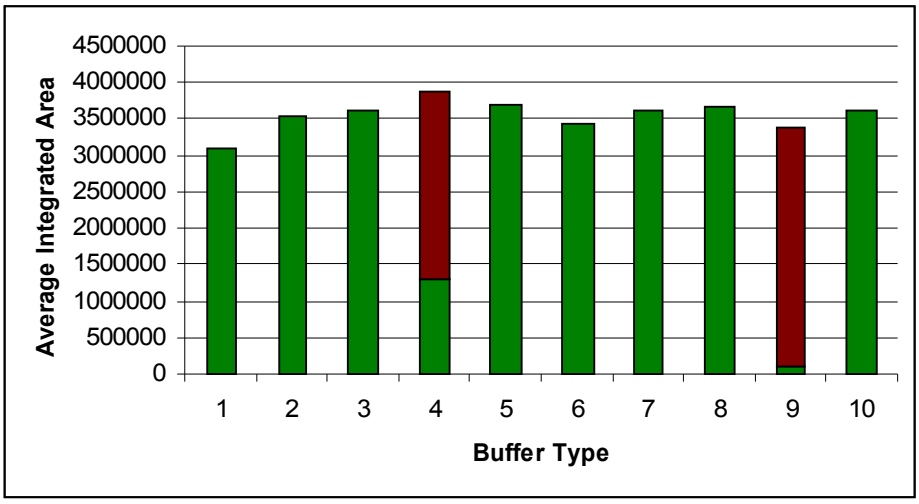


Figure 24: Relative levels of hydrocinnamonitrile measured in ten different buffer types by HPLC.

Rhodococcus rhodochrous supernatant was reacted with 20 mM hydrocinnamonitrile (▮) for 2 hrs at 30 °C with shaking (200 rev./min). The amount of substrate remaining and apparent product produced (▮) was measured in triplicate by HPLC.

Although buffers eight and ten contain 10 mM DTT, both also contain 10 mM EDTA which may have an inhibitory effect on activity against hydrocinnamonitrile. Polybuffer

exhibits almost negligible absorbance at 280 nm (A_{280} approximately 0.2) but is detected at 254 nm. HPLC data is extracted at 254 nm and therefore amounts of substrate or product present in reactions may be overestimated. The amount of 3-hydroxy-3-phenylpropionitrile only is over estimated in buffer 7. Conversely, the amount of benzonitrile is less in buffer 7 than any other buffer type tested. Buffers one, two, three, five and six appear to have similar effects on activity.

Results obtained from measuring activity by HPLC were therefore affected by the type of buffer used, as well as the compound being tested. Imidazole buffer is not suitable for analysis of nitrile conversion by HPLC.

3.3.4 pH Activity Profiles

The effect of pH on activity against benzonitrile was tested using Universal buffer at different pH's (Figure 25). The effect of pH on activity against benzonitrile in Polybuffer 74 can be seen in Figure 22. Benzoic acid formation from benzonitrile is highest at pH 6 (0.85 µmol) and pH 7 (0.87 µmol), and is present at all pH's except pH 4. Only trace amounts are formed at pH 5 (0.02 µmol) and pH 10 (0.08 µmol).

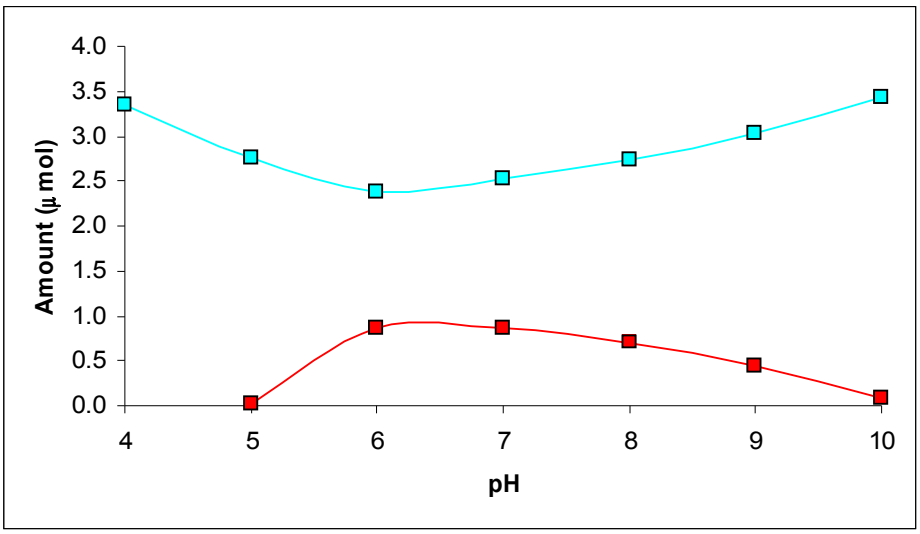


Figure 25: Amount of benzoic acid formed from benzonitrile at different pH's.

Benzonitrile (■) was reacted for 2 hrs at 30 °C with shaking (200 rev./min) in Universal buffer made up at different pH values and its conversion to benzoic acid (■) measured by HPLC.

3.3.5 Time Course Activity Study

The depletion of benzonitrile was monitored over 3 hrs and the amount of product formed measured (Figure 26). Benzamide was formed from benzonitrile within 60 minutes of reaction, with its amount peaking within 10 – 20 minutes. Concurrently, benzoic acid was formed from the benzamide produced and its amount steadily increased until reaching a plateau from approximately 120 minutes. The amount of benzonitrile in reaction rapidly drops within the first ten minutes, but after 90 minutes the amount utilised over time becomes negligible. Once approximately 1 μmol of benzonitrile remains in the reaction, it appears to no longer be converted and instead remains at a basal level (Figure 26).

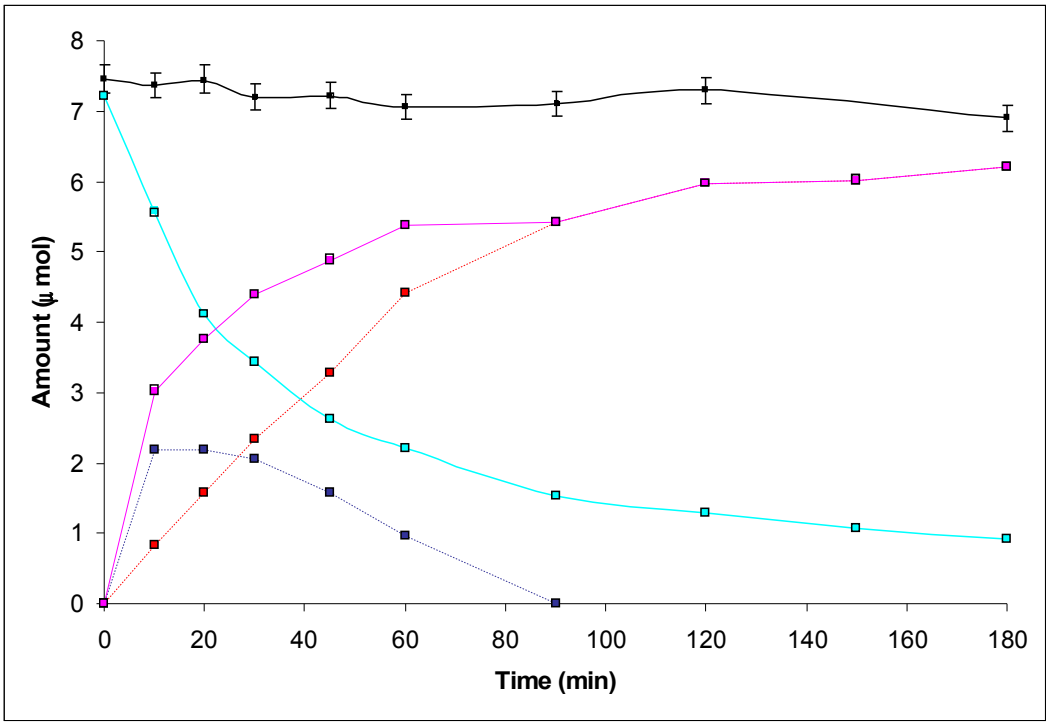


Figure 26: Conversion of 5 mM benzonitrile to benzamide and benzoic acid over three hours.

Benzonitrile (■) was added to reaction mix containing *Rhodococcus rhodochrous* supernatant (at 30 °C with stirring). Aliquots of the sample were withdrawn at given time points in triplicate and added to stop buffer. The average integrated area of substrate remaining and benzamide (■) and benzoic acid (■) produced was measured by HPLC, and converted to amount. The additive amount of benzamide and benzoic acid was plotted on the same axes (■). Benzonitrile was added to control reactions in which no enzyme was present (■) thereby demonstrating the stability of the substrate under these reaction conditions.

It can be seen that the amount of benzonitrile remaining in the reaction is not linear over the time span tested (Figure 26). The amount of benzamide formed from benzonitrile rapidly peaks after 10 minutes of reaction and plateaus between 10 and 30 minutes, but decreases as it is further converted to benzoic acid. The benzamide formed from benzonitrile is utilised within 60 minutes, since after 90 minutes benzamide is no longer detected in the reaction mix.

Benzoic acid is immediately produced from benzamide when benzamide is formed from benzonitrile. Benzoic acid continues to be formed over the full 3 hours of reaction, but the amount produced plateaus after 90 minutes when the substrate is depleted (Figure 26).

Activity against benzamide and its dependence on time was tested, and compared to reactions in which benzamide was first produced from benzonitrile. The average control amount of benzamide present in reactions where no enzyme was present was 5.4 µmol, with a standard deviation of 0.34 µmol (Figure 27).

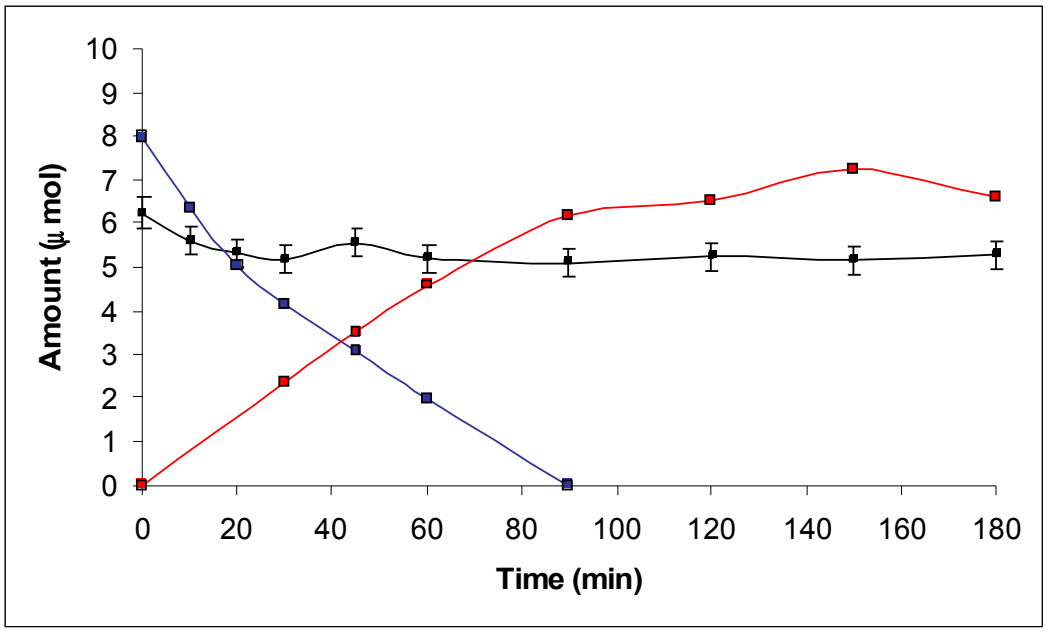


Figure 27: Conversion of 5 mM benzamide over three hours.

Benzamide was added to reaction mix containing *Rhodococcus rhodochrous* supernatant (at 30 °C with stirring). Aliquots of the sample were withdrawn at given time points in triplicate and added to stop buffer. The average integrated area of benzamide remaining (■) and benzoic acid produced (■) was measured by HPLC, and converted to amount. Benzamide was added to control reactions in which no enzyme was present (■) and measured in the same way.

After 60 minutes of reaction, there is no benzamide left in the reaction. Benzoic acid can be measured from 30 minutes onwards and its amount increases with time until it levels off after approximately 120 minutes. The formation of benzoic acid from benzamide is linear up to 90 minutes (Figure 28).

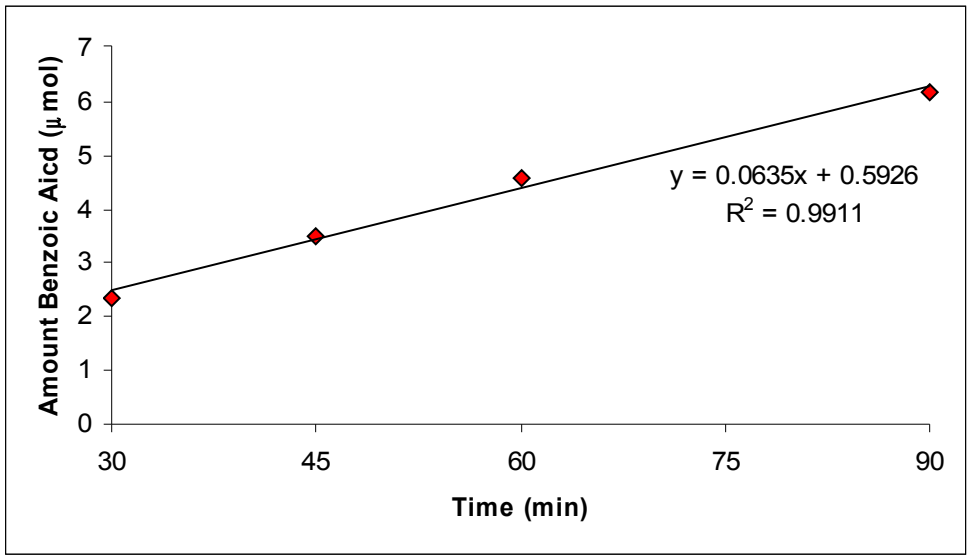


Figure 28: Formation of benzoic acid from benzamide over time.

Benzamide was added to reaction mix containing *Rhodococcus rhodochrous* supernatant (at 30 °C with stirring). Aliquots of the sample were withdrawn at given time points in triplicate and added to stop buffer. The average integrated area of benzamide remaining and benzoic acid produced (■) was measured by HPLC, and converted to amount.

The formation of product produced from 3-hydroxy-3-phenylpropionitrile over time is shown in Figure 29. After reaction times longer than 45 minutes, 3-hydroxy-3-phenylpropionitrile is no longer present in the reaction mix. Product appears within ten minutes and increases over time until 60 minutes where its amount is seen to level off. The amount of product remains more or less constant between 60 and 180 minutes.

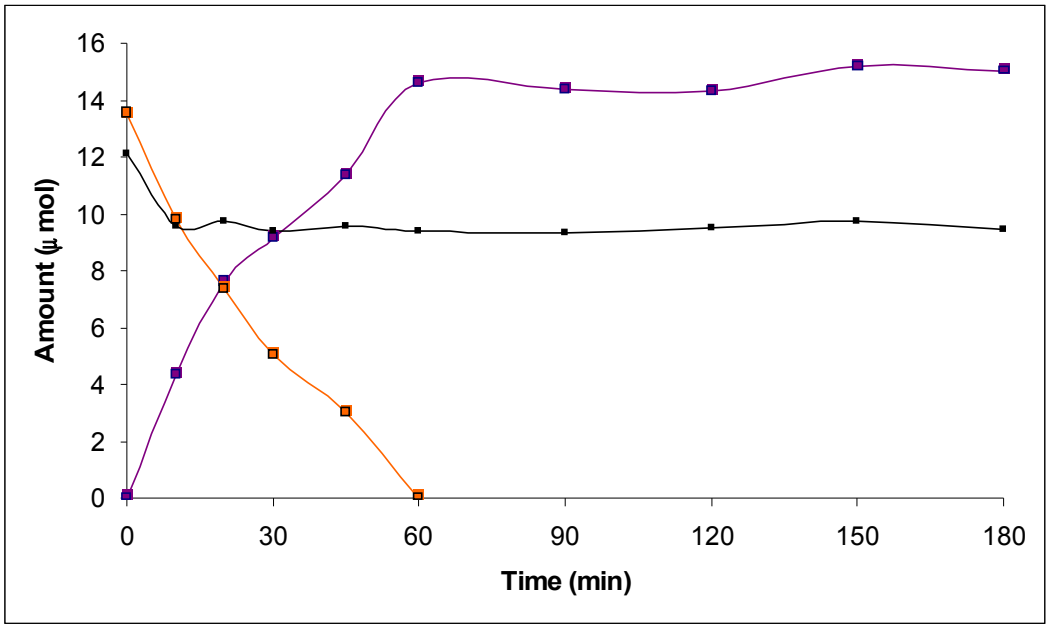


Figure 29: Conversion of 5 mM 3-hydroxy-3-phenylpropionitrile over three hours.

3-Hydroxy-3-phenylpropionitrile was added to reaction mix containing *Rhodococcus rhodochrous* supernatant (at 30 °C with stirring). Aliquots of the sample were withdrawn at given time points in triplicate and added to stop buffer. The average integrated area of 3-hydroxy-3-phenylpropionitrile remaining (■) and product formed (■) was measured by HPLC, and converted to amount. 3-Hydroxy-3-phenylpropionitrile was added to control reactions in which no enzyme was present (■) and measured in the same way.

The time scale of reaction against the substrates tested was reduced since it was evident that the production of amide from nitrile occurs in a much shorter time frame than expected. Indeed, in reactions occurring for 2 hours it would be assumed that benzoic acid is produced directly from benzonitrile since benzamide would not be noted. Benzonitrile conversion was tested over ten minutes and 3-hydroxy-3-phenylpropionitrile conversion over twenty minutes. The disappearance of 3-hydroxy-3-phenylpropionitrile as substrate, and appearance of its product, can be followed linearly over twenty minutes (Figure 30). The linear regression R^2 value is better for 3-hydroxy-3-phenylpropionitrile disappearance than for the appearance of product (R^2 = 0.99 as opposed to 0.94). When benzamide was reacted over 10 minutes, the appearance of benzoic acid could not be measured linearly by HPLC (data not shown), although disappearance of product was linear.

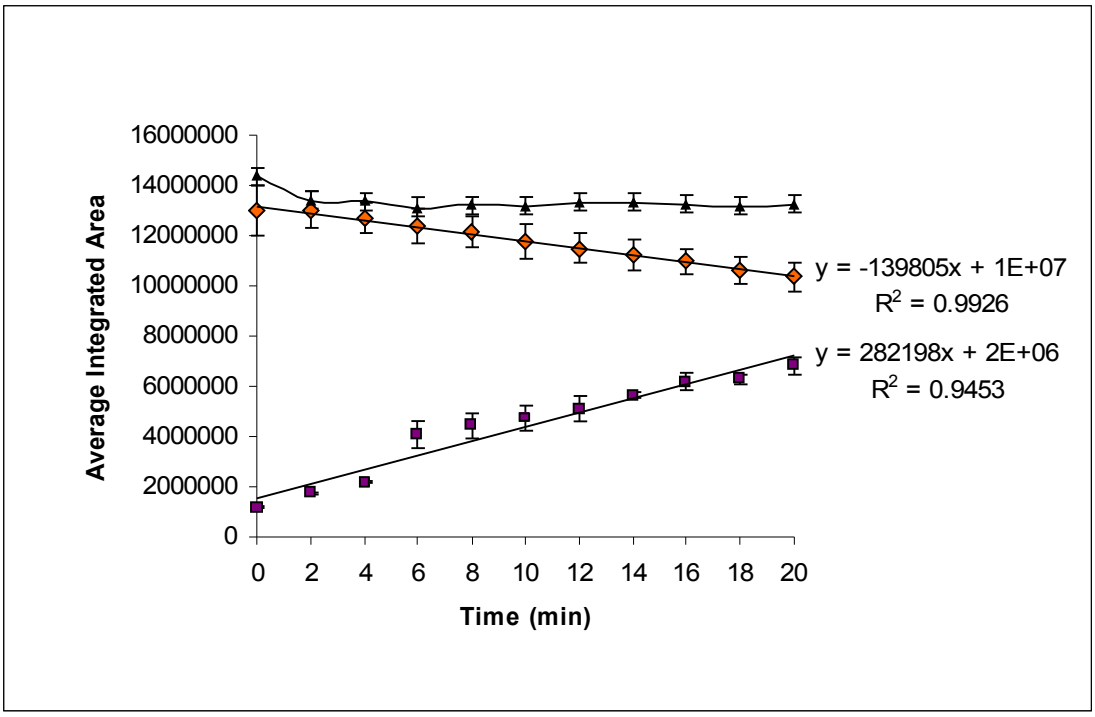


Figure 30: Conversion of 5 mM 3-hydroxy-3-phenylpropionitrile over a twenty minute reaction.

3-Hydroxy-3-phenylpropionitrile was added to reaction mix containing *Rhodococcus rhodochrous* supernatant (at 30 °C with stirring). Aliquots of the sample were withdrawn at given time points in triplicate and added to stop buffer. The average integrated area of 3-hydroxy-3-phenylpropionitrile remaining (■) and product formed (■) was measured by HPLC. 3-Hydroxy-3-phenylpropionitrile was added to control reactions in which no enzyme was present (■) and measured in the same way.

The average integrated area of benzonitrile reacted over ten minutes is also followed linearly. Time zero is an unreliable point assumed to arise from poor mixing technique and is omitted (Figure 31). The appearance of benzamide as product from benzonitrile can not be accurately measured within a ten minute reaction by HPLC, although the disappearance of substrate is already occurring. Benzamide appearance can only be measured after 10 minutes once the concentration of product is presumably within the instruments detection limitation range. The initial reaction rate of benzamide production can therefore not be calculated within the first few minutes of reaction.

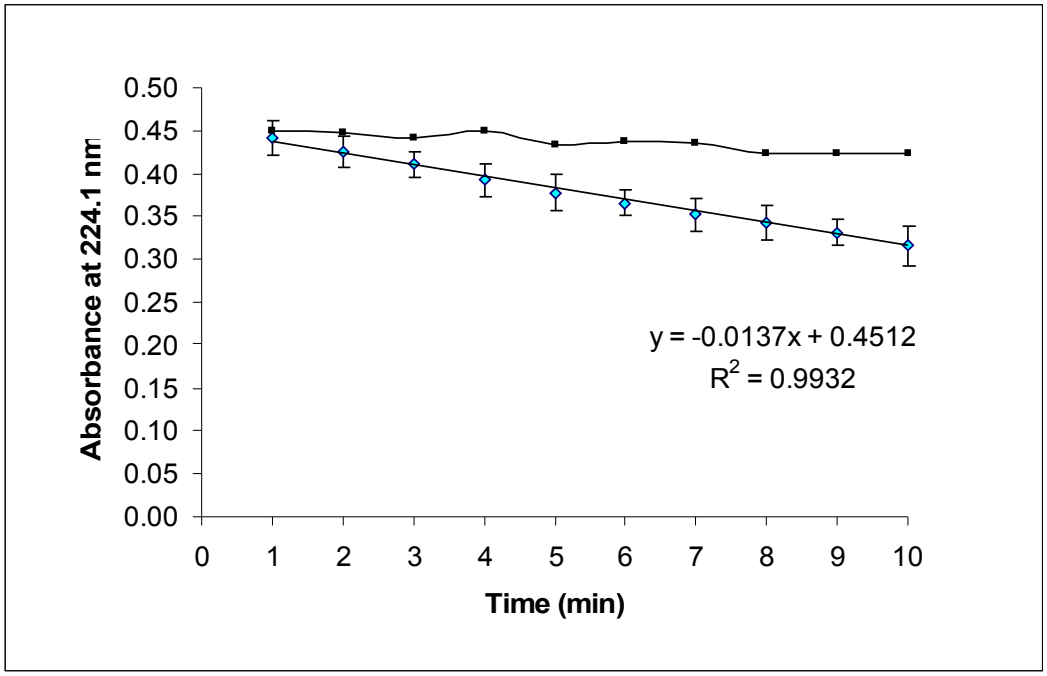


Figure 31: Conversion of 5 mM benzonitrile over a ten minute time reaction, excluding time zero.

Benzonitrile (□) was added to reaction mix containing *Rhodococcus rhodochrous* supernatant (at 30 °C with stirring). Aliquots of the sample were withdrawn at given time points in triplicate and added to stop buffer. The average absorbance of benzonitrile remaining (□) was measured by HPLC. Benzonitrile was added to control reactions in which no enzyme was present (■).

3.3.6 Protein Concentration Effects

Optimisation of the HPLC method for measuring activity has enabled quicker analysis times (10 minutes for benzonitrile and 20 minutes for 3-hydroxy-3-phenylpropionitrile and benzamide) in the linear activity regions for these enzymes. Also, activity may be traced as a change in absorbance of nitrile, or as a decrease in nitrile concentration, with an excellent degree of accuracy. Measuring activity as a function of appearance of substrate has been shown to be less reliable, especially if a certain concentration of product is required before it is detected by HPLC. The effect of enzyme concentration on activity against benzonitrile and benzamide was studied by HPLC. Reactions were linear with respect to time for both substrates up to 1.93 mg total protein per reaction (1.5 ml total volume). Benzonitrile depletion with increasing total protein concentration is shown in Figure 32.

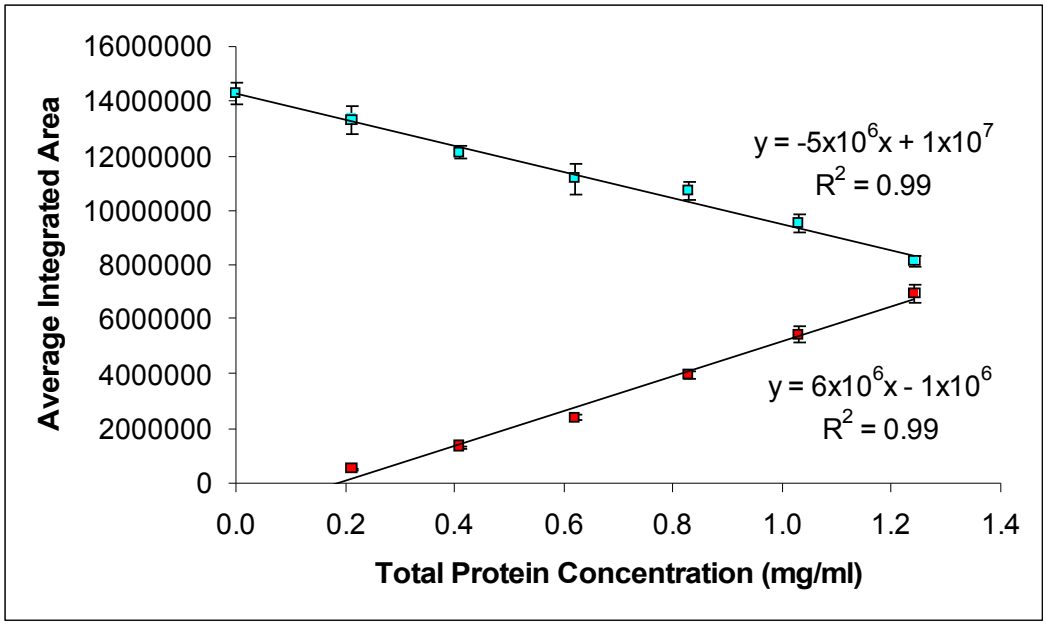


Figure 32: Formation of benzoic acid from benzonitrile with increasing protein concentration.

Different enzyme concentrations were incubated with benzonitrile for 20 min at 30 °C with shaking (200 rev./min). The disappearance of benzonitrile (□) and appearance of benzoic acid (■) was analysed in triplicate by HPLC and the average integrated area plotted ± S.D.

Benzoic acid formation from benzonitrile is evident with increasing protein concentration from 0.2 mg protein. No benzamide was detected in any of the samples tested showing it was concurrently converted to benzoic acid at all the protein concentrations tested. The effect of increasing protein concentration on substrate benzamide showed that at 0.83 mg of protein, benzamide is still present in the samples but is totally converted within 30 minutes of reaction when the protein concentration reaches 0.93 mg/ml. Benzoic acid formation from benzamide is evident from 0.93 mg/ml of protein (Figure 33). Benzonitrile conversion to benzamide occurs at much lower concentrations than benzamide conversion to benzoic acid.

There appears to be a delay between the consumption of the amide and release of the acid (Figure 33). A proportion of the benzamide may be bound to the amidase before benzoic acid is release as product. This may account for the slower benzoic acid formation from benzamide compared to benzamide formation from benzonitrile.

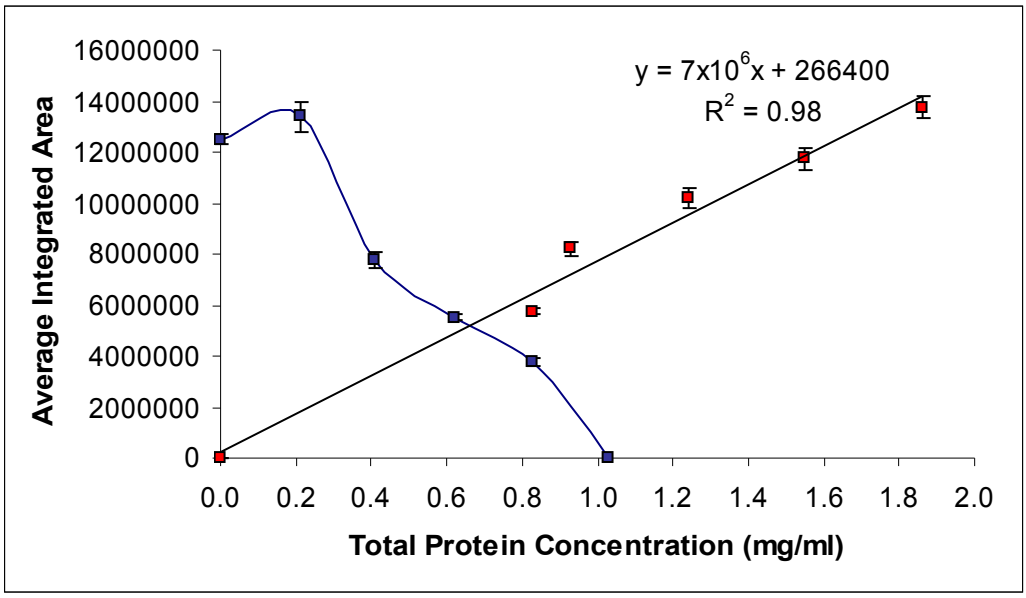


Figure 33: Formation of benzoic acid from benzamide with increasing protein concentration.

Different enzyme concentrations were incubated with benzamide for 30 min at 30 °C with shaking (200 rev./min). The disappearance of benzamide (◆) and appearance of benzoic acid (■) was analysed in triplicate by HPLC and the average integrated area plotted ± S.D.

When a linear regression curve is fitted to the average integrated area of benzoic acid as a function of protein concentration from 0.93 to 1.86 mg/ml only, the R^2 value is improved to 0.9978 (Figure 33). Formation of benzoic acid from benzamide is linear up to 1.93 mg/ml protein. The effect of increasing protein concentration on activity against benzonitrile and benzamide was repeated with lower reaction times and lower total protein concentration increments. When benzonitrile was used as the substrate, a reduced reaction time and lower protein concentration allowed its conversion to benzamide to be measured by HPLC, before it was further converted to benzoic acid.

During a 12 minute reaction, formation of benzamide from benzonitrile is evident from 0.3 mg to 0.9 mg/ml protein, and it was concurrently converted to benzoic acid in these samples. Benzoic acid formation from benzamide occurs from 0.3 mg/ml protein and its concentration increases in all further samples tested. The amount of benzamide and benzoic acid formed from benzonitrile is shown in Figure 34.

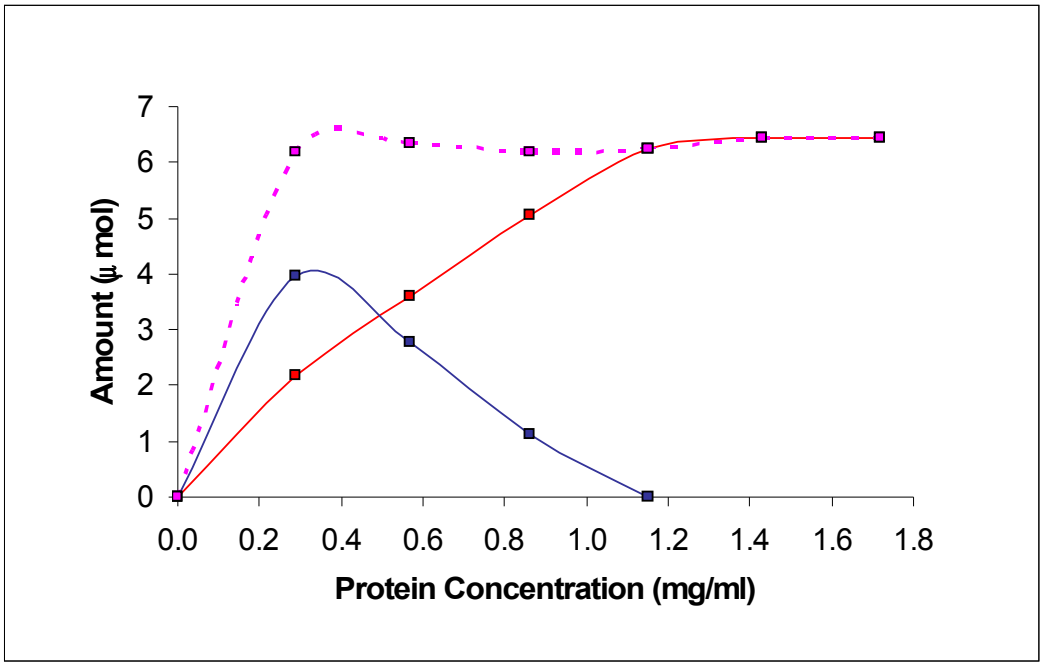


Figure 34: Amount of benzamide and benzoic acid formed from benzonitrile with increasing protein concentration.

Different enzyme concentrations were incubated with benzonitrile for 12 min at 30 °C with shaking (200 rev./min). The formation of benzamide (■) and benzoic acid (■) from benzonitrile was analysed in triplicate by HPLC and the amount of substrate and product plotted. All benzonitrile is converted to benzamide and consequently to benzoic acid. The additive amounts of both products, benzamide and benzoic acid (■), was plotted on the same axes, indicating the total conversion by a presumed nitrile hydratase.

Disappearance of substrate is "mirrored" by appearance of product, and when all benzamide is utilised, the amount of benzoic acid formed plateaus at approximately 6.5 µ mol. The starting amount of benzonitrile in the reaction was approximately 7.5 µmol. The additive amount of benzamide and benzoic acid is shown in Figure 34 – assuming that all the acid produced is due to amidase only, the total product formed shows the total activity profile against benzonitrile at increasing protein concentration.

When benzonitrile was the primary substrate, the amount of benzoic acid formed from benzamide, and disappearance of benzamide is linear at protein concentrations 0.29 to 0.86 mg/ml, and display linear regression analysis R^2 values of 1 and 0.99, respectively (data not shown).

To compare formation of benzoic acid directly from benzamide, and from benzamide that was first formed from benzonitrile, the effect of increasing protein concentration on activity was tested by reacting protein against benzamide for 25 minutes. The average integrated area of benzoic acid formation from benzamide with increasing protein concentration is shown in Figure 35. Benzoic acid formation from benzamide plateaus after protein concentrations of 0.9 mg/ml and all benzamide is converted at concentrations higher than 0.57 mg/ml. Activity against benzamide is linear at total protein concentrations from 0.3 to 0.9 mg ($R^2 = 0.99$ for benzamide disappearance, and $R^2 = 0.98$ for benzoic acid formation) and is in agreement with results where benzamide was first formed from benzonitrile (Figure 34).

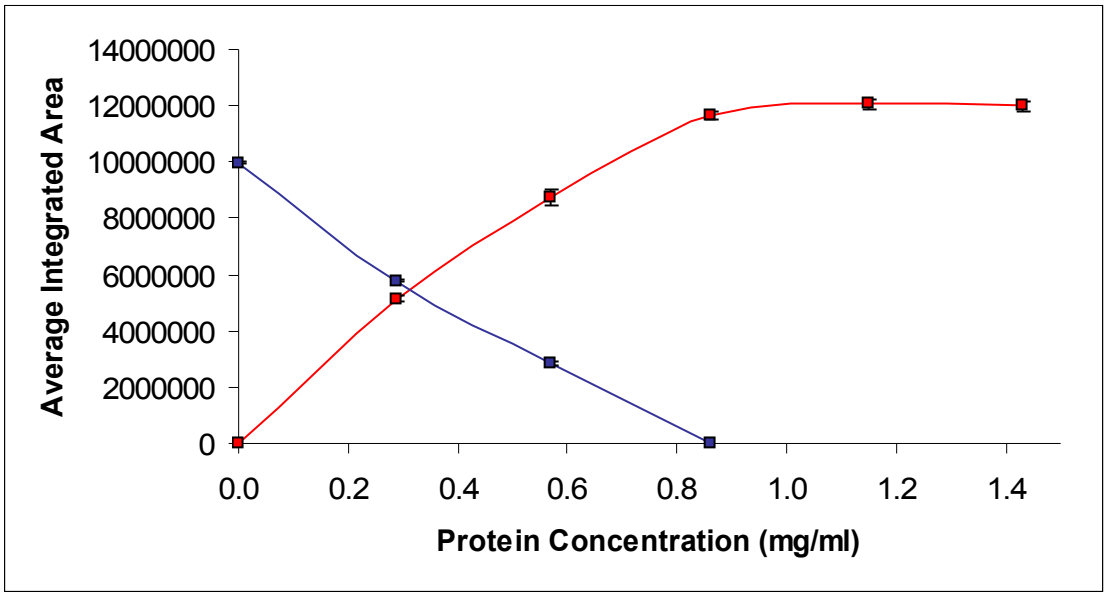


Figure 35: Average integrated area of benzoic acid formation from benzamide over a 25 minute reaction with increasing protein concentration.

Different enzyme concentrations were incubated with benzamide at 30 °C with shaking (200 rev./min). The formation of benzoic acid (■) from benzamide (■) was analysed in triplicate by HPLC and the average integrated area plotted ± S.D.

The effect of increasing protein concentration on product formation from 3-hydroxy-3-phenylpropionitrile was measured (Figure 36). 3-Hydroxy-3-phenylpropionitrile was not present at any protein concentration tested, indicating it was all converted to product. Total product formation from 3-hydroxy-3-phenylpropionitrile was linear up to 1.43 mg protein. Activity against benzonitrile and 3-hydroxy-3-phenylpropionitrile follows similar trends.

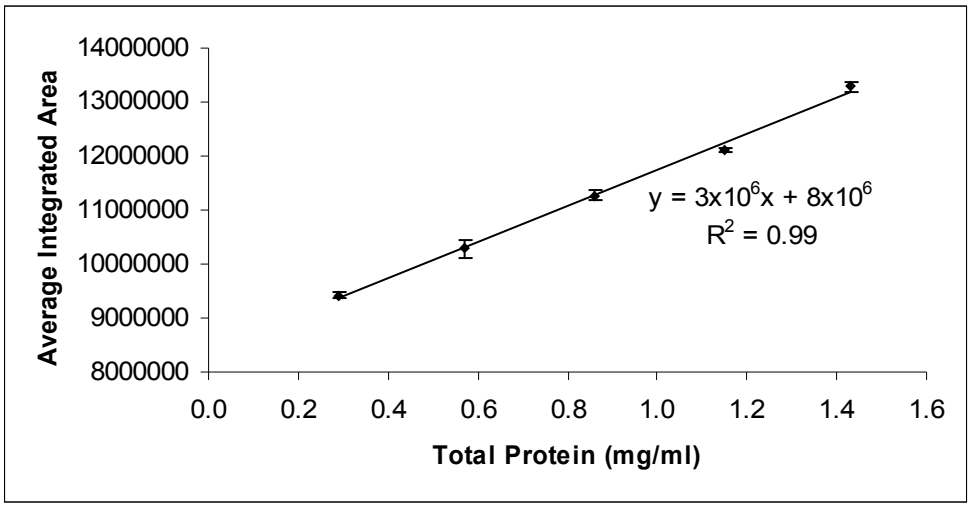


Figure 36: Average integrated area of product formed from 3-hydroxy-3-phenylpropionitrile over a 25 minute reaction.

Different enzyme concentrations were incubated with 3-hydroxy-3-phenylpropionitrile at 30 °C with shaking (200 rev./min). The formation of product (◆) was analysed in triplicate by HPLC and the average integrated area plotted ± S.D. The linear regression equation is shown.

Reaction against benzonitrile and 3-hydroxy-3-phenylpropionitrile is likely due to a common activity as the effect of increasing protein concentration is similar for both substrates. However, the reaction time against 3-hydroxy-3-phenylpropionitrile was 25 minutes as opposed to 12 minutes for benzonitrile, since the linear reaction times for their activities were proved to be different. The slower reaction kinetics against 3-hydroxy-3-phenylpropionitrile indicates that the suspected nitrile hydratase has a higher benzonitrile turnover.

3.4 Column Chromatography

Biotransformations using whole cells and cell extracts are commonly performed. In industrial applications of biocatalysts, a partially purified cell extract preparation containing activity of interest is often preferred to a highly purified enzyme due to the time and cost saving benefits. Previous studies concerning the substrate profile of *Rhodococcus rhodochrous* ATCC BAA-870 used whole cell and cell free extracts of the organism for biotransformations, with the whole cells generally exhibiting broader substrate ranges than the cell-free extracts [106]. Preparative separation of the nitrile hydratase and amidase activities from *Rhodococcus rhodochrous* ATCC BAA-870 was undertaken with the aim of

establishing a quick protocol for their separation for future activity profiling and enzyme stability studies, and to ensure that nitrile hydratase and amidase, and not nitrilase, was responsible for the activity found within the organism. Column chromatography was used for the separation of nitrile hydratase and amidase activities in a one-step process. If separate activities were required in a biocatalytic process, a simplified method for an enzyme preparation would be desirable in industry.

3.4.1 Chromatofocusing

Chromatofocusing is a powerful chromatographic technique that can be used to preparatively separate concentrated protein mixes, as well as protein isoforms. Chromatofocusing was the initial purification technique chosen to separate the enzyme/s of interest from the *Rhodococcus rhodochrous* ATCC BAA-870 soluble protein fraction (Figure 37). Due to the accuracy of the technique, a concentrated mixed protein sample can be applied to a chromatofocusing column and proteins purified to within 0.2 pH units difference in pI. An attempt at preparative separation of the nitrile-converting enzymes of interest was undertaken in which chromatofocusing was used to separate the enzymes based on pI differences, as well as to separate any isoforms of the enzymes.

The largest protein peak in chromatofocusing contained proteins at pI approximately 4 (Figure 37). It could be assumed that nitrile hydratase was contained within fractions of acidic pI (see Appendix 5.3 for nitrile hydratase theoretical pIs).

Each eluting fraction was tested against 5 mM of benzonitrile, hydrocinnamonitrile, (*R*)+mandelonitrile, 2-phenylglycinonitrile, 3-hydroxy-3-phenylpropionitrile, and 3-hydroxy-4-phenylvaleronitrile by HPLC. Control reactions without fraction samples were done (containing Polybuffer74 and substrate only, data not shown). All fractions showed no conversion of any of the substrates tested, and hence no detectable activity could be traced to any fractions. Unbound proteins also displayed no activity. BioRad protein concentration determination of the eluting fractions showed that protein was concentrated enough to afford activity as indicated by the protein concentration study (see Appendix 5.1 for example of standard curve). Fraction 100, for example contained 0.31 mg protein, a concentration at which benzonitrile, 3-hydroxy-3-phenylpropionitrile and benzamide were converted to products using the developed HPLC method.

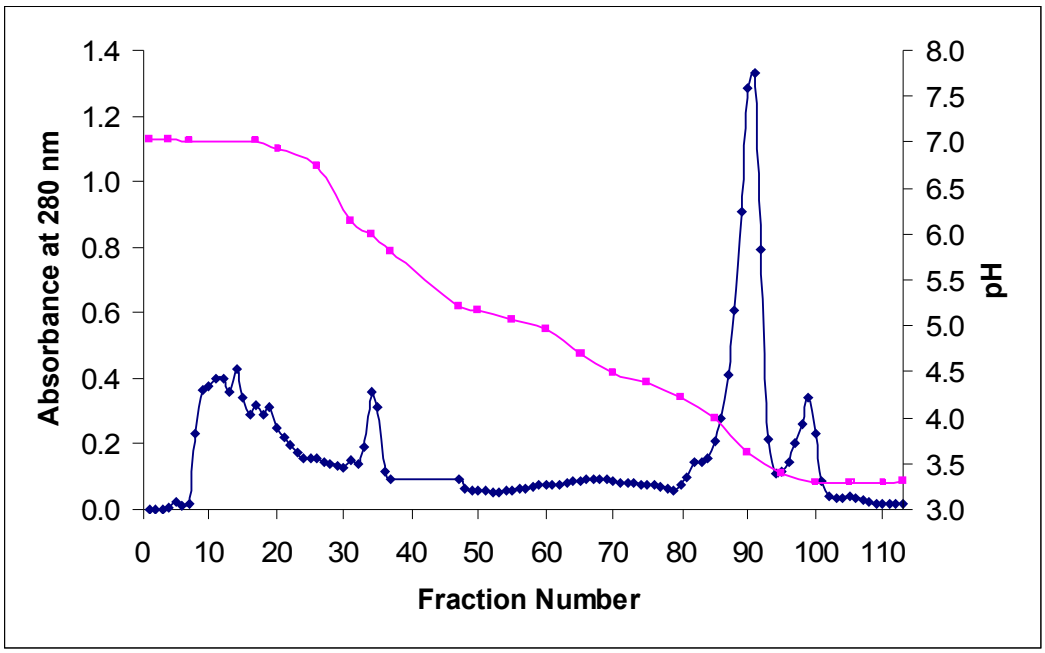


Figure 37: Polybuffer Exchanger 94 Chromatofocusing elution profile of the soluble protein fraction from *Rhodococcus rhodochrous* grown in minimal media.

Polybuffer 74 was used to elute the proteins with a pH 7 to 4 gradient (■). The elution of protein was monitored by measuring the absorbance at 280 nm of each fraction (◆).

In order to test whether the volume of fraction added to the reaction would significantly alter the overall pH of the reaction thereby causing a loss in activity, a pH test was performed. When 750 µl of Polybuffer 74 at pH 4 was added to reaction buffer at pH 7.4, the buffering capacity of the reaction buffer was enough to prevent any major changes in the reaction pH. The final pH was not changed by more than 0.3 pH units and therefore was not enough to have affected the pH of the reaction.

The fractions eluted from the chromatofocusing column showed no visible colour although an orange-coloured supernatant was originally loaded. The significance of the coloured fractions will be discussed later on in the study.

3.4.2 Gel Exclusion Chromatography

Sephacryl S-200 gel exclusion media with fractionation range (M_r) 5 000 – 250 000 was used to separate the enzymes present in supernatant of *Rhodococcus rhodochrous*. A protein standard elution profile and standard curve (Appendix 5.2) for Sephacryl S-200 was generated using molecular weight standards. The column void volume (46 ml) was

determined from the elution of Blue Dextran (2 000 kDa), and the apparent molecular weight of proteins within each fraction were estimated by comparison of the ratio of elution volume/void volume to those of the standards. A selectivity curve for Sephacryl S-200 media was generated in order to determine the size exclusion limits of the gel (Appendix 5.2). According to Figure 71, the exclusion limit for Sephacryl S-200 gel is log M_r 3.83 – 5.33, which equates to an M_r of approximately 6 700 – 213 800. The table of apparent average molecular weights of proteins within each eluted fraction (Table 8, Appendix 5.2) shows that the M_r of proteins within fractions 1 - 6 and 11 - 17 fall outside the exclusion limit for Sephacryl S-200, and therefore proteins falling outside this range may not be accurately sized.

Samples of crude protein mix from two batches of minimal media-grown cell-free extract from *Rhodococcus rhodochrous* were run on 10% SDS-PAGE (Figure 38).

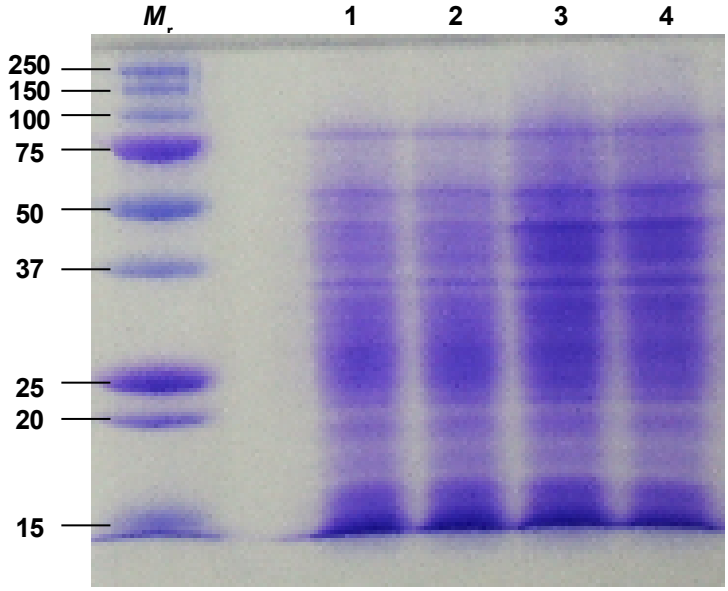


Figure 38: 10% SDS-PAGE of supernatant prepared from *Rhodococcus rhodochrous* grown in defined minimal media containing benzonitrile as inducer.

Lanes 1 and 2 are duplicate samples of supernatants of sonicates (15.5 μg of protein), while lanes 3 and 4 are duplicate samples of a second batch of cell-free extract (16 μg of protein). Precision plus protein markers from BioRad had relative molecular masses 250 000, 150 000, 100 000, 75 000, 50 000, 37 000 and 25 000. The gel was run at 150 volts using a BioRad mini Protean system.

A mixed protein sample from supernatant of *Rhodococcus rhodochrous* grown in minimal media was eluted on a Sephacryl S-200 gel exclusion column (Figure 39). The high

molecular weight fractions eluting first off the gel exclusion column showed activity. Fractions 5, 6, 7 and 8 (volume 40 – 64 ml) were active against benzonitrile, and converted it to benzamide (Figure 40). This indicates the presence of a nitrile hydratase since no benzoic acid was found. If so, this shows separation of nitrile hydratase activity from amidase activity, since no benzoic acid was present in any of the fraction samples analysed. Fractions 5, 6 and 7 also showed activity against 3-hydroxy-3-phenylpropionitrile. Again, activity against benzonitrile and 3-hydroxy-3-phenylpropionitrile was similar and shared in the same fractions (Figure 40).

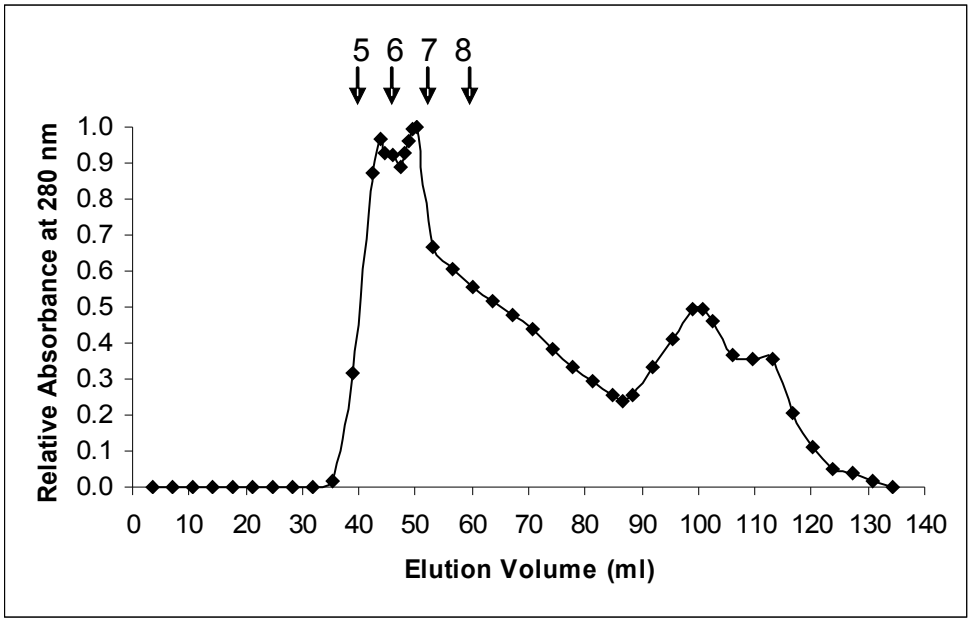


Figure 39: Protein elution from Sephacryl S-200 during gel exclusion of a cell free protein mix from *Rhodococcus rhodochrous*.

Proteins were eluted at room temperature with a flow rate of 0.7 ml/min using 100 mM potassium phosphate buffer, pH 7.4, containing 0.02% (w/v) sodium azide. A total of 9.46 mg protein was loaded onto the column and the A_{280} was monitored (♦). Fraction numbers are indicated by arrows.

Fractions at an elution volume higher than approximately 72 ml displayed no activity. From the standard curve of gel exclusion size standards created (Appendix 5.3), fractions eluting after 72 ml are in the size region approximately 20 kDa and smaller. Fractions with activity against benzonitrile contain proteins of average sizes roughly 700 kDa, 230 kDa and 93 kDa (fractions 5-7, respectively) and fraction 8 contains proteins of approximately 40 kDa (Figure 40). Fractions displaying activity all contain high molecular weight proteins, and elute with or just after the column void volume (43 ml).

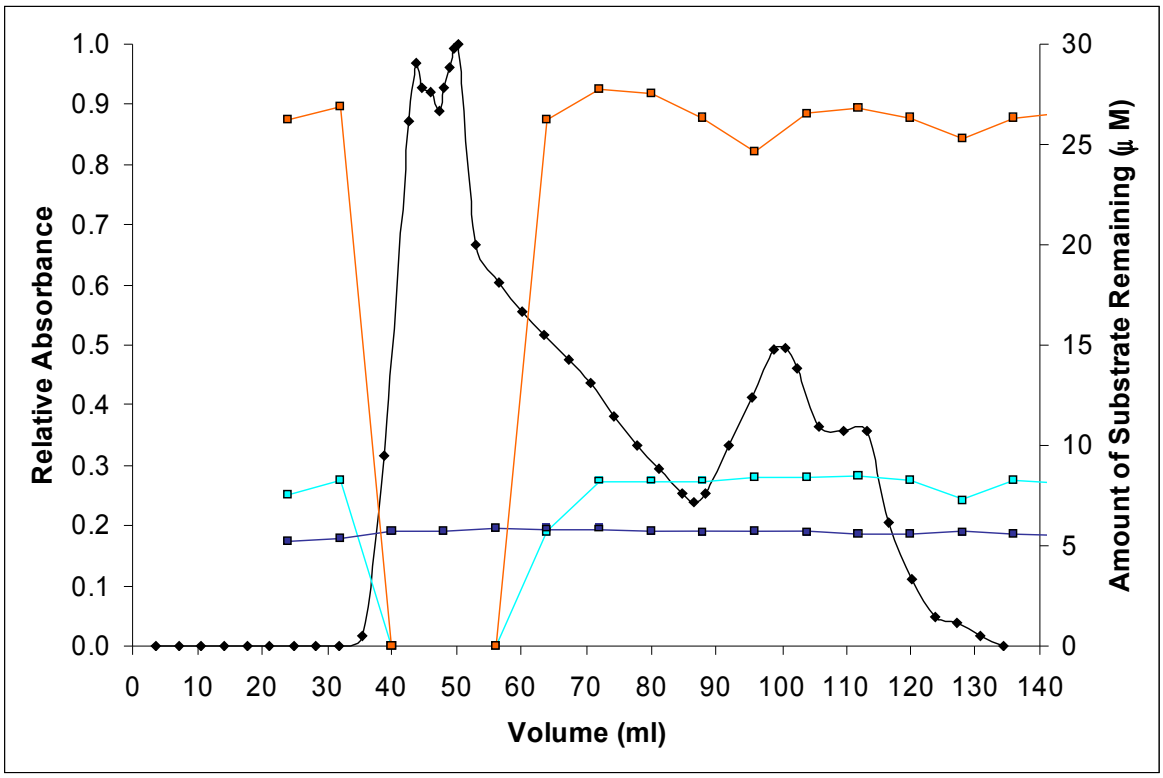


Figure 40: Nitrile hydrolytic activity profile of fractions from Sephacryl S-200 gel exclusion of a cell free protein mix from *Rhodococcus rhodochrous* showing residual substrate after reaction.

Benzonitrile (□), benzamide (■) or 3-hydroxy-3-phenylpropionitrile (■) was reacted in duplicate with each fraction at 30 °C with shaking (200 rev./min) and the amount of substrate remaining or product produced analysed by HPLC. Benzonitrile samples were reacted for 10 minutes, while benzamide and 3-hydroxy-3-phenylpropionitrile were reacted for 30 minutes. Proteins were eluted at room temperature with a flow rate of 0.7 ml/min using 100 mM potassium phosphate buffer, pH 7.4, containing 0.02% (w/v) sodium azide. A total of 9.46 mg protein was loaded onto the column and the A_{280} was monitored (◆).

Although the sample applied to the column showed amidase activity, it was not detectable in the fractions. Nitrile hydratase activity eluted at a volume of 40 – 56 ml. Proteins in this volume were resolved on a 10% SDS-PAGE gel; this yielded a prominent protein band at 48 kDa and two, less prominent bands, at 56 and 84 kDa after Coomassie staining (Figure 41). SDS-PAGE analysis showed that the active fractions also contained proteins of less than 25 kDa, however, a 10% polyacrylamide gel did not resolve in that molecular mass region. The sample did not contain proteins of less than 10 kDa since molecular cut-off filtration was used prior to gel exclusion, and contained no activity when tested by HPLC (data not shown).

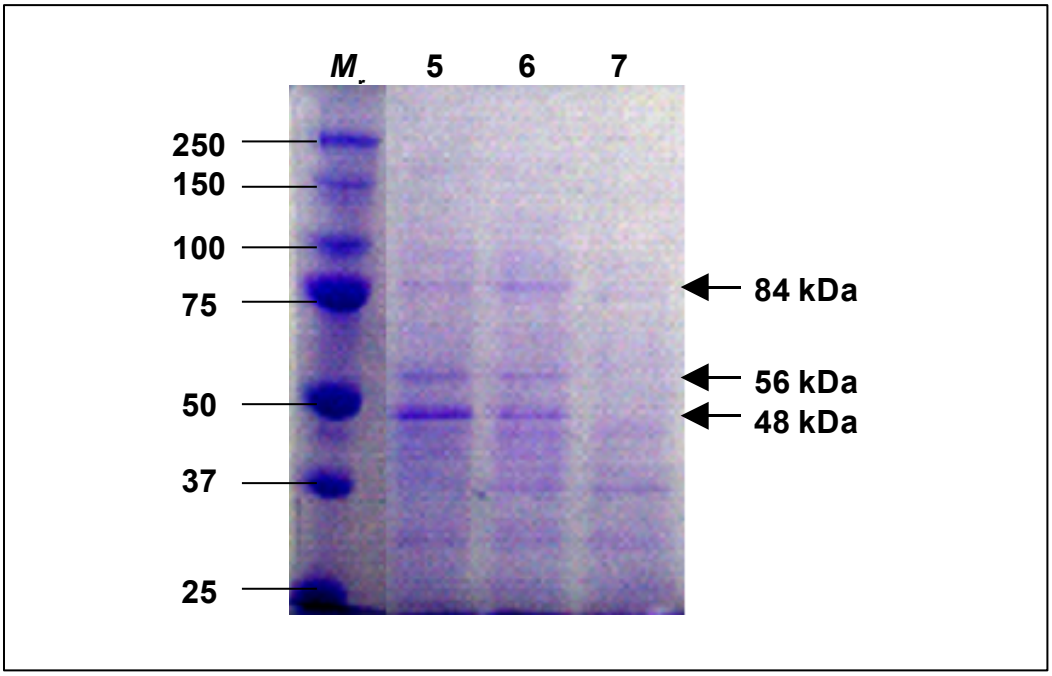


Figure 41: 12% SDS-PAGE of Sephacryl S-200 size exclusion chromatography fractions.

Samples of eluting gel exclusion fractions were prepared by adding 15 µl of each fraction to 10 µl sample loading buffer, and heating at 95 °C for 5 min prior to loading 20 µl of each sample. Lane 5 corresponds to fraction 5; lane 6, fraction 6 and lane 7, fraction 7. Protein size markers had relative molecular mass 250 000, 150 000, 100 000, 75 000, 50 000, 37 000 and 25 000. The gel was run at 150 volts using a BioRad mini Protean system. Arrows indicate sizes of resolved proteins.

Interestingly, fraction 5 with highest apparent molecular weight (lane 3, Figure 41) eluted orange-coloured. SDS-PAGE analysis showed a prominent 48 kDa band in this fraction which may be responsible if the colour is protein associated. Since the elution in fraction 5 occurred at high molecular weight, the colour is more likely protein-associated than due to a possible pigment contained within the sample.

Gel exclusion chromatography using Sephacryl S-200 was repeated to detect activity against benzamide, and to further resolve the apparent sizes of the enzymes responsible for activity. The protein sample was treated with polyethylenimine to remove any high molecular weight nucleic acid excess prior to loading (Figure 42). Fractions were collected in smaller volumes to further separate the activity against benzonitrile and 3-hydroxy-3-phenylpropionitrile.

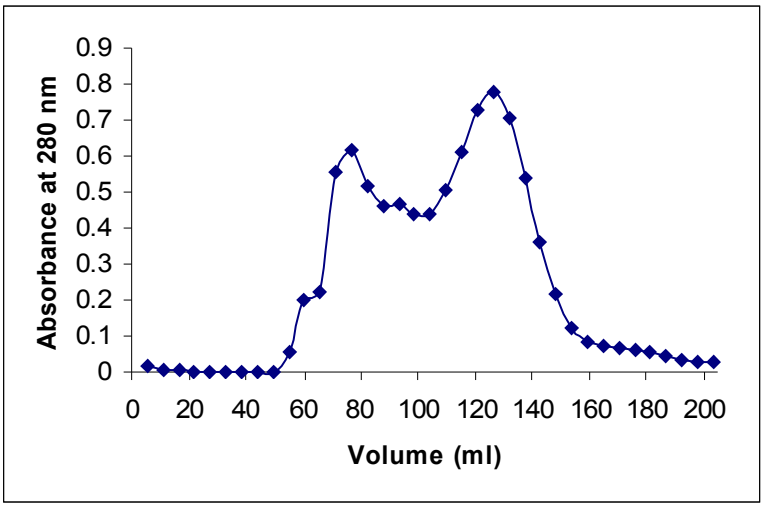


Figure 42: Sephacryl S-200 gel exclusion protein elution profile of *Rhodococcus rhodochrous* supernatant treated with polyethylenimine.

Supernatant was buffer exchanged using a 10 k cut-off filtration membrane after treatment with polyethylenimine. A 1 ml volume of a 10 mg/ml soluble protein mixture was loaded onto the column and eluted using 20 mM phosphate buffer, pH 7.4 with a 0.7 ml/min flow rate. The A_{280} was monitored (♦).

Reactions of eluted fraction samples were performed for 2 hours to ensure detection of activity and were therefore qualitative measures of activity. When fractions were reacted with benzonitrile, conversion to benzamide and benzoic acid was detected, indicating amidase activity was present. The profile of activity against benzonitrile showed distinct fractions where only benzamide was formed, and fractions where benzamide and benzoic acid were produced (Figure 43). Fractions reacted against benzamide confirmed amidase activity in fractions 15 and 16, with fractions 13 to 16 showing conversion to benzoic acid (Figure 44).

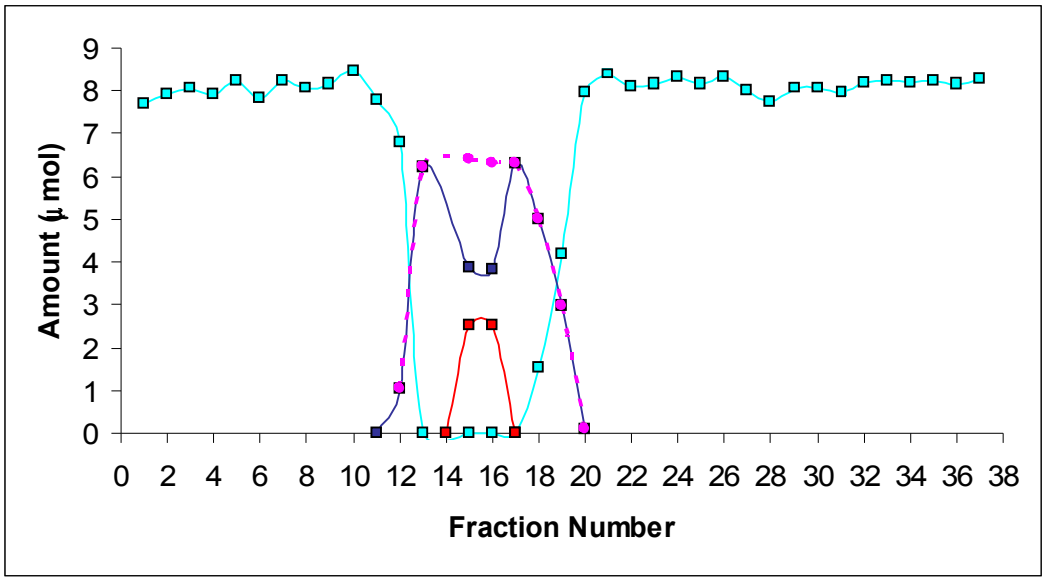


Figure 43: Conversion of benzonitrile to product in Sephacryl S-200 gel exclusion fractions showing total amount of product formation.

Benzonitrile (▫) was reacted in duplicate with each fraction for 2 hours at 30 °C with shaking (200 rev./min) and the amount of substrate remaining and product produced analysed by HPLC. Benzamide (▪) was produced from benzonitrile and benzoic acid (▪) produced concurrently from benzamide. The sum of benzamide and benzoic acid amounts is indicated to show total product formation (◆, dotted line).

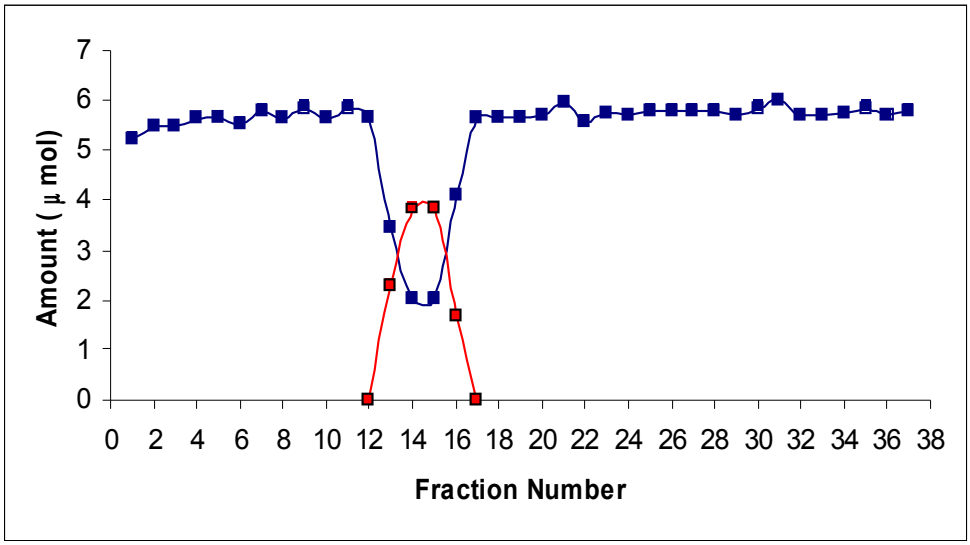


Figure 44: Conversion of benzamide to benzoic acid in Sephacryl S-200 eluted fractions.

Benzamide (▪) was reacted in duplicate with each fraction for 2 hours at 30 °C with shaking (200 rev./min) and the amount of substrate remaining and benzoic acid (▪) produced analysed by HPLC.

Activity against 3-hydroxy-3-phenylpropionitrile shared a similar profile with that of benzamide, with fractions 13 to 16 showing conversion to product (Figure 45). Unlike benzamide conversion, however, all the 3-hydroxy-3-phenylpropionitrile in fractions 14 and 15 was utilised.

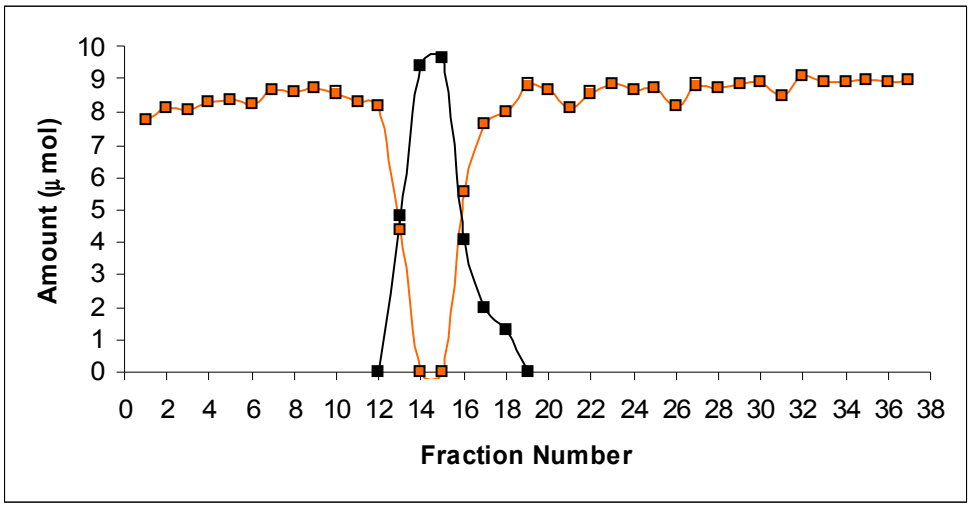


Figure 45: Conversion of 3-hydroxy-3-phenylpropionitrile to product in Sephacryl S-200 eluted fractions.

3-Hydroxy-3-phenylpropionitrile (□) was reacted in duplicate with each fraction for 2 hours at 30 °C with shaking (200 rev./min) and the amount of substrate remaining and product (■) produced analysed by HPLC.

Comparative activity profiles against benzonitrile, benzamide and 3-hydroxy-3-phenylpropionitrile are shown in Figure 46. Although their activities overlap somewhat, activity against 3-hydroxy-3-phenylpropionitrile had a wider fraction range than activity against benzamide since it was converted to product in fractions 13 to 18, whereas conversion of benzamide to benzoic acid occurs in fractions 13 to 16 (Figure 44 and Figure 45). Since the dilution of reacting enzyme from each fraction and the reaction time was the same for reactions against both substrates, it may be said that activity against 3-hydroxy-3-phenylpropionitrile is higher than that against benzamide.

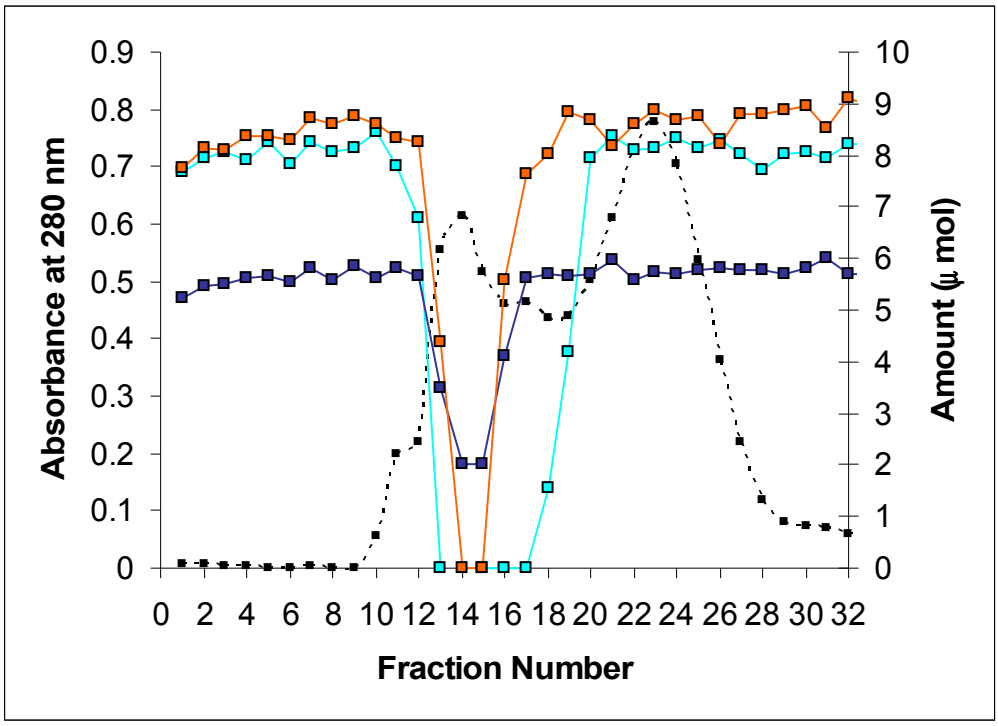


Figure 46: Conversion of benzonitrile, benzamide and 3-hydroxy-3-phenylpropionitrile in Sephacryl S-200 eluted fractions.

Benzonitrile (■), benzamide (■) or 3-hydroxy-3-phenylpropionitrile (■) were reacted in duplicate with each fraction at 30 °C with shaking (200 rev./min) and the amount of substrate remaining analysed by HPLC. Benzonitrile reactions were reacted for 10 minutes, while benzamide and 3-hydroxy-3-phenylpropionitrile were reacted for 30 minutes. Elution of protein was monitored at 280 nm (■).

Elution of smaller fraction volumes allowed better protein size distinctions possible for each fraction. Fractions 12 to 17 contained proteins of approximate relative molecular mass 34 500 to 5 500. Fraction 14 and 15 contained proteins of a range of approximate relative molecular mass between 17 000 and 25 000, respectively. Interestingly, activity against benzonitrile was due to proteins spanning a large size range, and may be an enzyme with mixed size species (similar to the low- and high-molecular mass nitrile hydratase of *Rhodococcus rhodochrous* J1). The apparent protein sizes affording activity in the second gel exclusion experiment are smaller (6 500 – 34 500) than sizes attributed to activity in the first experiment (42 000 – 700 000). Treatment of supernatant with polyethylenimine may have disrupted formation of high molecular weight enzyme aggregates in fractions of the second experiment.

SDS-PAGE of active fraction samples showed prominent bands in the 84, 56, 48 and 21 kDa region (Figure 41). Nitrile hydratase activity spans a native size range of approximately 2 000 – 68 000 in the second gel exclusion experiment, and 42 000 – 700 000 in the first experiment. Since cut-off filtration using an ultrafiltration membrane was used prior to loading the sample, the supernatant loaded onto the column should not contain proteins of less than 10 kDa. If multimer formation was inhibited in the second experiment, then functional αβ units in the 48 kDa range (made up of roughly 21 kDa monomers) may be the protein sizes responsible. If larger multimers formed in the first experiment, then a combination of αβ and $\alpha_2\beta_2$ (possibly 84 kDa), and even some larger multimers could be possible The native quaternary structures of bacterial nitrile hydratases are highly variable, but most are αβ heteromultimers, typically dimers or tetramers [102]. Stronger reducing conditions may be necessary for subunit disruption during denaturing PAGE – indeed, the reducing agents DTT and β-mercaptoethanol have been found to enhance the activity of nitrile hydratases (presumably by stabilising the catalytically active enzyme sulfhydryl groups) [103, 113], which may be further proof that the enzyme structure is not compromised by reducing agents. Although the addition of urea to SDS-PAGE serves to denature the native protein structure, urea itself is a known inducer of nitrile hydratase activity. High- and low-molecular mass nitrile hydrates in *Rhodococcus rhodochrous* has been selectively induced by reaction products (amides) and urea, respectively [17, 20, 114].

Again, orange-coloured fractions (fractions 13 – 15) appeared in the second gel exclusion elution experiment which correlated with maximum nitrile hydrolysing activity. A spectrophotometric wavelength absorbance scan of the coloured fractions (fraction number 14 and 15) compared to a clear protein-containing fraction was done (Figure 47), and showed increased absorption at 280 nm (due to higher protein levels) and a broad shoulder at 300 – 460 nm, which would result in a colour in the red to yellow visible range.

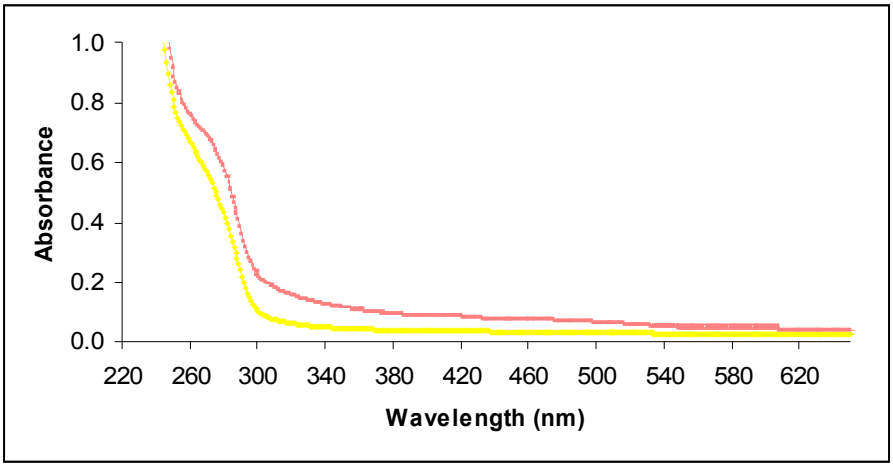


Figure 47: Wavelength scans of a coloured Sephacryl S-200 eluted gel exclusion fraction compared to other fractions.

All eluted fractions (■) were clear apart from the fractions containing nitrile hydratase activity (■) which was orange-pink in colour. Fractions were measured in quartz cuvettes using a DU 800 Spectrophotometer and are plotted as an average of three spectra.

The visual colour of fraction 14 and 15 was noted to be similar to the colour of *Rhodococcus rhodochrous* colonies or growth in media (Figure 13). It was originally assumed the colour was due to the pigment contained within the organism. Also, supernatant of *Rhodococcus rhodochrous* ATCC BAA-870, and therefore the cell free extract applied to the column, is orange in colour. Unbound proteins elute without colour, and colour is only preserved in proteins with nitrile hydrolysing activity.

3.4.3 Ion Exchange

Gel exclusion chromatography showed that nitrile hydratase and amidase in *Rhodococcus rhodochrous* ATCC BAA-870 are high molecular weight enzymes, and that their activities overlap in these fractions. Ion exchange chromatography of supernatant from *Rhodococcus rhodochrous* using Toyopearl SuperQ 650M ion exchange resin was performed to attempt separation of the nitrile hydratase and amidase activity which was not possible using gel exclusion. At first, twenty-one fractions were collected over a 42 ml salt gradient after unbound proteins were eluted from the column (Figure 48).

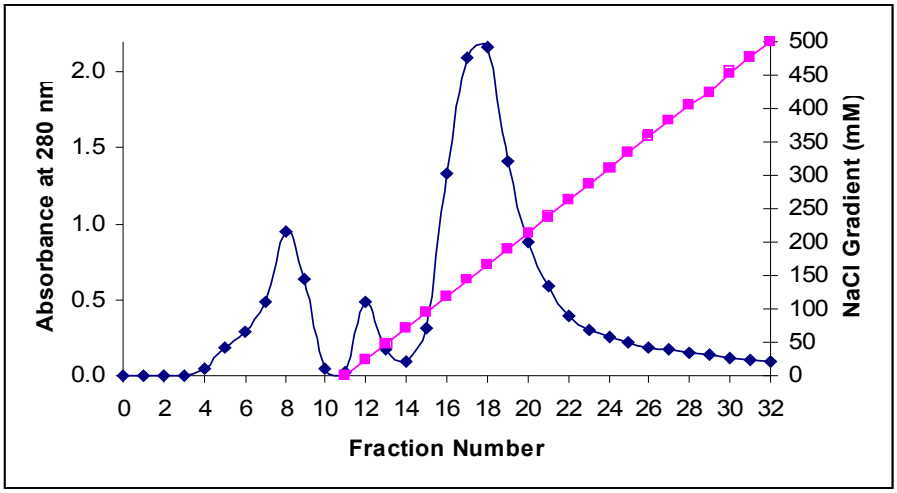


Figure 48: Protein elution profile from Toyopearl SuperQ 650M during ion exchange chromatography of supernatant from *Rhodococcus rhodochrous*.

The column was equilibrated using 20 mM Tris buffer, pH 8. Supernatant from *Rhodococcus rhodochrous* was buffer exchanged into 20 mM Tris buffer, pH 8, and 4.9 ml of a 10 mg/ml sample loaded onto the column. Unbound proteins were allowed to elute prior to elution of bound proteins using a 500 mM NaCl gradient over 42 ml (■). The fraction A_{280} was monitored (◆).

All ion exchange elution fractions were tested for activity against benzonitrile, benzamide and 3-hydroxy-3-phenylpropionitrile for 2 hours to ensure reactions ran to completion even if enzyme levels were not concentrated. No activity was detected in the fractions containing unbound protein. Figure 49 shows conversion of benzonitrile to benzamide and benzoic acid in ion exchange fractions. When benzonitrile was reacted, the benzamide produced was further converted to benzoic acid in fraction 17 and 18 (140 – 170 mM NaCl elution) and therefore both nitrile hydratase and amidase was present in these fractions. Fractions 19 and 20 (190 – 215 mM NaCl elution) contained benzamide only, and therefore only nitrile hydratase was present in those fractions since it was not further converted to benzoic acid even though it was reacted for 2 hours.

Based on the assumption that there is not a nitrilase present, an additive curve of amide produced as a sum of benzamide and benzoic acid gives a profile of the overall nitrile hydratase activity (Figure 49). Fraction 16 showed formation of 0.12 µmol of benzoic acid whereas no benzamide was detected in that fraction, and hence presumably all benzamide was converted to benzoic acid. When benzonitrile was the substrate, benzoic acid was formed in fractions 16, 17 and 18, and benzamide was formed in fractions 17, 18, 19 and 20. When benzamide was reacted with the ion exchange fractions, conversion to benzoic

acid was seen in the same fractions as those where benzonitrile was the substrate (Figure 49 and Figure 50). Fractions 16, 17 and 18 therefore contain amidase activity that elutes at 120 – 215 mM NaCl and is responsible for all benzoic acid generated in those fractions. There is no benzoic acid formed from benzamide in fractions 19 and 20, whereas the final product of benzonitrile in these fractions is benzamide.

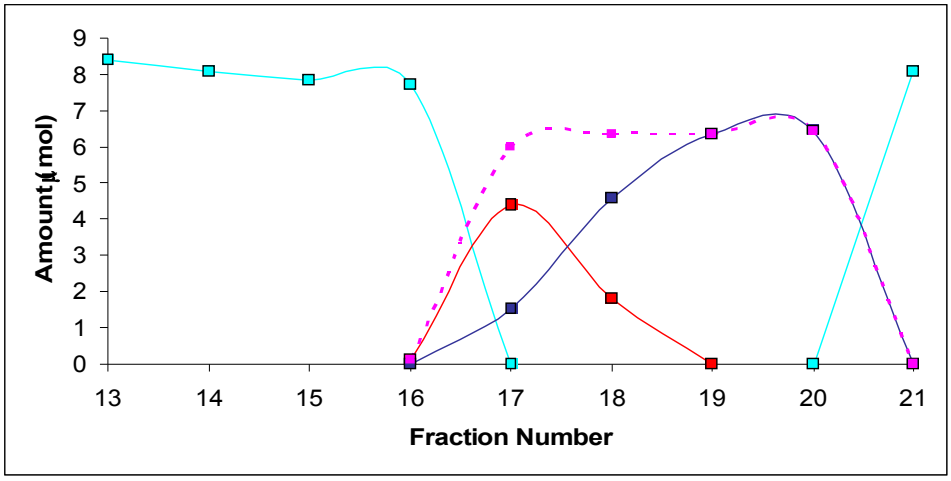


Figure 49: Conversion of benzonitrile to benzamide and benzoic acid in Toyopearl SuperQ 650M ion exchange eluted fractions.

Benzonitrile (■) was reacted in duplicate with each fraction for 2 hours at 30 °C with shaking (200 rev./min) and the amount of substrate remaining and benzoic acid (■) and benzamide (■) produced analysed by HPLC. The sum of benzamide and benzoic acid amounts is indicated to show total product formation from benzonitrile (■).

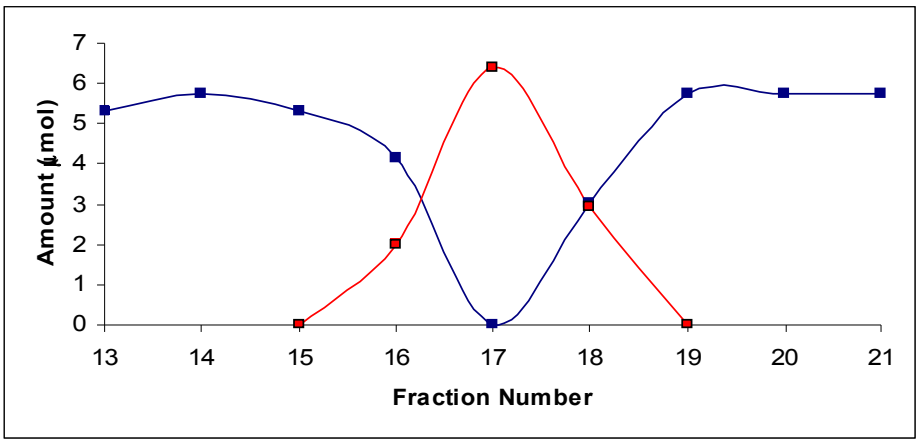


Figure 50: Conversion of benzamide to benzoic acid in Toyopearl SuperQ 650M ion exchange eluted fractions.

Benzamide (■) was reacted in duplicate with each fraction for 2 hours at 30 °C with shaking (200 rev./min) to generate benzoic acid (■) produced analysed by HPLC.

Conversion of 3-hydroxy-3-phenylpropionitrile to product in ion exchange fractions is shown in Figure 51. Fractions 16 to 20 (120 – 215 mM NaCl elution) contained activity against 3-hydroxy-3-phenylpropionitrile. Since all the 3-hydroxy-3-phenylpropionitrile was utilised in fractions 17, 18 and 19, it can be assumed that the product peak would not have levelled off if a higher enzyme dilution was used. The amidase activity profile does not level off (Figure 50), and since the enzyme dilutions are the same against both substrates it can be assumed that the nitrile hydratase has higher activity against 3-hydroxy-3-phenylpropionitrile than benzonitrile.

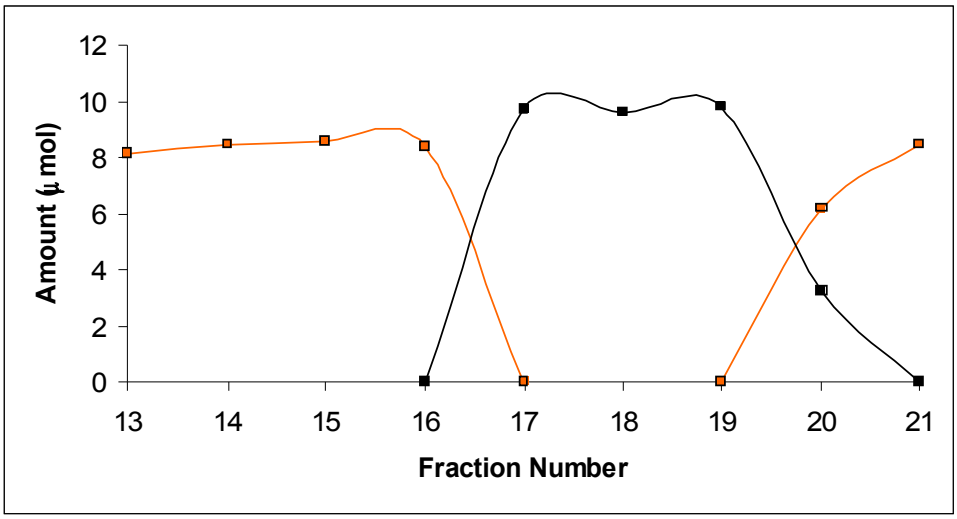


Figure 51: Conversion of 3-hydroxy-3-phenylpropionitrile to product in Toyopearl SuperQ 650M ion exchange eluted fractions.

3-Hydroxy-3-phenylpropionitrile (■) was reacted in duplicate with each fraction for 2 hours at 30 °C with shaking (200 rev./min) and the amount of substrate remaining and total product produced (■) analysed by HPLC.

The graphs of residual benzonitrile, benzamide and 3-hydroxy-3-phenylpropionitrile remaining in reactions using the ion exchange fractions as biocatalyst were superimposed and the overlapping activity profiles were studied (Figure 52). The profiles indicate that activity against nitrile substrates (namely, the nitrile hydratase) is the result of a single enzyme system that displays different affinities for the different substrates.

SDS-PAGE analysis of samples from fractions 16, 17 and 18 indicated different denatured protein profiles within the fractions (Figure 53). The common bands may be indicative of common activities found within the fractions. Fraction 16 and 17 both had proteins of sizes

84 kDa, 47 kDa and 21 kDa, while fractions 17 and 18 both had proteins with sizes of 56 kDa and 36 kDa. SDS-PAGE of gel exclusion fractions with activity displayed common subunit sizes to those found in ion exchange fractions (Figure 53). Gel exclusion fractions with nitrile hydratase activity contained subunits of sizes 84 kDa, 56 kDa, 48 kDa and a size less than 25 kDa (Figure 47), while ion exchange fractions show sizes 84 kDa, 56 kDa, 47 kDa, 36 kDa, 32 kDa and 21 kDa. Assuming the common subunit sizes are due to common activities, nitrile hydratase and amidase in *Rhodococcus rhodochrous* ATCC BAA-870 may be made up of one or more of these subunit sizes.

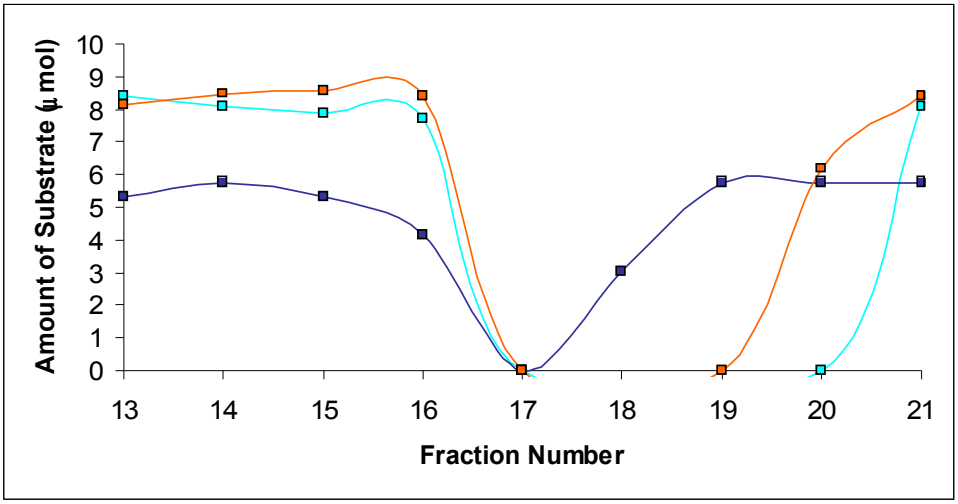


Figure 52: Amount of benzonitrile, benzamide and 3-hydroxy-3-phenylpropionitrile remaining in Toyopearl SuperQ 650M ion exchange eluted fractions.

Each fraction was reacted in duplicate with benzonitrile (■) for 10 min, and benzamide (■) and 3-hydroxy-3-phenylpropionitrile (■) for 30 min, at 30 °C with shaking (200 rev./min). The amount of substrate remaining was analysed by HPLC.

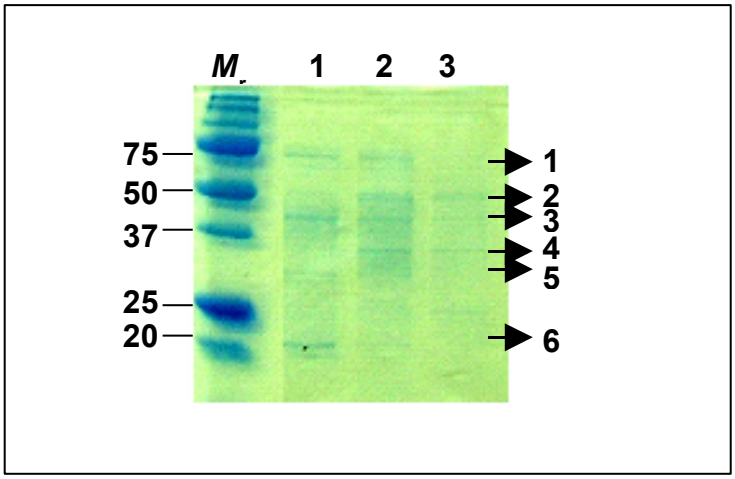


Figure 53: 10% SDS-PAGE of Toyopearl SuperQ 650M ion exchange eluted fractions.

Lane 1 corresponds to fraction 16; lane 2, fraction 17 and lane 3, fraction 18. Protein size markers had relative molecular mass 250, 150 and 100 (labels excluded for clarity), 75, 50, 37 and 25. Unknowns 1-6 correspond to sizes 84, 56, 47, 36, 32 and 21, respectively. Samples of eluting gel exclusion fractions were prepared by adding 80 µl of each fraction to 20 µl sample loading buffer, and heating at 95 °C for 5 min prior to loading 20 µl of each sample. The gel was run at 150 volts using a BioRad mini Protean system.

Ion exchange was repeated in an attempt to further separate the activities noted in eluted fractions. The number of fractions collected over the salt gradient was increased to 49 (Figure 54). Again, the unbound protein in the flow through contained no activity against any of the substrates tested. The activity profile and elution profile was significantly altered when the fraction number was increased and fraction volume decreased in the second ion exchange experiment, showing better protein peak separation and narrower activity elution profiles against benzonitrile and 3-hydroxy-3-phenylpropionitrile. Amidase activity was, however, not detected in any fractions from the second ion exchange experiment.

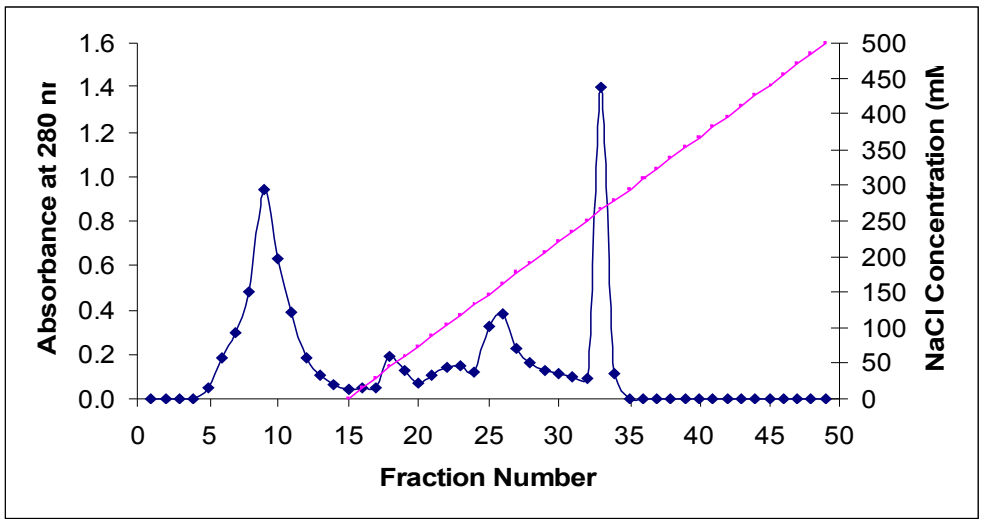


Figure 54: Toyopearl Super-Q 650M ion exchange chromatography of supernatant from *Rhodococcus rhodochrous* eluted with a 500 mM NaCl gradient.

The column was equilibrated using 20 mM Tris buffer, pH 8. Supernatant from *Rhodococcus rhodochrous* was buffer exchanged into 20 mM Tris buffer, pH 8, and 4 ml of a 10 mg/ml sample loaded onto the column. Unbound proteins were allowed to elute prior to elution of bound proteins using a 500 mM NaCl gradient over 42 ml. The fraction A_{280} was monitored.

Benzamide was formed from benzonitrile in fractions 18 and 19 (45 - 60 mM NaCl), and in fractions 22 to 28 (103 – 190 mM NaCl). All benzonitrile was converted to benzamide in fractions 23 to 25 (Figure 55). The amount of 3-hydroxy-3-phenylpropionitrile remaining in ion exchange fractions and its conversion to product is also shown in Figure 55. Fractions 23 to 27 (118 - 177 mM NaCl) converted 3-hydroxy-3-phenylpropionitrile to product, with fraction 24 converting it all to product.

The activity profiles were similar against both substrates, except that all 3-hydroxy-3-phenylpropionitrile was converted to product in fraction 24 only, whilst all benzonitrile was converted to benzamide in fractions 23, 24 and 25 (Figure 55). Also, trace activity against benzonitrile (forming benzamide only) is noted in fractions 18 and 19 while no activity against 3-hydroxy-3-phenylpropionitrile is noted in these fractions. Fractions 18 and 19 may contain a substrate-specific nitrile hydratase with low activity against benzonitrile whilst fractions 23 to 26 contain a nitrile hydratase with broad substrate specificity.

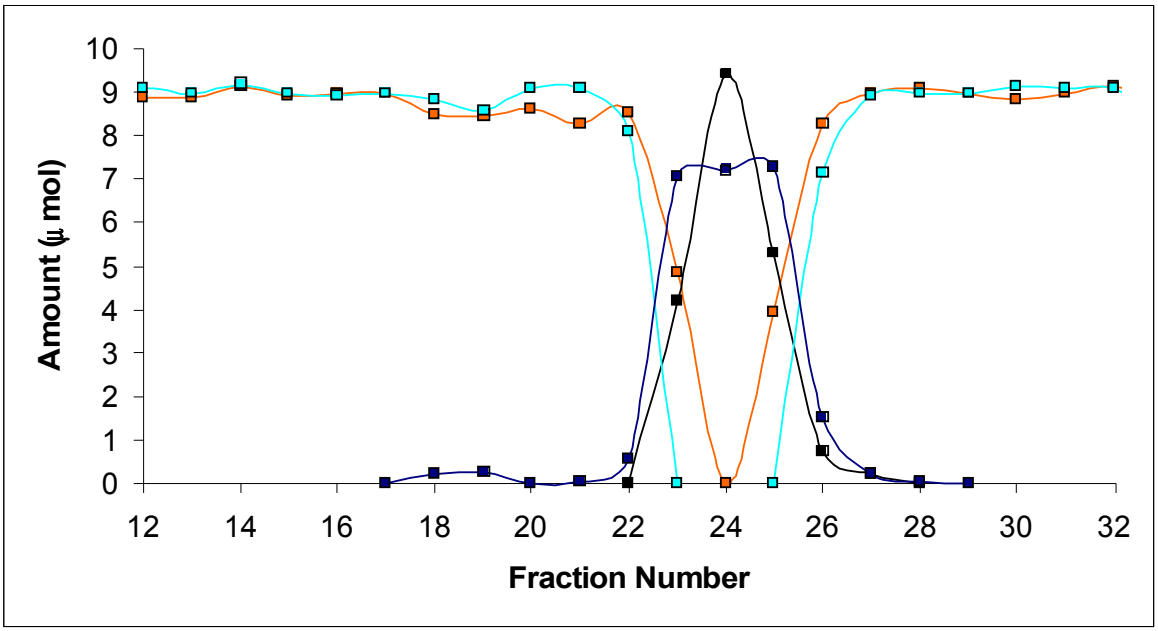


Figure 55: Amount of benzamide formed from benzonitrile, and conversion of 3-hydroxy-3-phenylpropionitrile in Toyopearl SuperQ 650M ion exchange eluted fractions.

Benzonitrile (▫) was reacted in duplicate with each fraction for 10 minutes at 30 °C with shaking (200 rev./min) and the amount of substrate remaining and benzamide (▪) produced analysed by HPLC. 3-Hydroxy-3-phenylpropionitrile (▫) was reacted in duplicate with each fraction for 30 minutes at 30 °C with shaking (200 rev./min) and the amount of substrate remaining and product produced (▪) analysed by HPLC.

Chapter 4

4 Discussion

The use of biocatalysts presents advantages for the synthetic chemist. These include a more ecofriendly approach to enzymatic conversions, with milder, cleaner chemistry, and the synthesis of products without excessive production of waste or unwanted by-products. A major problem in the development of a specific biotransformation reaction is finding a suitable biocatalyst. Unlike the common commercial enzymes, such as proteases, lipases and amylases for example, the study and application of nitrile hydrolysing enzymes is still at an early stage. When the availability of commercial enzyme preparations is scarce, exploring the use of a previously uncharacterised biocatalyst from a microbe has many advantages. Once the activity of interest is identified through the screening of organisms in a culture collection, the organism biomass can be isolated and bulked through enrichment culturing. A strain of *Rhodococcus rhodochrous* (ATCC BAA-870) was identified as a nitrile-metabolising organism, and its growth, nitrile substrate profile, and enzyme systems subsequently investigated.

4.1 Characteristics of the chosen biocatalyst, *Rhodococcus rhodochrous*

The *Rhodococcus* genus falls under the Nocardioform family. The *rhodochrous* species is so named due its rose-coloured appearance (Gr. n. *rhodon* the rose; Gr. n. *chrous*; L. adj. *rhodochrous* rose-coloured) and is easily identifiable. Most are isolated from soil, and are therefore readily obtainable from natural sources. Bergey's Manual of Systematic Bacteriology confirmed that *Rhodococcus rhodochrous* forms orange to red rough colonies on media such as glucose yeast extract agar, and that the life-cycle growth of *Rhodococcus rhodochrous* follows an elementary branching-rod-coccus morphogenetic sequence. The gram-positive organism is a practical, robust and easily cultured organism.

Rhodococcus rhodochrous ATCC BAA-870 was found to be a suitable organism for metabolism of selective nitriles. The nitrile activity of the organism could be easily induced using defined media and the activity of interest was extracellularly expressed,

eliminating the need for complicated recovery of enzyme. Although the cell doubling time of the organism in defined minimal media was at least 30 hours, induction of activity was easily achieved through addition of nitrile to the culturing media. Nitrilases from *Rhodococcus* have been known to be strongly induced by the addition of nitrile to the medium [109]. For example, the nitrilases of *Rhodococcus rhodochrous* K22 and *Rhodococcus rhodochrous* J1 can be induced by addition of isovaleronitrile to the medium [4, 115], with the latter induced nitrilase forming up to 35% of the total soluble protein [24]. The organism can be stored refrigerated on solid medium agar for many weeks without losing viability, and culturing of the organism by addition of a nitrile such as benzonitrile enables minimum use of antibiotics in the medium since the nitrile is toxic to many other bacterial strains. The cell disruption study showed that cell-free extract preparation from the organism is quick and simple. The *Rhodococcus rhodochrous* used in this study has presented interesting activity. Its ability to transform benzonitrile, and the β-hydroxynitrile, 3-hydroxy-3-phenylpropionitrile, makes it a particularly worthwhile subject for a potential commercial biocatalyst.

It is generally reported that nitrilases predominantly hydrolyse aromatic nitriles, whereas nitrile hydratase/amidase systems mainly have a preference for aliphatic nitriles [62, 68]. Nitrilases that utilize benzonitrile as a preferred substrate have, for example, been isolated from *Nocardia* sp. NCIB 11215, NCIB 11216, *Fusarium solani* and *Arthrobacter* sp., but only in small amounts since the enzymes were labile [115]. Benzonitrile was used in all the tests of activity performed on the organism in this study due to its preference and so-called adaptation to utilizing benzonitrile as a substrate. The enzyme/s suspected of being responsible for the metabolism of the aforementioned aromatic nitriles in *Rhodococcus rhodochrous* ATCC BAA-870 was a nitrile hydratase with aromatic nitrile specificity.

4.2 Towards Establishing an Activity Assay for Nitrile Hydratase

Enzymatic transformations are pivotal to biocatalysis and the move toward “greener” chemistry, whether in drug design or synthesis of commodity chemicals. However, the success of any development of an enzymatic transformation, enzyme discovery and/or enzyme engineering will depend mostly on the assay used to measure the activity of interest. Enzyme activity profiling may be used as a tool for identification and

classification of the activity of interest, but assay development plays a crucial role in taking an enzyme from the discovery phase, to one in which the enzyme is a viable commercial protein technology. There was a need for establishing a suitable and reliable assay for measuring nitrilase and/or nitrile hydratase activity in the organism studied herein. At first, an effort was made to find a qualitative assay that would allow quick and easy identification of nitrile-metabolising activity. Hence, a colorimetric assay method using pH-based colour changes was attempted.

Other researchers have determined the rate of nitrile hydrolysis for the isolates *Pseudomonas putida*, *Microbacterium paraoxydans* and *Microbacterium liquefaciens* by measurement using a pH-sensitive indicator-based colorimetric assay [81]. The faster reaction rate of *Pseudomonas putida* was followed by a quicker colour turn from green to yellow than the other organisms, but was confirmed by monitoring the percentage product conversion by HPLC. The colorimetric assay used in the present study was based on that developed by Banerjee *et al*. (2003) [116].

Bromothymol blue was chosen as the pH indicator since its pKa (7.0) is close to that of phosphate buffer. According to Kaul *et al*. (2004) [81] an appropriately matched indicator/buffer pair is required for accurate measurement of dehalogenase activity. Bromothymol blue is most sensitive to pH changes between pH 6.0 and 7.6, and changes from blue/green to yellow with increasing proton concentration generated by the enzyme activity. The BTB concentration in the assay was adjusted in order to increase the sensitivity while maximise the observable colour change. A colour change from blue/green to yellow was visible using both 0.05% and 0.01% (v/v) in solution (in cuvettes). However, the lower concentration was optimal since the colour change was more noticeable. This was also true for the colour change observed around agar wells in which reaction took place. Drawbacks to this assay include low sensitivity and poor differentiation between the reaction mix original colour (blue/green) and positive colour change (yellow). At the lower indicator concentration where colour change is more noticeable, the colour differentiation is poor. High concentrations of purified enzyme were required for a positive colour change suggesting a colorimetric assay of this nature is only selective for either potent or concentrated enzyme. Colour change was not noted when *Rhodococcus rhodochrous* cells were used in the reaction mix, although this culture previously tested positive for nitrilase activity. The organism itself may have its own buffering capacity which masks any colour

change produced by the enzyme. It was also not established whether the kinetic parameters of the enzyme changed upon changing pH, and therefore this assay may only be used as a qualitative indication of acid-forming activity. Indeed, released ammonia could itself buffer carboxylic acid formation. The assay did not seem applicable to whole cell reactions.

Phenylglycinonitrile was acidic (pH approximately 3.5) in both buffer concentrations and therefore not a suitable substrate for this assay. Very hydrophobic nitriles such as adiponitrile would cause solubility problems in the pH-based indicator assay which relies on a buffered solution system for measuring activity. Many nitriles are acidic or relatively hydrophobic in nature and would therefore also be excluded from this assay. Even concentrated commercial enzyme samples separated on non-denaturing PAGE gels could not be detected using colour change, and therefore the assay could not be applied to detecting activity using an overlay method.

After unsuccessful attempts at establishing colorimetric activity assays for the enzymes of interest (based on electrophoretic separation of the enzymes and changes in pH on reaction), a more sensitive fluorimetric assay was tested. The fluorescence-based OPA assay was compared to the HPLC method previously used to detect activity. Fluorimetric methods of measuring enzyme activity are generally far more sensitive than spectrophotometric methods.

The reported nitrilase assay in which the release of ammonia reacted with *o*-phthaldialdehyde and 2-mercaptoethanol forms a fluorescent isoindole derivative is a potentially simple and commercially viable assay [82]. In contrast to the HPLC assay method, the fluorimetric method proved to be unreliable or unreproducible. The linearity of the ammonia standard curve obtained in this study did not compare with that reported by the authors. Activity identification on non-denaturing PAGE gels was tested using the fluorimetric method, but also proved unsuccessful. To be detected, the signal generated requires high concentrations of substrate (100 mM) which implies that only highly concentrated enzyme preparations that are stable in the presence of high concentrations of substrate can be measured using this assay.

Although the assay was originally used testing whole cells of *Rhodococcus rhodochrous* by Banerjee *et al*. 2003 [116], using ammonia release by whole cell suspensions of an

organism to determine activity is also non-specific since ammonia-forming activity may be due to other metabolic activities such as protein turnover. Hence, the origin of ammonia in whole cell suspensions is not defined using this method, and activity measured may be over or under estimated.

4.3 High Performance Liquid Chromatography and Mass Spectrometry

Since HPLC was previously used for measuring nitrilase activity qualitatively and is a well-documented method in nitrilase literature, the development of the method as a reliable and reproducible procedure was undertaken. The commercial nitrilases tested showed different substrate specificity and the relative activities could be accurately and reliably quantified by HPLC. Another advantage of the HPLC method used in the present study is that disappearance of nitrile substrate and appearance of product can be measured simultaneously, providing an internal molar balance with which to ascertain the validity of the results.

Interestingly, the commercial nitrilase from *Rhodococcus rhodochrous* showed only slight activity against benzonitrile, while the NIT-1005 converted all benzonitrile to benzoic acid. Even though it is widely suggested that nitrilases generally have a preference for aromatic substrates, there is large variability amongst nitrilases from different sources [106, 108].

The development of the HPLC method for assaying nitrile converting activity included analysis of nitrile standards, commercial nitrilase reactions, and construction of standard curves of concentration versus absorbance, retention area, and amount for nitrile standards (including benzonitrile, benzamide, benzoic acid, hydrocinnamonitrile, 3-hydroxy-3-phenylpropionitrile and 3-hydroxy-3-phenylpropionic acid). Benzonitrile is less polar than its hydrolytic products, benzoic acid and benzamide, with the latter eluting earliest. Separation of the nitrile and its corresponding amide and acid is effectively achieved using the isocratic elution method described, and the three compounds have roughly one minute time separation in their respective elutions. Benzonitrile and its products can be easily identified by HPLC owing to their predictable elution times and differing lambda maximum absorbance values. The compounds with longer chains, namely

hydrocinnamonitrile, 3-hydroxy-3-phenylpropionitrile and 3-hydroxy-3-phenylpropionic acid, have lambda maximum values closer to each other and are much lower (closer to 200 nm) than benzonitrile and its corresponding acid and amide. Although it is generally not considered reliable to measure compounds in the 200 nm range by HPLC (since many HPLC solvents display absorbance at or near this wavelength), control samples containing reaction buffer and the acidic stop reagent/ elution solvent did not absorb in this region.

Standard curves of the six compounds showed that all were reliably measured in the concentration range zero to ten millimolar, and all displayed linear dependence curves (with R^2 values close to one) of concentration versus absorbance, retention area, and amount. All the compounds, except benzamide, had stable absorbance maxima values in the concentration range tested. At concentrations higher than 7 mM, the absorbance maximum of benzamide was seen to drop slightly, and remained at the lowered value up to 10 mM. The current method used for measuring activity against nitriles or amides, however, uses substrates at a concentration of 5 mM which is within the accurate region for benzamide. In cases where other substrates are tested for activity, the concentration range in which absorbance, retention area and amount are linear should be measured.

Since it was shown that HPLC could be used to measure the six compounds (Table 5) and their conversion accurately in a wide concentration range, the method was further extended to investigate the relationship between activity and time for reactions against benzonitrile, benzamide and 3-hydroxy-3-phenylpropionitrile.

Mass spectral analysis of the above-mentioned 6 nitrile standards was done to confirm the structures, but more importantly to elucidate the subtle differences between 3-hydroxy-3-phenylpropionitrile and its corresponding amide and acid. Due to the relatively lower absorbance lambda maximum values of the arylaliphatic compounds, HPLC may not be the best method of analysis for these compounds. Although their respective retention times differ (4.15 minutes for the nitrile, 3.4 minutes for the amide and 3.8 minutes for the acid), the wavelength maxima of the nitrile and acid are identical (206.5 nm) and the amide product very similar (200.7 nm). This would not normally pose a problem since the data obtained for each have almost negligible standard deviations, but the accuracy of following substances close to 200 nm is not ideal when analysed by HPLC.

Nitriles generally give poor mass spectral data. The smaller nitriles are not well suited to mass spectral analysis and some are too volatile to be measured with certainty. Benzonitrile, benzamide and benzoic acid are problematic in that regard, and even higher sample concentrations did not improve the spectra. The larger nitriles with longer, aliphatic chains, and the products thereof, however, gave better spectra and results comparable with those from a database and the Millenium internal spectra library. 3-Hydroxy-3-phenylpropionitrile and 3-hydroxy-3-phenylpropionic acid could be matched with approximately 97% and 96% certainty to internal standards, and mass spectral analysis is therefore a good method for these types of compounds. Hydrocinnamonitrile, although similar in structure to 3-hydroxy-3-phenylpropionitrile did not give good mass spectral results and could not be matched to internal standards.

Mass spectral analysis could not be used to confirm the structure of the corresponding amide produced from 3-hydroxy-3-phenylpropionitrile. However, the intermediate product produced by *Rhodococcus rhodochrous* ATCC BAA-870 when 3-hydroxy-3-phenylpropionitrile is converted to 3-hydroxy-3-phenylpropionic acid has a stable retention time, and elutes earlier than the nitrile and acid (as expected, and similar to benzonitrile and its corresponding amide and acid). Gas chromatography may be a more suitable method for analysis of the arylaliphatic and volatile nitriles and the corresponding amide and acid thereof.

4.3.1 Different Buffer Types

By HPLC, reactions against benzonitrile, 3-hydroxy-3-phenylpropionitrile and hydrocinnamonitrile were analysed in ten different buffer types to optimise buffer conditions and test the efficacy of the buffer system used for chromatofocusing. Activity observed was qualitative only and the differences observed in the buffers were comparatively measured.

EDTA did not affect the activity against benzonitrile whilst DTT on its own appeared to have a slightly negative effect on activity. The nitrilase activity of *Rhodococcus rhodochrous* J1 was not affected by chelating agents such as EDTA or azide, indicating it lacked a metal-ion requirement [115], and was also unaffected by Fe^{2+} and Mn^{2+} that are inhibitory toward the *Nocardia* sp. NCIB 11216 [117]. The activity of nitrile hydratase

from *Bacillus pallidus* Dac521 was not affected by EDTA [103]. However, it is suggested that chelating data can be misleading since *Rhodococcus rhodochrous* J1 nitrile hydratase reportedly contains 11 atoms of cobalt per mol of active enzyme and its activity is unaffected when dialysed with EDTA for 1 week [113], whereas nitrile hydratase of *Myrothecium verrucaria* which contains 4 mol of zinc per mol of enzyme lost 90% of its activity after dialysis with EDTA for 15 minutes [18].

DTT is included in the buffer as a reducing agent to counteract oxidation of the enzyme. DTT had no negative effect on nitrile hydratase activity in *Rhodococcus rhodochrous* ATCC BAA-870, suggesting that the cysteine residues are maintained in a reduced state at the active site with the concentrations tested. The *Rhodococcus rhodochrous* J1 nitrilase is inactivated by some thiol reagents [115]. The activity of purified J1 nitrilase in the presence of dithiothreitol was six times higher than activity measured without the presence of reductant [115], and DTT was the most effective in restoring activity of nitrilase inhibited by other thiol reagents.

Reactions against hydrocinnamonitrile in different buffer types indicated buffers which caused anomalous effects when measuring substrate levels by HPLC since it was not utilised by the organism. A reduction in the measurable levels of hydrocinnamonitrile at pH 4 was presumably a pH-induced effect, while DTT caused the measurable levels of the substrate to almost completely disappear. HPLC is therefore not suited to measurement of reactions in all buffer types, and is particularly not suited to measurement in buffers that display a wavelength maximum at or near that of the compound being measured (such as imidazole which has the same absorbance maximum as hydrocinnamonitrile and 3-hydroxy-3-phenylpropionitrile).

4.3.2 pH Profiles

The effect of pH on activity (pH 4 to 10) was tested using benzonitrile and hydrocinnamonitrile. Again, no activity was seen against hydrocinnamonitrile at any pH, confirming previous results that showed no product formation from this substrate. The activity maximum against benzonitrile was broad between pH 6 and 7, with the activity gradually decreasing at higher pH but more rapidly at lower pH. The *Rhodococcus rhodochrous* J1 pH profile was examined using benzonitrile as substrate [115], and showed

maximum activity at pH approximately 7.5. The J1 nitrilase had a narrow pH range compared to the broad nitrilase pH ranges found in *Nocardia* NCIB 11215 nitrile hydratase [118] and *Fusarium* [119].

Nitrile hydratase from *Bacillus pallidus* Dac521 had optimum activity between pH 7 and 7.5 and retained greater than 50% activity between pH 6.2 and 8.7 [103]. Its activity rapidly decreased as pH was reduced from the optimum, and at pH 5 it still retained activity although it was 21-fold less than at pH 7. The pH profile of nitrile hydratase from *Bacillus pallidus* Dac521 is similar to the one tested in this study, and similar to the pH dependence of mesophilic enzymes which have pH optima in the pH 7 – 7.5 range [103, 120]. It is not known whether the rapid loss of activity at reduced pH is due to subunit dissociation, denaturation, or a change in ionization of critical active site residues. A change in ionization states is probable since catalytic thiol residues generally have a pK_a of approximately 4.6, and in nitrile hydratase may play a role in the catalytic mechanism of the enzyme. However, according to Huang *et al*. (1997) [34], the thiolate ligands of *Rhodococcus* sp. R312 nitrile hydratase coordinate the Fe^{III} cofactor rather than participate in the catalytic process itself. All known mesophilic nitrile hydratases contain a catalytic metal ion cofactor. *Rhodococcus rhodochrous* N771 [121] and *Rhodococcus* R312 [122] nitrile hydratases, for example, contain Fe^{III} chelated by thiolate ligands, *Rhodococcus rhodochrous* J1 nitrile hydratase contains non-corrinoid cobalt [123] and *Myrothecium verrucaria* nitrile hydratase contains zinc [18].

It is possible that the enzymes may precipitate out at their isoelectric point, and hence their activity may not be accurately quantified even though the enzyme is viable. Protein solubility is affected by pH and is minimal at its isoelectric point. Most proteins have a pI in the acidic range. The broad pH range in which *Rhodococcus rhodochrous* ATCC BAA-870 activity can be measured suggests flexible assaying procedures may be possible with this organism, and highlights its use as a potential industrial bioconversion tool.

4.3.3 Time Course Activity Study

The activity of interest displayed by the isolated *Rhodococcus rhodochrous* was explored, and reaction times were optimised to ensure sampling for HPLC was done in the linear region. The activity of this organism was previously sampled after reaction for two hours

[106]. The linear region of activity against benzonitrile occurs within the first ten minutes of reaction, and hence the sampling time for this activity has been dramatically reduced. The benzamide produced from benzonitrile is itself utilised within 60 minutes, and if the reaction time was extended and sampled after this, it could easily be assumed that benzoic acid is the only product. Reactions against benzamide only confirmed the activity against benzamide which was first produced from benzonitrile, and also showed that benzamide is utilised within 60 minutes of reaction. The linear sampling times when testing activity against benzamide and 3-hydroxy-3-phenylpropionitrile is now performed in 20 minutes, again a much reduced reaction time.

The activity against the amide in *Rhodococcus rhodochrous* ATCC BAA-870 is likely the rate-limiting step in production of acid from nitrile. The production of acid is rapid and occurs in under ten minutes, whereas production of amide from this acid occurs over a much longer time frame. The nitrile hydratase may be an efficient enzyme with high turnover (relative to the amidase). It is possible that although the two enzymes are co-transcribed, the amidase may be transcribed at a lower rate than the nitrile hydratase. However, it is more likely that the two enzymes differ with respect to their kinetics towards the selected unnatural substrates.

The stoichiometry of nitrile consumption and amide or acid formation from the hydrolysis of nitrile was examined in reaction mixture containing 50 mM potassium phosphate pH 7.4, 6.2 ± 0.2 μmol benzonitrile, and enzyme in a final reaction volume of 1.5 ml. After the chosen reaction incubation time, the amounts of benzonitrile, benzamide and benzoic acid in the reaction mix were determined. The maximum amounts of benzamide and benzoic acid formed from benzonitrile was 2.2 μmol and 6 μmol respectively. All the benzamide was converted to benzoic acid. The amount of benzonitrile remaining after the reaction was run until completion was 2 μmol. The results indicated that the total amount of benzoic acid and benzamide formed from benzonitrile was approximately 6.2 μmol, and product formation is stoichiometric with the consumption of benzonitrile. The possibility of the reverse reaction was investigated (data not shown) but the formation of amide or nitrile from benzoic acid was not detected, even when reacted for over 2 hours. Utilisation of benzamide shows that the amide is an intermediate in the nitrile hydrolysis pathway of the nitrile-metabolising enzymes involved, and hence it is suspected that the nitrile hydrolyis is

due to a nitrile hydratase and amidase combination rather than a nitrilase. During enzyme kinetic studies of the J1 nitrilase, it was shown that benzamide was not formed from benzonitrile, and benzoic acid was formed stoichiometrically with the consumption of nitrile [115].The major product of a ricinine nitrilase purified from a pseudomonad was the corresponding acid, but approximately 9% of the substrate was converted to the amide [124].

Conversion of 3-hydroxy-3-phenylpropionitrile to product was linear over 20 minutes under the conditions used. Elution of nitrile hydratase activity for benzonitrile in chromatography experiments was seen to always coincide with activity against 3-hydroxy-3-phenylpropionitrile, and therefore the reaction kinetics of nitrile hydratase against benzonitrile and 3-hydroxy-3-phenylpropionitrile is different. Benzonitrile is converted to benzamide more rapidly than the conversion of the arylapliphatic nitrile 3-hydroxy-3-phenylpropionitrile, and therefore the nitrile hydratase in *Rhodococcus rhodochrous* ATCC BAA-870 has a preference for the small aromatic nitrile.

Although most biocatalysts are inherently labile, the proposed nitrile hydratase and amidase enzymes responsible for nitrile metabolism in the organism studied, are reasonably stable. When reacted for 2 hours at 30 degrees, all substrate is converted to product, and since no starting material remains, it can be safely assumed that the biocatalyst itself does not lose activity within the given reaction time frame. In addition, the relatively wide pH profiles and ability to convert substrate in the presence of methanol support the notion that the catalyst stability is high when activity is derived from cell extracts.

4.3.4 Protein Concentration Effects

The previous assay tested required at least 1 mg/ml of purified commercial enzyme preparation to detect activity (the pH-based colorimetric assay) and the OPA-based fluorimetric assay showed no measurable activity even at this concentration. The levels of protein required to measure activity by HPLC are, however, considerably lower. The activity of interest was part of a total protein cell-free extract and not purified enzyme. Benzonitrile conversion to benzoic acid (via benzamide) is evident at concentrations as low as 0.2 mg/ml protein when reacted for 20 minutes, and formation of benzoic acid was

linear with respect to concentration. However, since benzamide was not detected and presumably immediately converted to benzoic acid, the concentration of protein used was reduced and the reactions were reacted for only ten minutes. Appearance of benzamide produced from benzonitrile, and its subsequent conversion to benzoic acid can be followed when the concentration of protein is reduced and reacted for ten minutes. When benzamide was the substrate, its conversion to benzoic acid occurred at higher concentrations than when it was first formed from benzonitrile. The level of benzamide dropped at concentrations higher than 0.4 mg/ml and was completely converted to benzoic acid only when the concentration reached 0.9 mg/ml. The results once again suggest that the formation of benzoic acid from benzamide is rate-limiting, while formation of benzamide from benzonitrile occurs within seconds to minutes. Interestingly, conversion of 3-hydroxy-3-phenylpropionitrile to product also occurs at protein concentrations lower than 0.29 mg/ml, and all substrate was converted within the given reaction time. Activity against 3-hydroxy-3-phenylpropionitrile and benzonitrile follow similar trends and therefore may be due to the same enzyme, or perhaps two different enzymes with great affinity for both substrates (e.g. isozymes). The amidase activity, however, has clearly different reaction characteristics to the activity attributed to nitrile hydratase. *Rhodococcus rhodochrous* ATCC BAA-870 was previously selected on 3-hydroxy-3-phenylpropionitrile and the organism therefore has a natural affinity for the substrate.

Reactions against both benzonitrile and benzamide are linear up to 1.93 mg total protein concentration per reaction (1.5 ml total volume). This effectively will reduce the concentration of enzyme used for these reactions since they can be measured at concentrations lower than those previously used. Also, since this is total protein, and not necessarily purified, the levels of purified protein needed for reaction was possibly very low. It was highly probable that these enzymes of interest were either potent with high activity per mg protein, or that a large proportion of the protein was induced enzyme. It is suggested that the nitrile-converting enzymes in *Rhodococcus rhodochrous* ATCC BAA-870 are more likely very active against the substrates tested, rather than concentrated.

4.4 Column Chromatography

4.4.1 Chromatofocusing

Prior to attempting chromatofocusing of the cell-free extract of the *Rhodococcus rhodochrous* biocatalyst, the pI profiles of other organisms were evaluated. Ampholyte electrofocusing of *Rhodococcus rhodochrous* J1 indicated the nitrilase had a pI of 5.6, which was similar to a calculated pI derived from a *Klebsiella* bromoxynil-specific enzyme nucleotide sequence [115]. *Bacillus pallidus* Dac521 has two nitrile hydratase isoforms with pIs of 4.7 and 5.48. Generally, mesophilic nitrile hydratases have pI values ranging from 3.6 [51] to 5.7 [125]. Within the nitrilase/nitrile hydratase enzyme classes, it is evident that the enzyme properties differ greatly according to species and that isoforms of the enzymes with differing properties exist. Although measured pI values for these enzymes differ, it can generally be said that they fall within the acidic range. The theoretical pI for all known Rhodococcal and Pseudomonal nitrile hydratases from the Swiss-Prot and TrEMBL database was calculated based on their known sequences and compared (Appendix 5.3). Rhodococcal theoretical pI values ranged from 4.87 to 5.3 and all were acidic. The theoretical pI for the cobalt-containing high-molecular weight NHase (P21219 and P21220) was calculated using the ProtParam tool at the Expasy Proteomics Server [126]. Based on the primary sequence of the enzyme, the theoretical pI for the heterodimeric enzyme was calculated to be 5.3 (see Table in Appendix 5.3). A pH 7 to 4 elution gradient was therefore proposed to be suitable for the attempt of this technique.

The elution profile obtained showed the majority of proteins contained in the soluble protein fraction of *Rhodococcus rhodochrous* eluted at pH 4 and less. Unfortunately, while the protein mix initially applied to the column was active against nitriles, none of the fractions tested positive for activity and hence no detectable activity could be traced to any fractions. Although Polybuffer does not reportedly interfere with many protein assays, components of Polybuffers adhere to certain proteins thereby affecting their assaying methods. For example, Polybuffer forms a complex with copper ions and therefore interferes with the Lowry method for measuring protein concentration. It may be possible that the ampholytes in Polybuffer inhibit nitrile-hydrolysing enzyme activity, either by binding at the enzyme active site, or by blocking the formation of active enzyme multimers.

The pH of the post fractionation assay mixture showed that the pH of the reaction mix was not responsible for the lack of detectable activity. The lack of measurable activity may possibly be due to a dilution problem. It has been previously reported that nitrile hydratases are labile to dilution, and can be stabilised by addition of organic acids such as valerate or butyrate [120]. When dialysed against buffer that did not contain organic acid, the iron-containing nitrile hydratase from *Rhodococcus* sp. R312 released iron molecules essential to catalytic activity [29]. The same has not been reported with cobalt-containing nitrile hydratase.

Another possible problem was that the buffer system used with chromatofocusing may not have been compatible with the current method of HPLC analysis. The amount of benzoic acid formed from benzonitrile when reacted with Polybuffer 74 containing 5 mM DTT was shown to be different at different pH's even though reaction conditions were identical. Figure 34 showed more benzoic acid produced at pH 6 than at pH 7.4, with the least amount produced at pH 4. Since activity against the same substrate may be different at different pH's, fractions eluting from a chromatofocusing column should be brought to the same pH before adding it to the reaction mixture. This could, however, cause further dilution problems which may also affect the ability to quantitatively detect activity. Benzoic acid formation from benzonitrile could be measured when reacted in imidazole buffer and therefore the chromatofocusing buffer should not have affected measurable activity.

The loss of orange colour from supernatant applied to the chromatofocusing column (colour which was associated with nitrile-converting activity in both gel exclusion- and ion exchange chromatography-eluted fractions) may indicate a reason for loss of detectable activity within those fractions. Since activity could be associated with the colour, loss of colour may likewise indicate a loss of activity, and may prove that metal chelation at the enzyme active site was interfered with by the polybuffer ampholytes, either directly (by binding to the active site metal) or through interaction with the sulphur containing residues (including the modified oxidised ones). Nitrile hydratase has two cysteine residues and three histidine residues involved in catalysis at the active site. Chromatofocusing has not been done by anyone else on this class of enzymes to the best of our knowledge.

Chromatofocusing has given insight as to the pI range of the enzymes of interest in the organism, but may not necessarily be used in conjunction with the current HPLC method of measuring or screening for activity. To overcome the problem of loss of activity with separation using chromatofocusing, traditional methods of chromatographic separation of enzymes were applied.

4.4.2 Gel Exclusion

Most NHase, amidase and nitrilase enzymes are high molecular weight, multimeric assemblies, and many of these form multimers in the presence of substrate only. *Nocardia* enzymes [117, 118] and *Fusarium* enzyme [119] form active high-molecular-mass aggregates. This could be the case for the amidase activity seen in this organism. Unexpectedly, although the sample applied to the column showed amidase activity, it was absent in the collected fractions. The amidase in this organism may be made up of α- and β-subunits greatly differing sizes, and hence may have eluted in different fractions. Although it was shown using protein concentration studies that the enzyme concentration required for benzamide hydrolysis was higher than that required for benzonitrile, the reactions were reacted for at least 2 hours, during which measurable levels of product should have been detected by HPLC.

Since the fractions containing activity of interest eluted near the column void volume, it was estimated that the enzymes responsible for the activity are high molecular weight multimeric enzymes. This is not uncommon for nitrilases, nitrile hydratases or amidases. A nitrilase from *Rhodococcus* sp. NCIB 11216 forms a benzonitrile-induced 560-kDa dodecamer from association of a 47-kDa monomer, and this is accelerated by increased temperature and enzyme concentration [117, 127]. Similarly, *Rhodococcus* ATCC 39484 nitrilase has a substrate-induced aggregation of 40-kDa subunits to form a 560-kDa complex [26]. An enantiomeric homooctomeric amidase purified from *Agrobacterium tumefaciens* strain d3 was estimated to be 490 kDa and composed of 63 kDa subunits [128].

The subunit molecular weights estimated using SDS-PAGE show that the putative nitrile and amide hydrolysing enzymes may be made up of 21, 48, 56, or 84 kDa subunits. The 48 kDa band density was double that of the smaller bands, indicating that subunits of that size

are in the majority. The 56 and 84 kDa protein bands were of similar density and therefore may represent the subunits of a two-subunit heteromer. NHases generally contain two subunits (α and β), with both subunits having a molecular weight of approximately 23 kDa, and two αβ heterodimers associate to form the $(\alpha\beta)_2$ tetramer. Mesophilic nitrile hydratases have native molecular masses ranging from 54 kDa (*Pseudomonas putida* [129]) to 530 kDa (*Rhodococcus rhodochrous* J1 [113]) and are usually composed of distinct α and β subunits which are typically between 22 and 29 kDa, respectively [57, 130]. The cyanide dihydratase of *Bacillus pumilus* is a multimer of 18 subunits with a total molecular mass of 672 kDa [131]. The α subunit is, by convention, the smaller subunit in nitrile hydratase enzymes. It is possible that the same enzyme may be a mixed molecular weight species such as the high and low molecular mass nitrile hydratase from *Rhodococcus rhodochrous* J1. *Rhodococcus rhodochrous* J1 produces two forms of nitrile hydratase, a high-molecular mass enzyme of approximately 520 kDa and a low-molecular mass enzyme of approximately 130 kDa, depending on the inducer added to the culturing media. Both enzymes are composed of α and β subunits, with the high-molecular mass enzyme made up of nine or ten subunits, and the smaller enzyme of two of each subunit. In *Rhodococcus rhodochrous* J1, the expression of both high- and low-molecular mass nitrile hydratases is regulated at the transcriptional level by the levels of reaction product (amide) present [132].

Gel exclusion chromatography has shown that the activity of interest in *Rhodococcus rhodochrous* ATCC BAA-870 is a result of high-molecular weight protein, and possibly is higher than the previously reported values for nitrile hydratase. Many amidases are high molecular weight enzymes. For example, *Rhodococcus erythropolis* MP50 is 480 kDa [50] and *Agrobacterium tumefaciens* d3 is a 490 kDa protein made up of 63 kDa subunits [128]. The notion that nitrile hydratase and amidase in *Rhodococcus rhodochrous* ATCC BAA-870 are both made of relatively big subunits is therefore supported by the previously published values. If the α- and β-subunits of nitrile hydratase *Rhodococcus rhodochrous* ATCC BAA-870 were roughly 21-26 kDa in size, it may be possible that tightly associated αβ units were responsible for the 48 kDa size, and $\alpha_2\beta_2$ units for the 84 kDa size noted in SDS-PAGE gels. This would be true only if the reducing conditions in SDS-PAGE were not strong enough to ensure complete separation of the subunits making up the proposed high molecular weight nitrile hydratase. The amidase subunits would then be due to the 56

kDa band noted, which is the most commonly reported subunit size for amidase enzymes [128].

The rose colour evident in fraction five adds an interesting point for thought. The colour can be correlated with high activity, and good cell disruption shows increasing colour intensity. Not only is this colour a useful marker, but it is associated with NHase activity and is an interesting route for further investigation. It is possible that, although not confirmed, the colour may be due to cobalt or iron ions contained within the active site of nitrile hydratase.

4.4.3 Ion Exchange

It is suggested that the benzonitrile degradation activity detected in fractions was only due to a nitrile hydratase and amidase, and not a nitrilase as was previously thought. All purification procedures were carried out at room temperature, indicating the thermal stability of the enzymes was reasonably high. Most mesophilic nitrile degrading enzymes (such as *Nocardia* sp. 11216 nitrilase [117] and *Pseudomonas chlororaphis* nitrile hydratase [120]) are purified at temperatures below 4 °C due to their thermal instabilities.

Although previously postulated on the basis of gel exclusion studies that the enzyme, when induced, may form a large proportion of the total protein, it is seen in the elution profile that the activity peaks do not necessarily correspond with elution peaks in which protein is concentrated. Therefore, the assumption that the activity of interest is due to a potent, rather than concentrated enzyme, is further supported.

Gel exclusion chromatography indicated that nitrile hydratase activity eluted at high molecular weight which constituted the majority of eluting proteins. It could be said that a large proportion of the soluble protein fraction of *Rhodococcus rhodochrous* ATCC BAA-870 contains nitrile hydratase and that the organism overproduces the enzyme. The relatively slow reaction kinetics against 3-hydroxy-3-phenylpropionitrile would support this. However, elution of proteins using ion exchange chromatography indicated that although the activity eluted within a protein peak, it did not constitute the majority of eluted proteins. Nitrile hydratase is therefore produced in the organism in fair amounts, but is more likely a potent enzyme.

Ion exchange fractions with activity also had a rose-coloured appearance. The absorbance spectrum obtained confirmed the difference in absorbance between the coloured and clear fractions, with the coloured fraction showing a broad absorbance shoulder between 300 to 500 nm. The colouring of active fractions is likely enzyme-associated, and may be due to the type of ion associated at the active site. *Pseudomonas* [120] and *Brevibacterium* [122] nitrile hydratases are composed of two subunits (α and β) containing tightly bound iron [38], and exhibit broad absorptions in the visible range with an absorption maximum at 720 nm and a broad shoulder at 300 – 500 nm. A concentrated solution of highly purified cobalt-containing nitrile hydratase from *Rhodococcus rhodochrous* J1 exhibited a broad absorption spectrum in the visible range, with an absorption maximum at approximately 410 nm [113]. With one cobalt atom per α-subunit, a high molecular weight nitrile hydratase concentrated in one or two fractions could very likely exhibit colour.

Separation of nitrile hydratase and amidase activities suggests the nitrile hydratase and amidase enzymes in *Rhodococcus rhodochrous* can be purified using ion exchange chromatography alone. In conjunction with gel exclusion chromatography, a quick and simple method of purification for the nitrile-hydrolysing enzymes is possible, and is a vast improvement from the previously reported laborious eight- and six-step purification protocols for nitrile hydratase [104, 133]. The isolation of nitrile hydratase and amidase enzymes from *Rhodococcus rhodochrous* ATCC BAA-870 to a great degree of purity may not be necessary provided that no interfering contaminating activity is present. The degree of purity of commercial enzymes ranges from highly purified to raw protein preparations depending on the application. A partially purified enzyme preparation is more cost effective for industrial application and therefore preferred to highly purified enzymes. The application of the enzyme preparation from *Rhodococcus rhodochrous* ATCC BAA-870 is suited to analytical purposes since it is free of stabilizers and preservatives, and is easy to pipette. It is also easily stored frozen for long periods of time without a loss in activity. Only benzamide was formed from benzonitrile in ion exchange fractions when the procedure was optimised, and therefore nitrile hydratase was in those fractions. The activity against 3-hydroxy-3-phenylpropionitrile in the same fractions supports the findings that nitrile hydratase converts the β-hydroxy substrate. Amidase activity was lost when fractions were separated using the shallower salt gradient in ion exchange, and when gel exclusion fractions were collected over a longer elution. It is suggested that the amidase in

Rhodococcus rhodochrous ATCC BAA-870 either requires some other component of protein for activity, or is easily disassociated into subunits which eliminates activity.

4.5 General Discussion

Monosubstituted benzonitrile derivatives with hydroxyl groups were suitable substrates for the enzymes found in *Rhodococcus rhodochrous*. Hydrocinnamonitrile was not hydrolysed but 3-hydroxy-3-phenylpropionitrile could be utilised. The *Rhodococcus rhodochrous* ATCC BAA-870 enzymes are suited to hydrolysis of the aromatic nitrile, benzonitrile, and arylaliphatic nitrile, 3-hydroxy-3-phenylpropionitrile. It is postulated that the enzyme's nitrile-binding site may have a high affinity for an aromatic ring. It has generally been accepted that aliphatic-specific nitrile hydratases have low specificity for aromatic nitriles. However, it is possible that certain nitriles act as high affinity inhibitors rather than substrates, as suggested by some studies. For example, benzonitrile-induced inhibition of *Bacillus pallidus* Dac521 nitrile hydratase activity is irreversible [103], and nitrile hydratases of *Corynebacterium nitrilophilus* [134] and *Rhodococcus* R312 [122] are inhibited by α-hydroxynitriles and isobutyronitrile respectively. Absence of activity against certain nitriles may be due to structural gene expression repression or inhibition of expressed nitrile hydratase activity.

Hydrocinnamonitrile appears to not be utilised/ converted by any enzyme present in supernatant of *Rhodococcus rhodochrous* when tested routinely according to the protocol laid out in the methods section. The bulkiness of the substrate should not be a factor in its inability to be utilized, since 3-hydroxy-3-phenylpropionitrile was converted even though it has an extra hydroxyl group in its structure.

Most nitrilases produce only the corresponding acid and ammonia as products. However, purified nitrilases from *Rhodococcus rhodochrous* ATCC39484 [26], *Pseudomonas* DSM7155 [93] and *Fusarium oxysporum* f.sp. *melonis* [135] produce a small amount of amide product, and therefore have nitrile hydratase activity as well. In these cases the amount of amide produced is less than 5% of the total product formed. The AtNIT1 enzyme of *A. thaliana* has high nitrile hydratase activity against some substrates but not with others. For example, the ratio of amide to acid produced from fumaronitrile was 93:7,

while from crotonitrile it was 1:99 [136]. The nitrilase of *Rhodococcus rhodochrous* J1 utilises benzamide at a rate of 0.00022% compared to benzonitrile, and therefore has measurable nitrile hydratase activity [15]. The enzyme mechanism proposed by Kobayashi *et al*. (1998) explains the activities mentioned above by proposing two possible routes of nitrile degradation. The tetrahedral intermediate formed by nucleophilic attack of the nitrile carbon atom by nitrilase is broken down to the acid in most cases, but can also be released as an amide. Whether the amide product is a by-product from nitrile hydratase activity, or a result of premature release of substrate from the enzyme-ligand complex, many organisms have dual nitrilase and nitrile hydratase/amidase enzyme systems. It is therefore possible for an organism to have both the nitrilase and nitrile hydratase/amidase enzyme systems, while only one system is selectively used depending on the conditions of induction and/or reaction. Nitrilase in *Rhodococcus rhodochrous* J1, for example, can be selectively induced using valeronitrile without affecting the expression of nitrile hydratase and amidase, and vice versa [15].

Although the organism studied herein shows distinct nitrile hydratase/amidase activity as measured by the conversion of benzonitrile and 3-hydroxy-3-phenylpropionitrile to their respective amides, the existence of a nitrilase within *Rhodococcus rhodochrous* ATCC BAA-870 can not be entirely ruled out. A wider set of reaction substrates, or indeed different induction substrates, could show the presence of a nitrilase. In general, the ability of one nitrile-converting organism to selectively use an enzyme set depending on reaction parameters and/or induction conditions, further lends favour to their versatility as biocatalysts in industrial applications.

4.6 Conclusion

Enzymes that hydrolyse nitriles have enormous potential as industrial biocatalysts in that they can provide the common functional groups of amides and carboxylic acids subsequent to the facile chemical addition of a carbon to a simpler (and cheaper) substrate. Using a chosen nitrile substrate such as benzonitrile as the sole nitrogen source during simple enrichment culturing isolates bacterial enzyme systems that are adapted to metabolism of the substrate of interest. The microorganism which formed the basis of the current study, *Rhodococcus rhodochrous* ATCC BAA-870, converted benzonitrile to benzamide and benzoic acid, and also converted the β-hydroxynitrile, 3-hydroxy-3-phenylpropionitrile to the corresponding amide and acid. Increasing the concentration of biocatalyst caused faster conversions, and extending the reaction time allowed complete conversion of all substrate to product. The mild hydrolysis of the β-hydroxynitrile would be of value as a biotransformation process since the substrate is prone to elimination reactions in harsh reaction conditions.

The main objective of a biocatalytic process would be a high degree of selective substrate conversion within the shortest possible time, and for this reason the benzonitrile-converting enzyme found in *Rhodococcus rhodochrous* (which converted 5 mM benzonitrile to benzamide in less than 10 minutes) is identified as an enzyme worthy of further investigation for practical applications in industry. The reasonably stable enzymes would allow flexibility in an industrial bioconversion process. The enzyme system was identified as a nitrile hydratase that converts the aromatic benzonitrile to the corresponding amide, and a putative amidase subsequently converts the aromatic amide, benzamide, to benzoic acid. Inhibiting the amidase would allow stopping the reaction at the amide intermediate.

Although certain colorimetric assays may be useful in detecting potent nitrile-hydrolysing activity during the biocatalyst screening process, they are unreliable and nonspecific. HPLC remains the most reliable quantitative method for determination of nitrile activity, but is not suitable for high-throughput screening. The multistep process of measuring activity by HPLC may be a drawback to the assay, as is the lengthy processing of samples.

Nitrile hydratase activity in *Rhodococcus rhodochrous* ATCC BAA-870 has useful colour-association, and can be separated from amidase activity using ion exchange chromatography. Gel exclusion chromatography has shown that both the nitrile hydratase and amidase enzymes in *Rhodococcus rhodochrous* ATCC BAA-870 are high molecular weight native structures, and are suited to conversions of mono-substituted aromatic nitriles such as benzonitrile and the β-hydroxy nitrile, 3-hydroxy-3-phenylpropionitrile. The enzymes appear to have a broad pH range, fast reaction times, and are relatively stable. Nitrile hydratase and amidase from *Rhodococcus rhodochrous* ATCC BAA-870 are potentially useful enzymes which could be applied to biocatalysis in industry.

5 Appendix

5.1 Standard Curves

Ammonia concentration standard curve:

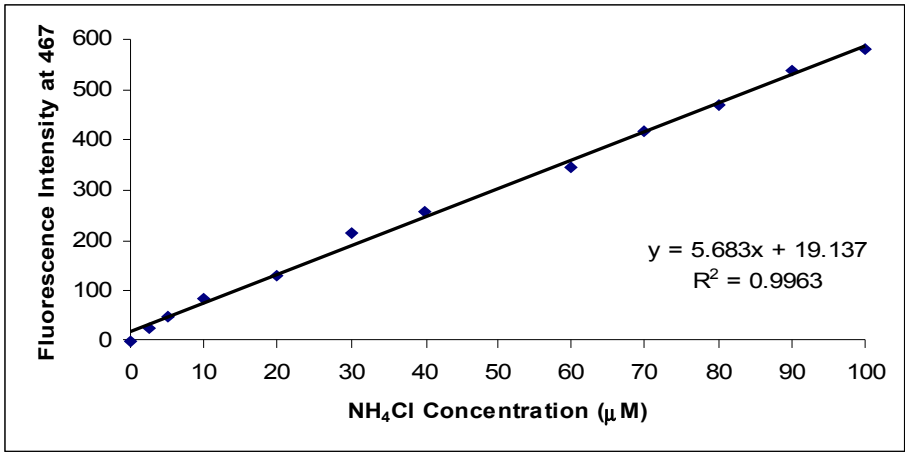


Figure 56: NH_4Cl Standard curve.

Increasing concentrations of *o*-phthaldialdehyde derivatised ammonia were measured using a PerkinElmer LS 55 fluorescence spectrometer. Excitation and emission wavelengths were set at 412 and 467 nm respectively.

Example of a bovine serum albumin concentration standard curve using the BioRad assay:

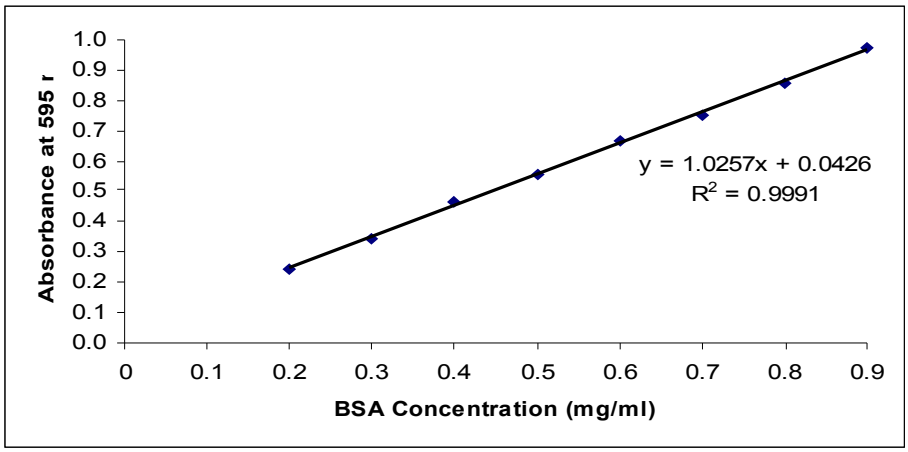


Figure 57: Sample BioRad protein concentration determination standard curve.

BSA standards in the range 0.2 – 0.9 mg/ml were prepared in duplicate, and 100 µl of each added to 5 ml protein concentration determination dye reagent. Standards were incubated at room temperature for a minimum of 5 minutes. The absorbance at 595 nm was read using a Beckman Coultier DU 800 Spectrophotometer. Unknown samples were prepared and the concentration determined from the standard curve.

Example of an SDS-PAGE size marker standard curve:

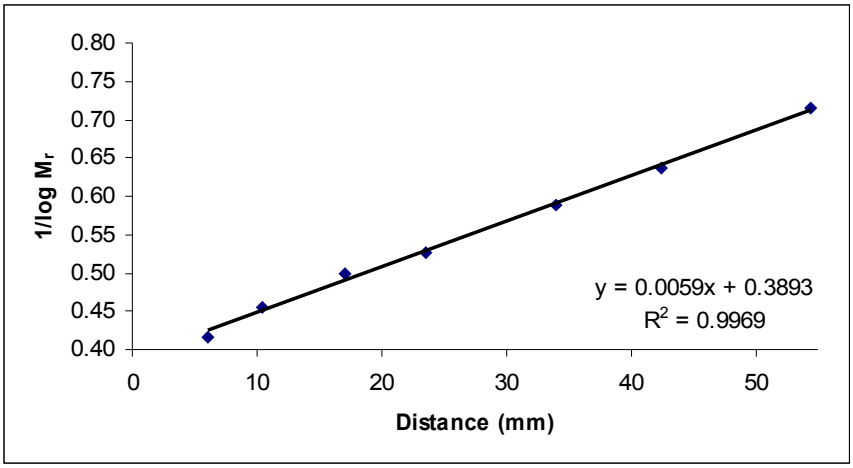


Figure 58: Standard curve of 10% SDS-PAGE size markers.

Relative molecular mass markers 250 000, 150 000, 100 000, 75 000, 50 000, 37 000 and 25 000 were run on a 10% SDS polyacrylamide gel at 150 V using a BioRad mini Protean gel system, and their distances measured. A standard curve was constructed for estimation of unknown sizes by plotting the marker 1/log M_r versus distance (mm).

Gel exclusion standard curve:

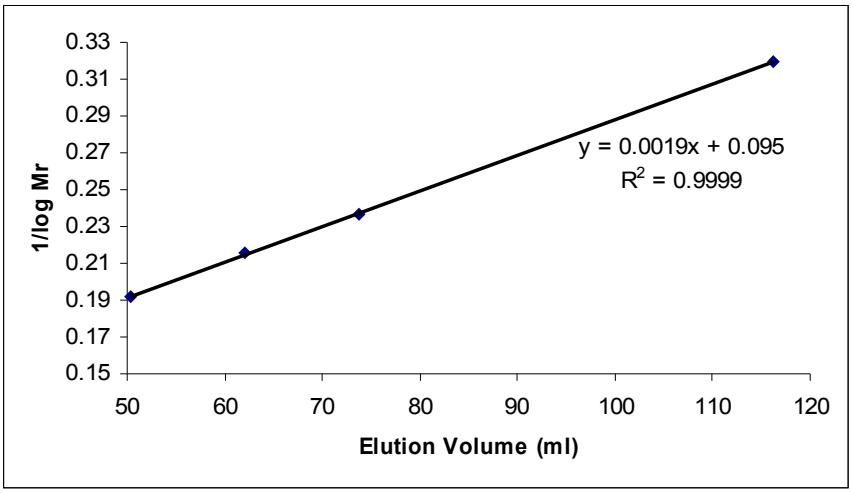


Figure 59: Sephacryl S-200 gel exclusion standard curve.

Gel exclusion standards were eluted from a Sephacryl S-200 gel exclusion column run at a 0.7 ml/min flow rate using 100 mM potassium phosphate buffer, pH 7.4, containing 0.02% (w/v) sodium azide. A standard curve of 1/log M_r versus elution volume was constructed for estimation of eluting proteins of unknown size.

5.2 Chromatography

The elution profile of Sephacryl S-200 gel exclusion size standards from BioRad is shown in Figure 60.

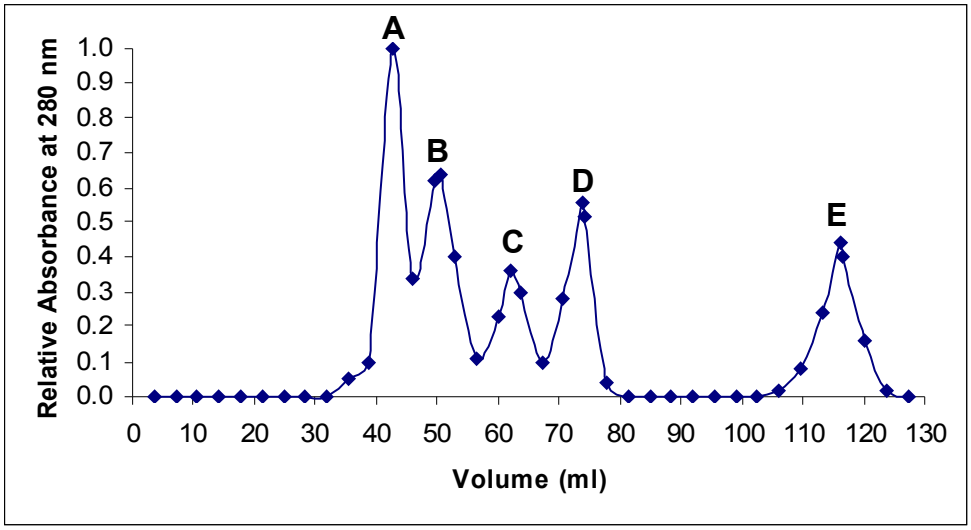


Figure 60: Sephacryl S-200 gel exclusion standard elution profile.

Protein Standards of relative molecular mass A to B are Thyroglobulin (670 000), Gamma globulin (158 000), Ovalbumin (44 000), Myoglobin (17 000) and Vitamin B_{12} (1 350). The column was equilibrated using 100 mM potassium phosphate buffer, pH 7.4, containing 0.02% (w/v) sodium azide, and 1 ml of a 4.5 mg total standard concentration loaded. Standards were eluted using a flow rate of 0.7 ml/min and the A_{280} monitored.

A selectivity curve was constructed according to the protocol in the Gel Filtration Handbook by Amersham Biosciences. The curve shows the molecular weight size ranges that elute with accuracy using the Sephacryl S-200 gel exclusion column (Figure 61). The column void volume (V_o) was determined from the elution of Blue Dextran (2 000 000 Da) and found to be 43 ml. Molecular weights were estimated by comparison of the ratio of Blue Dextran elution volume/void volume to those of the standards. The calibration curve was prepared by measuring the elution volumes of several standards and calculating their corresponding K_{av} values:

$$K_{av} = V_e - V_o / V_t - V_o$$

where V_e = 43 ml, Vt = 111 ml, and V_o the elution volume for each standard. The standard Kav values were then plotted versus the logarithm of their molecular weight (Figure 61).

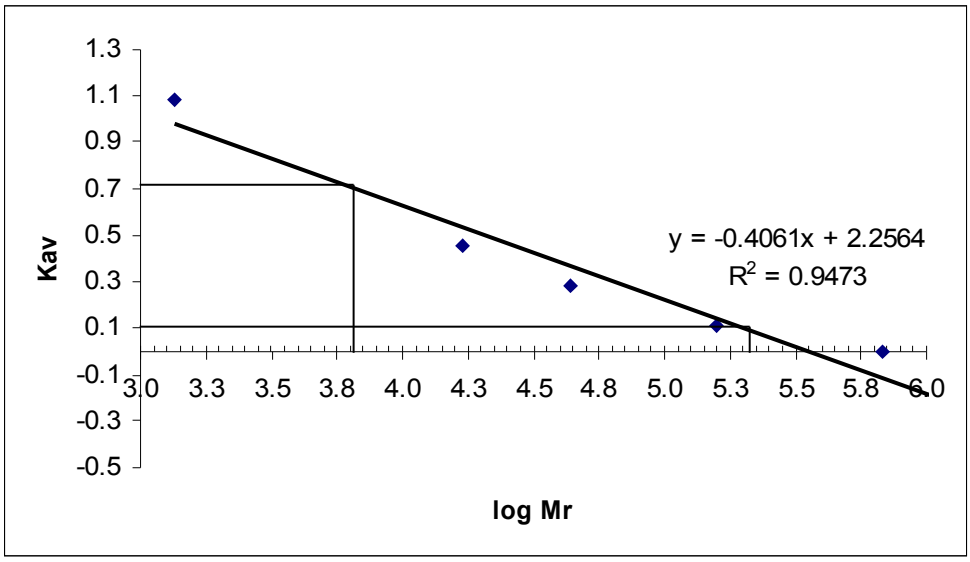


Figure 61: Sephacryl S-200 gel exclusion selectivity curve.

The column void volume (V_o) was determined from the elution of Blue Dextran (2 000 kDa) at 0.7 ml/min using 100 mM potassium phosphate buffer, pH 7.4, containing 0.02% (w/v) sodium azide. Molecular weights were estimated by comparison of Blue Dextran elution volume/void volume ratio to that of standards. Standards and unknowns were eluted using a flow rate of 0.7 ml/min and the A_{280} monitored.

The K_{av} = 1 to K_{av} = 7 is the accepted linear range for a selectivity curve and determines the fractionation range of the gel exclusion medium. The exclusion limit indicates the size of molecule that is excluded from the gel pores and therefore elutes in the void volume.

The apparent molecular weight contained within each eluting fraction was calculated for the Sephacryl S-200 column (Table 8). The molecular weight of an unknown substance can be determined from the calibration curve once its K_{av} value is calculated from its measured elution volume.

Table 8: Apparent molecular weight of the proteins within each Sephacryl S-200 gel exclusion fraction as estimated by comparison of the ratio of elution volume/void volume of Blue Dextran to that of molecular weight standards

Fraction Number	Elution Volume	Apparent Molecular Weight Within Each Fraction
1	8	1174897600
2	16	93325400
3	24	12882500
4	32	2630300
5	40	707900
6	48	234400
7	56	93330
8	64	41690
9	72	20420
10	80	11220
11	88	6460
12	96	3980
13	104	2630
14	112	1780
15	120	1260
16	128	910
17	136	680

The column was run at a 0.7 ml/min flow rate using 100 mM potassium phosphate buffer, pH 7.4, containing 0.02% (w/v) sodium azide.

5.3 Nitrile Hydratase Theoretical pI

Table 9: Theoretical pI values of different nitrile hydratase enzymes from Rhodococcal and Pseudomonad species

NHase Type	Swiss-Prot Number and Code		Organism	Reference	Theorotical pI*		
	α subunit	β subunit			α subunit	β subunit	αβ unit
Cobalt-containing	Q7SID2 NHAA_PSETH	Q7SID3 NHAB_PSETH	*Pseudonocardia thermophila*	Yamaki *et al.* (1997)	4.89	5.42	**5.12**
Cobalt-containing	P97051 NHAA_PSEPU	P97052 NHAB_PSEPU	*Pseudomonas putida*	Payne *et al.* (1997)	5.44	5.97	**5.71**
Cobalt-containing low molecular weight	P29378 NHA2_RHORH	P29379 NHB2_RHORH	*Rhodococcus rhodochrous*	Kobayashi *et al.* (1991)	4.93	4.92	**4.93**
Cobalt-containing high molecular weight	P21219 NHA1_RHORH	P21220 NHB1_RHORH	*Rhodococcus rhodochrous*	Kobayashi *et al.* (1991)	4.85	5.86	**5.3**
Iron-containing	P27764 NHAA_PSECL	P27763 NHAB_PSECL	*Pseudomonas chlororaphis*	Nishiyama *et al.* (1991)	5.16	5.8	**5.55**
Iron-containing	P13448 NHAA_RHOER	P13449 NHAB_RHOER	*Rhodococcus erythropolis*	Ikehata *et al.* (1989)	4.79	4.93	**4.87**
Iron-containing	Q53118 NHAA_RHOSO	Q53117 NHAB_RHOSO	*Rhodococcus* sp.	Mayaux *et al.* (1991)	4.57	5.12	**4.79**

*Theorotical pI values were calculated using the ProtParam tool from ExPasy [Gasteiger *et al*. (2005)] as deduced from the protein sequence and assuming there is no post-translational modification of the protein.

5.4 Mass Spectra

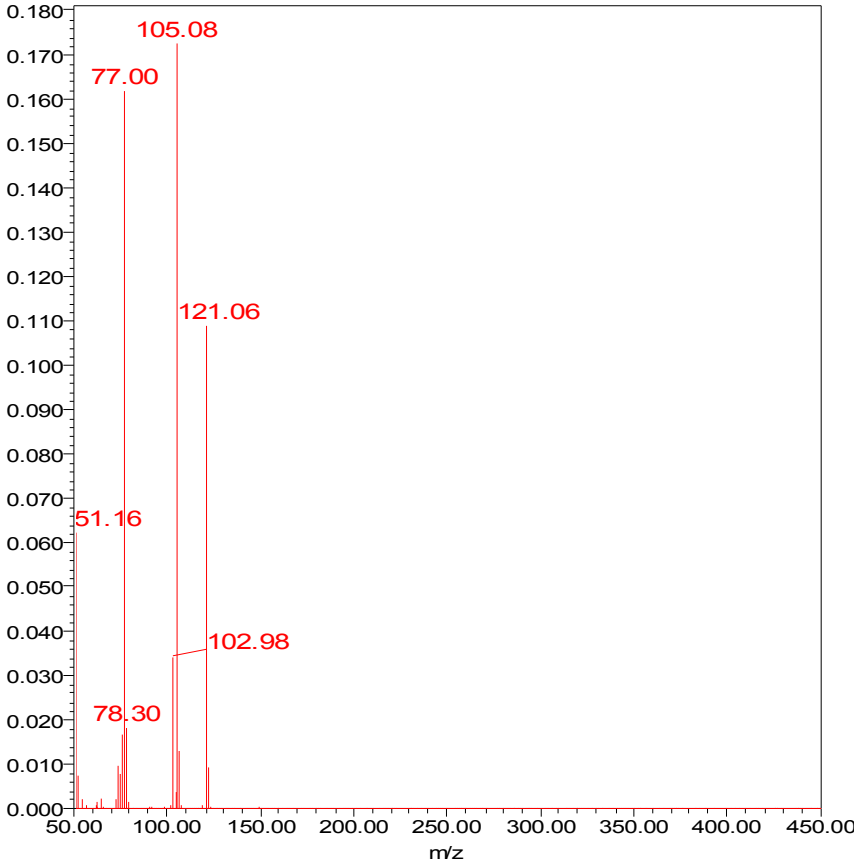


Figure 62: Benzamide mass spectrum.

The parent compound peak is at m/z 121. Mass spectral results were obtained using the Waters Integrity™ System with photodiode array detector and Thermabeam™ mass detector using a 20 µl injection volume and a 30 min run time. Initial elution was 0.2 ml/min 0.1% (v/v) formic acid for the first 15 min, followed by 2 min of a 0.3 ml/min 50% methanol:50% acetonitrile elution, 5 min of a 0.25 ml/min 0.1% (v/v) formic acid and lastly 8 min of 0.1% (v/v) formic acid at 0.2 ml/min.

The mass spectrum peak break down for benzamide (Figure 62) is summarised by Figure 63:

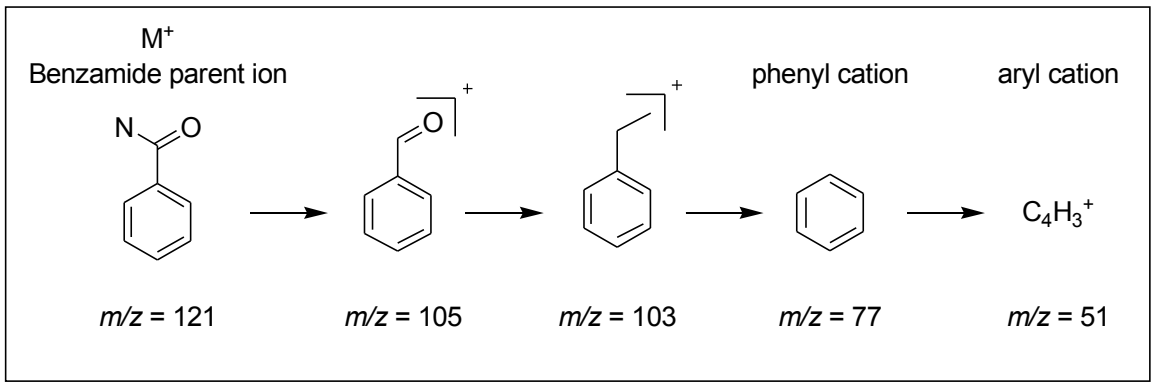


Figure 63: Mass spectrum breakdown for benzamide showing the mass/charge ratio of possible peak components.

Only the components of the main identification peaks are shown. Structures were drawn using *ChemDraw® Ultra* version 8.0 (by CambridgeSoft Corporation, 2003).

The mass spectrum peak break down for 3-hydroxy-3-phenylpropionitrile (Figure 65) is summarised by Figure 64:

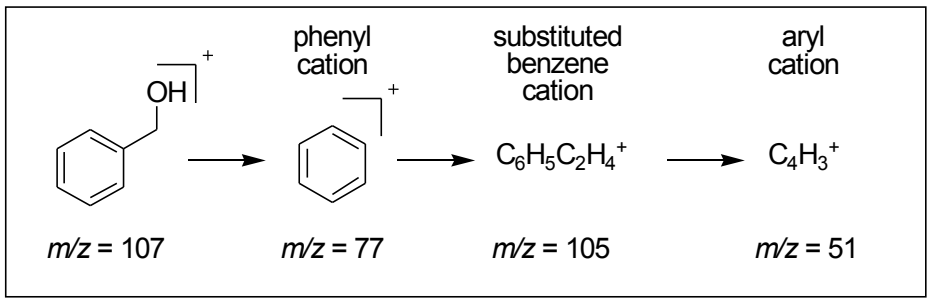


Figure 64: Mass spectrum breakdown for 3-hydroxy-3-phenylpropionitrile showing the mass/charge ratio of identified peak components.

Only the components of the main identification peaks are shown. Structures were drawn using *ChemDraw® Ultra* version 8.0 (by CambridgeSoft Corporation, 2003).

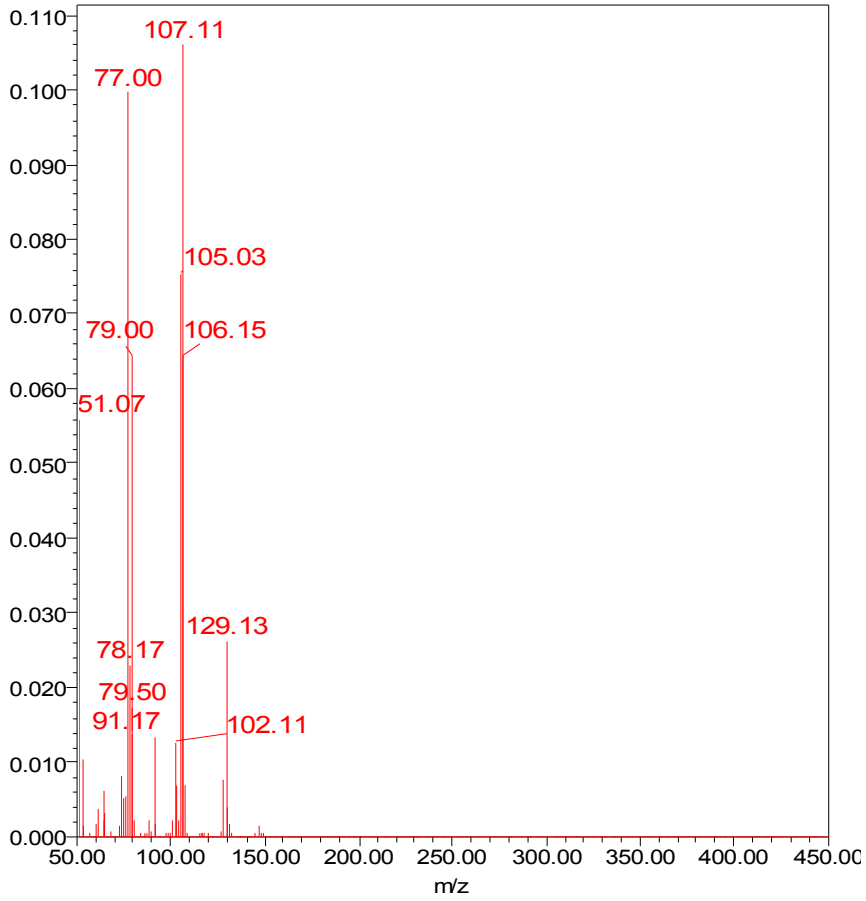


Figure 65: 3-Hydroxy-3-phenylpropionitrile mass spectrum.

The parent compound peak would be at m/z 147.18 but is too weak to be observed. Mass spectral results were obtained using the Waters Integrity™ System with photodiode array detector and Thermabeam™ mass detector using a 20 µl injection volume and a 30 min run time. Initial elution was 0.2 ml/min 0.1% (v/v) formic acid for the first 15 min, followed by 2 min of a 0.3 ml/min 50% methanol:50% acetonitrile elution, 5 min of a 0.25 ml/min 0.1% (v/v) formic acid and lastly 8 min of 0.1% (v/v) formic acid at 0.2 ml/min.

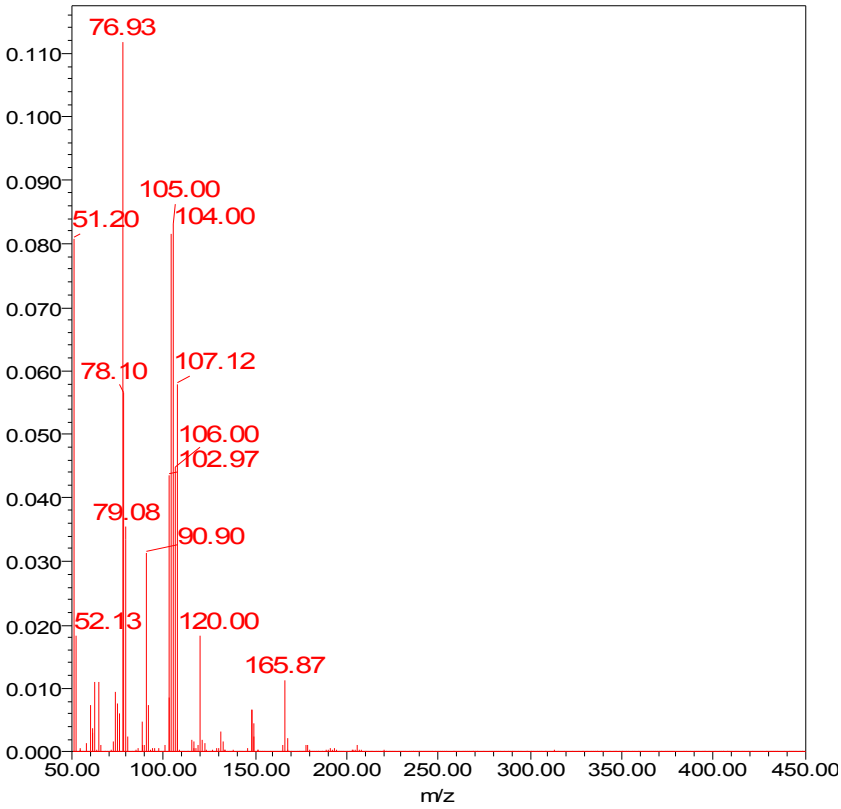


Figure 66: 3-Hydroxy-3-phenylpropionic acid mass spectrum.

Mass spectral results were obtained using the Waters Integrity™ System with photodiode array detector and Thermabeam™ mass detector using a 20 µl injection volume and a 30 min run time. Initial elution was 0.2 ml/min 0.1% (v/v) formic acid for the first 15 min, followed by 2 min of a 0.3 ml/min 50% methanol:50% acetonitrile elution, 5 min of a 0.25 ml/min 0.1% (v/v) formic acid and lastly 8 min of 0.1% (v/v) formic acid at 0.2 ml/min.

The mass spectrum peak break down for 3-hydroxy-3-phenylpropionic acid (Figure 66) is summarised by Figure 67:

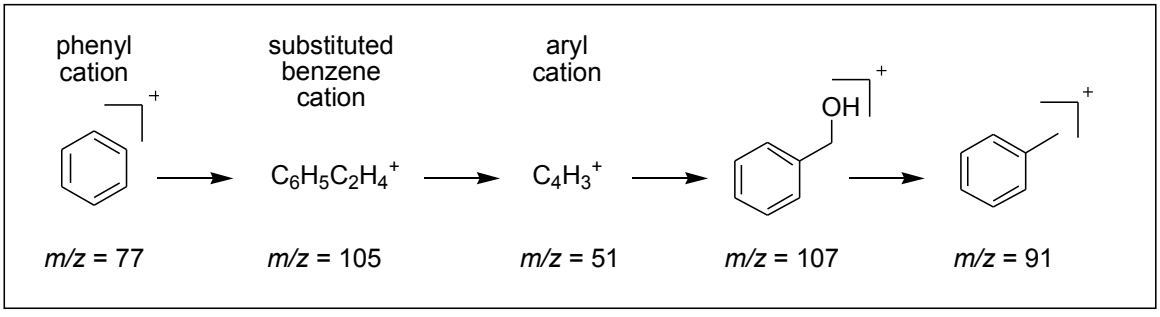
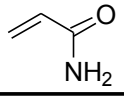
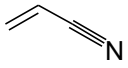
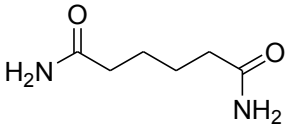
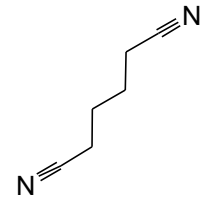
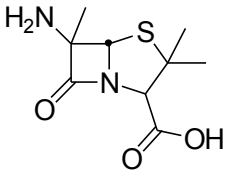
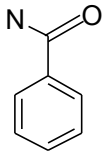
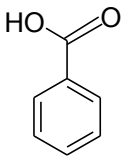
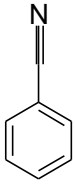


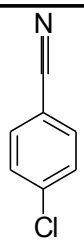
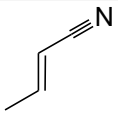
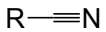
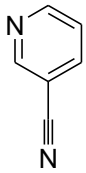
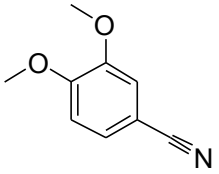
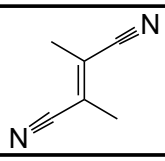
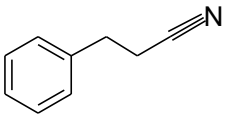
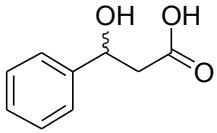
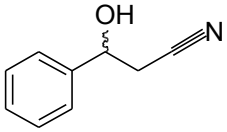
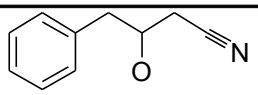
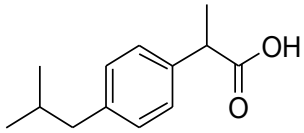
Figure 67: Mass spectrum breakdown for 3-hydroxy-3-phenylpropionic acid showing the mass/charge ratio of identified peak components.

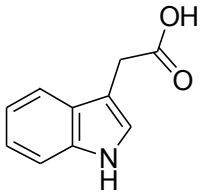
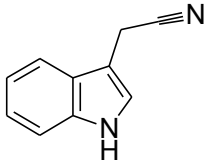
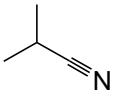
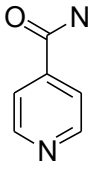
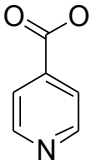
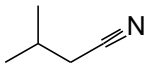
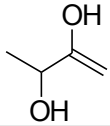
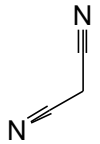
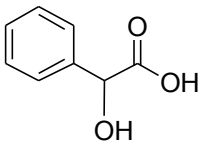
Only the components of the main identification peaks are shown. Structures were drawn using *ChemDraw® Ultra* version 8.0 (by CambridgeSoft Corporation, 2003).

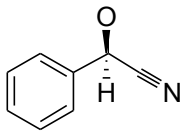
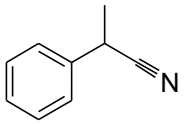
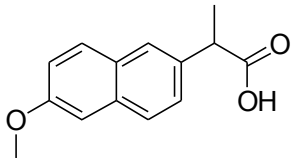
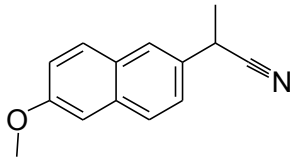
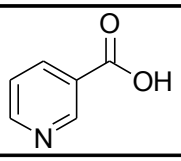
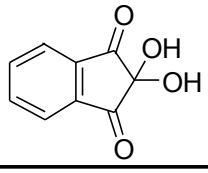
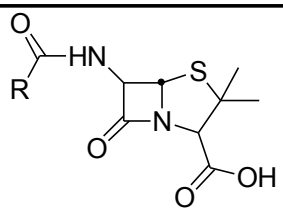
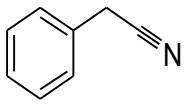
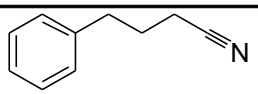
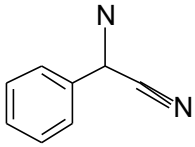
5.5 Structures

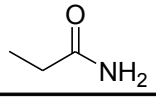
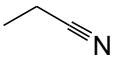
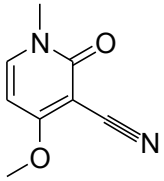
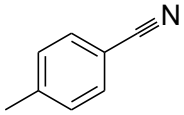
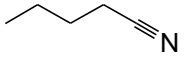
Table 10: Table of compounds and structures referred to in this study

Compound Name	Alternate Name/s	Structure	Classification
Acetonitrile	Methyl cyanide; Cyanomethane; Ethanenitrile		Aliphatic mononitrile
Acrylamide	2-Propenamide		Aliphatic amide
Acrylonitrile	Propenenitrile; Vinyl cyanide; Cyanoethylene; Acritet; Fumigrain; Ventox		Aliphatic mononitrile
Adipamide	Hexanediamide; Hexanedioic diamide		
Adiponitrile	Hexanedinitrile		Aliphatic dinitrile
6-Aminopenicillanic acid	6-Amino-3,3-dimethyl-7-oxo-4-thia-1-azabicyclo; Heptane-2- carboxylic acid		Aromatic acid; Penicillin synthesis precursor
Benzamide	Benzoylamide; Benzoic acid amide; Phenylcarboxyamide		Aromatic amide
Benzoic acid	Benzenecarboxylic acid; Benzeneformic acid; Phenyl carboxylic acid; Phenyl formic acid; Dracylic acid		Aromatic acid
Benzonitrile	Phenyl Cyanide; Cyanobenzene		Aromatic mononitrile
Benzyl nitrile	See Phenylacetonitrile		

Compound Name	Alternate Name/s	Structure	Classification
4-Chlorobenzonitrile			Aromatic mononitrile
Crotonitrile	Crotonic nitrile; Cyanopropene; Propenyl cyanide		Aliphatic mononitrile
Cyanide	Isocyanide		Aliphatic mononitrile
3-Cyanopyridine	Nicotinonitrile; 3-Pyridine-carbonitrile; 3-Pyridinenitrile; 3-Azabenzonitrile; Nicontinic acid nitrile		Aromatic mononitrile
3,4-Dimethoxybenzonitrile			Aromatic mononitrile
Fumaronitrile	Trans-1,2-dicyanoethylene; (E)-But-2-enedinitrile		Aliphatic dinitrile
Hydrocinnamonitrile	3-Phenylpropionitrile; Benzenepropanenitrile; 2-Cyanoethylbenzene; Phenethyl cyanide; 3-Phenyl-propanenitrile		Aromatic mononitrile
3-Hydroxy-3-phenylpropionic acid	β-Hydroxyphenyl-propionic acid; 3-Hydroxybenzene-propanoic acid		Aromatic acid
3-Hydroxy-3-phenylpropionitrile	β-Hydroxy-benzenepropanenitrile; 3-Phenyl-hydracrylonitrile		Beta-substituted aryl-aliphatic mononitrile
3-Hydroxy-4-phenylvaleronitrile			Aromatic mononitrile
Ibuprofen	2-(p-Isobutyl-phenyl)-propionic acid; 2-(4-Isobutyl-phenyl)-propionic acid		Aromatic acid; Non-steroidal anti-

Compound Name	Alternate Name/s	Structure	Classification
			inflammatory drug
Indole-3-acetic acid	Heteroauxin; Indoleacetic acid		Aromatic acid; Plant phytohormone (auxin)
Indole-3-acetonitrile	3-Indoleacetonitrile; 3-Indolylacetonitrile; 3-Cyanomethyl-indole; 1H-Indole-3-acetonitrile		Aromatic mononitrile
Isobutyronitrile	2-Methyl-propanenitrile; Isopropylcyanide; 2-Cyanopropane		Aliphatic mononitrile
Isonicotinamide	4-Carbamoylpyridine; Isonicotinic acid amide; Gamma-Pyridine-carboxamide; 4-Pyridine-carboxamide		Aromatic amide
Isonicotinic acid	Cinnamylidene-hydrazide; Pyridine-4-carboxylic Acid; 4-Pyridinecarboxylic acid; 4-Picolinic acid		Aromatic acid
Isovaleronitrile			Aliphatic mononitrile
Lactic acid	2-Hydroxypropanoic acid		Aliphatic acid
Malononitrile	Propanedinitrile; Dicyanomethane		Aliphatic dinitrile
Mandelic acid	α-Hydroxy-benzeneacetic acid; α-Hydroxy-phenylacetic acid; Amygdalic acid; Uromaline		Aromatic acid

Compound Name	Alternate Name/s	Structure	Classification
(*R*)+Mandelonitrile	α-Hydroxy-benzeneacetonitrile; Benzaldehyde; cyanohydrin; Mandelic acid nitrile		Aromatic mononitrile
α-Methylbenzyl cyanide	α–Methylphenyl-acetonitrile; α-2-Phenyl-propionitrile		Aromatic mononitrile
Naproxen	2-(6-Methoxy-naphthalen-2-yl)-propanoic acid; (S)-6-Methoxy-α-methyl-2-naphthaleneacetic acid		Aromatic acid; Non-steroidal anti-inflammatory drug
Naproxen nitrile			Aromatic mononitrile
Nicotinic acid	Vitamin B_3; Niacin		Aromatic acid; Essential amino acid
Ninhydrin			Colorimetric reagent
Penicillin	Penicillin-G		β-Lactam antibiotic
Phenylacetonitrile	Benzyl nitrile; α-Cyanotoluene; Benzeneacetonitrile; α-Tolunitrile		Aromatic mononitrile
Phenylbutyronitrile			Arylaliphatic mononitrile
Phenylglycinonitrile	Amino-phenyl-acetonitrile		Alpha-substituted aryl-aliphatic mononitrile
3-Phenylpropionitrile	See Hydrocinnamonitrile		

Compound Name	Alternate Name/s	Structure	Classification
Propionamide			Aliphatic amide
Propionitrile	Propylnitrile; Ethyl cyanide; Cyanoethane; Propiononitrile		Aliphatic mononitrile
Ricinine	1,2-Dihydro-4-methoxy-1-methyl-2-oxo-3-pyridine-nitrile		Aromatic mononitrile; Plant toxin
p-Tolunitrile			Aromatic mononitrile
Valeronitrile	Pentanenitrile; 1-Cyanobutane; Butyl cyanide		Aliphatic mononitrile

Structures were drawn using *ChemDraw® Ultra* version 8.0 (by CambridgeSoft Corporation, 2003).

6 References

1 Kobayashi, M., Nagasawa, T. and Yamada, H. (1992) Enzymatic synthesis of acrylamide: a success story not yet over. TRENDS Biotechnol. **10**, 402-408

2 Hjort, C. M., Godtferedson, S. E. and Emborg, C. (1990) Isolation and characterisation of a nitrile hydratase from a *Rhodococcus* sp. J. Chem. Technol. Biotechnol. **48**, 217-226

3 Takashima, Y. (1995) Process for the production of amide compounds using microorganisms. In European Patent Application, 95-101282.2, pp. 10

4 Kobayashi, M., Yanaka, N., Nagasawa, T. and Yamada, H. (1990) Purification and characterization of a novel nitrilase of *Rhodococcus rhodochrous* K22 that acts on aliphatic nitriles. J. Bacteriol. **172**, 4807-4815

5 Lu, J., Zheng, Y., Yamagishi, H., Odaka, M., Tsujimura, M., Maeda, M. and Endo, I. (2003) Motif CXCC in nitrile hydratase activator is critical for NHase biogenesis *in vivo.* FEBS Lett. **553**, 391-396

6 Gradley, M. L., Deverson, C. J. F. and Knowles, C. J. (1994) Asymmetric hydrolysis of R-(–),S(+)-2-methylbutyronitrile by *Rhodococcus rhodochrous* NCIMB 11216. Arch. Microbiology **161**, 246-251

7 Meth-Cohn, O. and Wang, M.-X. (1997) An in-depth study of the biotransformation of nitriles into amides and/or acids using *Rhodococcus rhodochrous* AJ270. J. Chem. Soc. Perkin Trans. **1**, 1099-1104

8 Brenner, C. (2002) Catalysis in the nitrilase superfamily. Curr. Opin. Struct. Biol. **12**, 775-782

9 Pace, H. C. and Brenner, C. (2001) The nitrilase superfamily: classification, structure and function. Genome Biology **2**, 1.1-1.9

10 Novo, C., Farnaud, S., Tata, R., Clemente, A. and Brown, P. R. (2002) Support for a three-dimensional structure predicting a Cys-Glu-Lys catalytic triad for *Pseudomonas aeruginosa* amidase comes from site-directed mutagenesis and mutations altering substrate specificity. Biochem. J. **365**, 731-738

11 Stevenson, D. E., Feng, R. and Storer, A. C. (1990) Detection of covalent enzyme-substrate complexes of nitrilase by ion-spray mass spectroscopy. FEBS Lett. **277**, 112-114

12 Kobayashi, M., Komeda, H., Yanaka, N., Nagasawa, T. and Yamada, H. (1992) Nitrilase from *Rhodococcus rhodochrous* J1: sequencing and overexpression of the gene and identification of an essential cysteine residue. J. Biol. Chem. **267**, 20746-20751

13 Grifantini, R., Pratesi, C., Galli, G. and Grandi, G. (1996) Topological mapping of the cysteine residues of N-carbamyl-D-amino-acid amidohydrolase and their role in enzymatic activity. J. Biol. Chem. **271**, 9326-9331

14 Kobayashi, M., Fujiwara, Y., Goda, M., Komeda, H. and Shimizu, S. (1997) Identification of active sites in amidase: Evolutionary relationship between amide bond- and peptide bond-cleaving enzymes. Proc. Natl. Acad. Sci. USA **94**, 11986-11991

15 Kobayashi, M., Goda, M. and Shimizu, S. (1998) Nitrilase Catalyzes Amide Hydrolysis as Well as Nitrile Hydrolysis. Biochem. Biophys. Res. Comm. **253**, 662-666

16 Kobayashi, M., Yanaka, N., Nagasawa, T. and Yamada, H. (1992) Primary structure of an aliphatic nitrile-degrading enzyme, aliphatic nitrilase from *Rhodococcus*

rhodocrous K22 and expression of its gene and identification of its active site residue. Biochemistry **31**, 9000-9007
17 Yamada, H. and Kobayashi, M. (1996) Nitrile hydratase and its application to industrial production of acrylamide. Biosci. Biotech. Biochem. **60**, 1391-1400
18 Maier-Greiner, U. H., Obermaier-Skrobranek, B. M. M., Estermaier, L. M., Kammerloher, W., Freund, C., Wülfing, C., Burkert, U. I., Matern, D. H., Breuer, M., Eulitz, M., Küfrevioglu, Ö. I. and Hartmann, G. R. (1991) Isolation and properties of a nitrile hydratase from the soil fungus *Myrothecium verrucaria* that is highly specific for the fertilizer cyanamide and cloning of its gene. Proc. Natl. Acad. Sci. USA **88**, 4260-4264
19 Komeda, H., Kobayashi, M. and Shimizu, S. (1996) Characterization of the gene cluster of high-molecular-mass nitrile hydratase (H-NHase) induced by its reaction product in *Rhodococcus rhodocrous* J1. Proc. Natl. Acad. Sci. USA **93**, 4267-4272
20 Komeda, H., Kobayashi, M. and Shimizu, S. (1996) A novel gene cluster including the *Rhodococcus rhodocrous* J1 nhIBA genes encoding a low molecular mass nitrile hydratase (L-NHase) induced by its reaction product. J. Biol. Chem. **271**, 15796-15802
21 Wieser, M., Takeuchi, K., Wada, Y., Yamada, H. and Nagasawa, T. (1998) Low-molecular-mass nitrile hydratase from *Rhodococcus rhodocrous* J1: purification, substrate specificity and comparison with the analogous high-molecular-mass enzyme. FEMS Microbiol. Lett. **169**, 17-22
22 Kobayashi, M., Izui, H., Nagasawa, T. and Yamada, H. (1993) Nitrilase in biosynthesis of the plant hormone indole-3-acetic acid from indole-3-acetonitrile: cloning of the Alcaligenes gene and site directed mutagenesis of cysteine residues. Proc. Natl. Acad. Sci. USA **90**, 247-251
23 Bartling, D., Seedorf, M., Schmidt, R. C. and Weiler, E. W. (1994) Molecular characterization of two cloned nitrilases from *Arabidopsis thaliana*: key enzymes in biosynthesis of the plant hormone indole-3-acetic acid. Proc. Natl. Acad. Sci. USA **91**, 6021-6025
24 Kobayashi, M. and Shimizu, S. (1994) Versatile nitrilases: nitrile-hydrolyzing enzymes. FEMS Microbiol. Lett. **120**, 217-224
25 Pace, H. C., Hodawadekar, S. C., Draganescu, A., Huang, J., Bieganowski, P., Pekarsky, Y., Croce, C. M. and Brenner, C. (2000) Crystal structure of the worm NitFhit Rosetta Stone protein reveals a Nit tetramer binding two Fhit dimers. Curr. Biol. **10**, 907-917
26 Stevenson, D. E., Feng, R., Dumas, F., Groleau, D., Mihoc, A. and Storer, A. C. (1992) Mechanistic and structural studies on *Rhodococcus* ATCC 39484 nitrilase. Biotechnol. Appl. Biochem. **15**, 283-302
27 Nagasawa, T., Wieser, M., Nakamura, T., Iwahara, H., Yoshida, T. and Gekko, K. (2000) Nitrilase of *Rhodococcus rhodochrous* J1, conversion into the active form by subunit association. Eur. J. Biochem. **267**, 138-144
28 Kobayashi, M. and Shimizu, S. (1998) Metalloenzyme nitrile hydratase: structure, regulation, and application to biotechnology. Nat. Biotechnol. **16**, 733-736
29 Okada, M., Noguchi, T., Nagashima, T., Yohda, M., Yabuki, S., Hoshino, M., Inoue, Y. and Endo, I. (1996) Location of the non-heme iron center on the a-subunit of photoreactive nitrile hydratase from *Rhodococcus* sp. N-771. Biochem. Biophys. Res. Commun. **221**, 146-150
30 Miyanaga, A., Fushinobu, S., Ito, K., Shoun, H. and Wakagi, T. (2004) Mutational and structural analysis of cobalt-containing nitrile hydratase on substrate and metal binding. Eur. J. Biochem. **271**, 429-438

31 Hourai, S., Miki, M., Takashima, Y., Mitsuda, S. and Yanagi, K. (2003) Crystal structure of nitrile hydratase from a thermophilic *Bacillus smithii*. Biochem. Biophys. Res. Comm. **312**, 340-345
32 Nagashima, S., Nakasako, M., Dohmae, N., Tsujimura, M., Takio, K., Odaka, M., Yohda, M., Kamiya, N. and Endo, I. (1998) Novel non-heme iron center of nitrile hydratase with a claw setting of oxygen atoms. Nat. Struct. Biol. **5**, 347-351
33 Nojiri, M., Kawano, Y., Hashimoto, K. and Kamiya, N. (To be published) X-ray snap shots of inhibitor binding process in photo-reactive nitrile hydratase.
34 Huang, W., Jia, J., Cummings, J., Nelson, M., Schneider, G. and Lindqvist, Y. (1997) Crystal structure of nitrile hydratase reveals a novel iron centre in a novel fold. Structure **5**, 691-699
35 Berman, H. M., Westbrook, J., Feng, Z., Gilliland, G., Bhat, T. N., Weissig, H., Shindyalov, I. N. and Bourne, P. E. (2000) The Protein Data Bank. Nuc. Acids Res. **28**, 235-242
36 Brennan, B. A., Cummings, J. G., Chase, D. B., Turner, I. M. J. and Nelson, M. J. (1996) Resonance Raman spectroscopy of nitrile hydratase, a novel iron-sulfur enzyme. Biochemistry **35**, 10068-10077
37 Nelson, M. J., Jin, H., Turner, I. M. J., Grove, G., Scarrow, R. C., Brennan, B. A. and Que, L. J. (1991) A novel iron-sulfur center in nitrile hydratase from Brevibacterium sp. J. Am. Chem. Soc. **113**, 7072-7073
38 Sugiura, Y., Kuwahara, J., Nagasawa, T. and Yamada, H. (1987) Nitrile hydratase: the first non-heme iron enzyme with a typical low spin Fe(III) active centre. J. Am. Chem. Soc. **109**, 5848-5850
39 Jin, H., Turner, I. M. J., Nelson, M. J., Gurbiel, R. J., Doan, P. E. and Hoffman, B. (1993) Coordination sphere of the ferric ion in nitrile hydratase. J. Am. Chem. Soc. **115**, 5290-5291
40 Doan, P. E., Nelson, M. J., Jin, H. and Hoffman, B. (1996) An Implicit TRIPLE Effect in Mims Pulsed ENDOR: A Sensitive New Technique for Determining Signs of Hyperfine Couplings. J. Am. Chem. Soc. **118**, 7014-7015
41 Scarrow, R. C., Brennan, B. A., Cummings, J. G., Jin, H., Duong, D. J., Kindt, J. T. and Nelson, M. J. (1996) X-ray spectroscopy of nitrile hydratase at pH 7 and 9. Biochemistry **35**, 10078-10088
42 Nagashima, S., Nakasako, M., Dohmae, N., Tsujimura, M., Takio, K., Odaka, M., Yohda, M., Kamiya, N. and Endo, I. (1998) Novel non-heme iron center of nitrile hydratase with a claw setting of oxygen atoms. Nat. Struct. Biol. **5**, 347-351
43 Shearer, J., Jackson, H. L., Schweitzer, D., Rittenberg, D. K., Leavy, T. M., Kaminsky, W., Scarrow, R. C. and Kovacs, J. A. (2002) The First Example of a Nitrile Hydratase Model Complex that Reversibly Binds Nitriles. J. Am. Chem. Soc. **124**, 11417-11428
44 Honda, J., Kandori, H., Okada, T., Nagamune, T., Shichida, Y., Sasabe, H. and Endo, I. (1994) Spectroscopic observation of the intramolecular electron transfer in the photoactivation processes of nitrile hydratase. Biochemistry **33**, 3577-3583
45 Endo, I., Odaka, M. and Yohda, M. (1999) An enzyme controlled by light: the molecular mechanism of photoreactivity in nitrile hydratase. TRENDS Biotechnol. **17**, 244-249
46 Noguchi, T., Honda, J., Nagamune, T., Sasabe, H., Inoue, Y. and Endo, I. (1995) Photosensitive nitrile hydratase intrinsically possesses nitric oxide bound to the non-heme iron center: evidence by Fourier transform infrared spectroscopy. FEBS Lett. **358**, 9-12

47 Endo, I. and Odaka, M. (2000) What evidences were elucidated about photoreactive nitrile hydratase? J. Mol. Catal. B: Enzymatic **10**, 81-86
48 Popescu, V.-C., Münck, E., Fox, B. G., Sanakis, Y., Cummings, J. G., Turner, I. M. J. and Nelson, M. J. (2001) Mössbauer and EPR Studies of the Photoactivation of Nitrile Hydratase. Biochemistry **40**, 7984-7991
49 Banerjee, A., Sharma, R. and Banerjee, U. C. (2002) The nitrile-degrading enzymes: current status and future prospects. Appl. Microbiol. Biotechnol. **60**, 33-44
50 Hirrlinger, B., Stolz, A. and Knackmuss, H.-J. (1996) Purification and characterization of an amidase from *Rhodococcus erythropolis* MP 50 which enantioselectively hydrolyzes 2-arylpropionamides. J. Bacteriol. **178**, 3501-3507
51 Asano, Y., Fujishiro, K., Tany, Y. and Yamada, H. (1982) Aliphatic nitrile hydratase from *Arthrobacter* sp. J1: Purification and characterisation. Agric. Biol. Chem. **46**, 1165-1174
52 Stelkes-Ritter, U., Wyzgol, K. and Kula, M. (1995) Purification and characterization of a newly screened microbial peptide amidase. Appl. Microbiol. Biotechnol. **44**, 393-398
53 Rawlings, N. D. and Barrett, A. J. (2000) MEROPS: the peptidase database. Nucleic Acids Res. **28**, 323-325
54 Zalkin, H. and Smith, J. L. (1998) Enzymes utilizing glutamine as an amide donor. Adv. Enzymol. Relat. Areas Mol. Biol. **72**, 87-144
55 Patricelli, M. P. and Cravatt, B. F. (2000) Clarifying the catalytic roles of conserved residues in the amidase signature family. J. Biol. Chem. **275**, 19177-19184
56 Mayaux, J. F., Cerbelaud, E., Soubrier, F., Faucher, D. and Petre, D. (1990) Purification, cloning, and primary structure of an enantiomer-selective amidase from *Brevibacterium* sp. strain R312 - structural evidence for genetic coupling with nitrile hydratase. J. Bacteriol. **172**, 6764-6773
57 Nishiyama, M., Horinouchi, S., Kobayashi, M., Nagasawa, T., Yamada, H. and Beppu, T. (1991) Cloning and characterization of genes responsible for metabolism of nitrile compounds from *Pseudomonas chlororaphis* B23. J. Bacteriol. **173**, 2465-2472
58 Rolf, M. J. and Lim, H. C. (1985) In Comprehensive Biotechnology (Moo-Young, M., ed.), pp. 165-174, Pergamon Press, Oxford
59 Shaw, N. M., Naughton, A., Robins, K., Tinschert, A., Schmid, E., Hischier, M.-L., Venetz, V., Werlen, J., Zimmerman, T., Brieden, W., de Riedmatten, P., Roduit, J.-P., Zimmerman, B. and Neumüller, R. (2002) Selection, Purification, Characterisation, and Cloning of a Novel Heat-Stable Stereo-Specific Amidase from *Klebsiella oxytoca*, and Its Application in the Synthesis of Enantiomerically Pure (R)- and (S)-3,3,3-Trifluoro-2-hydroxy-2-methylpropionic Acids and (S)-3,3,3-Trifluoro-2-hydroxy-2-methylpropionamide. Organic Process Res. & Dev. **6**, 497-504
60 Shaw, N. M., Robins, K. T. and Kiener, A. (2003) Lonza: 20 Years of Biotransformations. Adv. Synth. Catal. **345**, 425-435
61 Conn, E. E. (1981) Biosynthesis of cyanogenic glycosides. In Cyanide in Biology (Vennesland, B., Conn, E. E., Knowles, C. J., Westley, J. and Wissing, F., eds.), pp. 183-196, Academic Press, London
62 Wyatt, J. M. and Linton, E. A. (1988) in Ciba Foundation Symposium 140 (Evered, D. and Harnett, S., eds.), pp. 32-48, Wiley, Chichester
63 Bhalla, T. C., Miura, A., Wakamoto, A., Ohba, Y. and Furuhashi, K. (1992) Asymmetric hydrolysis of alpha aminonitriles to optically active amino acids by a nitrilase of *Rhodococcus rhodochrous* PA-34. Appl. Microbiol. Biotechnol. **37**, 184-190

64 Faber, K. (1995) In Biotransformations in Organic Chemistry, Springer-Verlag, Berlin
65 Yamamoto, K., Ueno, Y., Otsubo, K., Kawakami, K. and Komatsu, K.-I. (1990) Production of S-(+)-ibuprofen from a nitrile compound by *Acinetobacter* sp. strain AK226. Appl. Environ. Microbiol. **56**, 3125-3129
66 Layh, N., Stoltz, A., Böhme, J., Effenberger, F. and Knackmuss, H.-J. (1994) Enantioselective hydrolysis of racemic naproxen nitrile and naproxen amide to S-naproxen by new bacterial isolates. J. Biotechnol. **33**, 175-182
67 Effenberger, F. and Böhme, J. (1994) Enzyme-catalysed enantioselective hydrolysis of racemic naproxen nitrile. Bioorg. Med. Chem. **2**, 715-721
68 Nagasawa, T. and Yamada, H. (1990) In Biocatalysis (Abramowicz, D. A., ed.), pp. 277-318, Van Nostrand Reinhold, New York
69 Wieser, M. and Nagasawa, T. (2000) Stereoselective Nitrile-Converting Enzymes. In Stereoselective Biocatalysis (Patel, R. N., ed.), pp. 467-486
70 Crosby, J., Moilliet, J., Parratt, J. S. and Turner, N. J. (1994) Regioselective hydrolysis of aromatic dinitriles using a whole cell catalyst. J. Chem. Soc. Perkin Trans. **I**, 1679-1687
71 Kobayashi, M. and Shimizu, S. (2000) Nitrile hydrolases. Curr. Opin. Chem. Biol. **4**, 95-102
72 Christian, H.-J., Hollergeschwandner, C., Peitzsch, M., Ress-Loeschke, M., Hauer, B., Brandao, P. F., Bunch, A., Robinson, G., Bull, A. T. and Syldatk, C. (2001) in 5th Int. Symp. on Biocatalysis and Biotransformation, pp. 140, Darmstadt
73 Yamamoto, K., Oishi, K., Fujimatsu, I. and Komatsu, K.-I. (1991) Production of R-(-) mandelic acid from mandelonitrile by Alcaligenes faecalis ATCC 8750. Appl. Environ. Microbiol. **57**, 3028-3032
74 Dufour, É., Storer, A. C. and Ménard, R. (1995) Engineering nitrile hydratase activity into a cysteine protease by a single mutation. Biochemistry **34**, 16382-16388
75 Dufour, É., Tam, W., Nägler, D. K., Storer, A. C. and Ménard, R. (1998) Synthesis of amidrazones using an engineered papain nitrile hydratase. FEBS Lett. **433**, 78-82
76 Nagasawa, T., Shimizu, S. and Yamada, H. (1993) The superiority of the third-generation catalyst, *Rhodococcus rhodochrous* J1 nitrile hydratase, for industrial production of acrylamide. Appl. Microbiol. Biotechnol. **40**, 189-195
77 Prepechalová, I., Martínková, L., Stoltz, A., Ovesná, M., Bezouska, K., Kopecký, J. and Kren, V. (2001) Purification and characterization of the enantioselective nitrile hydratase from *Rhodococcus equi* A4. Appl. Microbiol. Biotechnol. **55**, 150-156
78 Kruse, J. M. and Mellon, M. G. (1953) Colorimetric Determination of Cyanide and Thiocyanate. Anal. Chem. **25**, 1188-1192
79 Fawcett, J. K. and E., S. J. (1960) A rapid and precise method for the determination of urea. J. Clin. Pathol. **13**, 156-159
80 Dadd, M. R., Sharp, D. C. A., Pettman, A. J. and Knowles, C. J. (2000) Real-time monitoring of nitrile biotransformations by mid-infrared spectroscopy. J. Microbiol. Methods **41**, 69-75
81 Kaul, P., Banerjee, A., Mayilraj, S. and Banerjee, U. C. (2004) Screening for enantioselective nitrilases: kinetic resolution of racemic mandelonitrile to (R)-(–)-mandelic acid by new bacterial isolates. Tetrahedron: Asymmetry **15**, 207-211
82 Banerjee, A., Sharma, R. and Banerjee, U. C. (2003) A rapid and sensitive fluorimetric assay method for the determination of nitrilase activity. Biotechnol. Appl. Biochem. **37**, 289-293
83 Mana and Spohn. (2000) Rapid and selective determination of ammonia by fluorimetric flow injection analysis. Fresenius' J. Anal. Chem. **366**, 825-829

84 Goddard, J.-P. and Reymond, J.-L. (2004) Enzyme assays for high-throughput screening. Curr. Opin. Biotech. **15**, 314-322
85 Preiml, M., Hönig, H. and Klempier, N. (2004) Biotransformation of b-amino nitriles: the role of the N-protecting group. J. Mol. Biocat. B: Enz **29**, 115-121
86 Garner, P. and Ramakanth, S. (1986) Stereodivergent Syntheses of threo- and erythro-6-Amino-6-deoxyheptosulose Derivatives via an Optically Active Oxazolidine Aldehyde. J. Org. Chem. **51**, 2609-2612
87 Czernecki, F., Franco, S. and Valery, J.-M. (1997) Further Study toward Amipurimycin: Synthesis of the Northern Part. J. Org. Chem. **62**, 4845-4847
88 Davies, S. G., Smyth, G. D. and Chippindale, A. M. (1999) Syntheses of derivatives of L-daunosamine and its C-3 epimer employing as the key step the asymmetric conjugate addition of a homochiral lithium amide to tert-butyl (E,E)-hexa-2,4-dienoate. J. Chem. Soc. Perkin Trans. **1**, 3089-3104
89 Davies, S. G., Ichihara, O., Lenoir, I. and Walters, I. A. S. (1994) Asymmetric-synthesis of (-)-(1R,2S)-cispentacin and related cis-2-amino and trans-2-amino cyclopentane-1-carboxylic and cyclohexane-1-carboxylic acids. J. Chem. Soc. Perkin Trans. **1**, 1411-1415
90 Theil, F. and Ballschuh, S. (1996) Chemoenzymatic synthesis of both enantiomers of cispentacin. Tetrahedron: Asymmetry **7**, 3565-3572
91 Sone, H., Nemoto, T., Ishiwata, H., Ojika, M. and Yamada, K. (1993) Isolation, structure, and synthesis of dolastatin D, a cytotoxic cyclic depsipeptide from the sea gare *Dolabella auricularia*. Tetrahedron Lett. **34**, 8449-8452
92 Martínková, L. and Kren, V. (2002) Nitrile- and Amide-converting Microbial Enzymes: Stereo-, Regio- and Chemoselectivity. Biocatal. Biotrans. **20**, 73-93
93 Layh, N., Parratt, J. S. and Willetts, A. (1998) Characterization and partial purification of an enantioselective arylacetonitrilase from *Pseudomonas fluorescens* DSM7155. J. Mol. Catal. B: Enzymatic **5**, 467-474
94 Dhillon, J., Chhatre, S., Shanker, R. and Shivaraman, N. (1999) Transformation of aliphatic and aromatic nitriles by a nitrilase from *Pseudomonas* sp. Can. J. Microbiol. **45**, 811-815
95 Langdahl, B. R., Bisp, P. and Ingvorsen, K. (1996) Nitrile hydrolysis by *Rhodococcus erythropolis* BL1, an acetonitrile-tolerant strain isolated from a marine sediment. Microbiology **142**, 145-154
96 Heald, S. C., Brandao, P. F., Hardicre, R. and Bull, A. T. (2001) Physiology, biochemistry and taxonomy of deep-sea nitrile metabolising *Rhodoccocus* strains. Antonie Van Leeuwenhoek **80**, 169-183
97 Layh, N., Hirrlinger, B., Stolz, A. and Knackmuss, H.-J. (1997) Enrichment strategies for nitrile-hydrolysing bacteria. Appl. Microbiol. Biotechnol. **47**, 668-674
98 Kato, Y., Ooi, R. and Asano, Y. (1998) Isolation and characterization of a bacterium possessing a novel aldoxime-dehydration activity and nitrile-degrading enzymes. Arch. Microbiology **170**, 85-90
99 Brandão, P. F. B., Clapp, J. P. and Bull, A. T. (2002) Diversity and taxonomy of geographically diverse strains of nitrile-metabolising actinomycetes using chemometric and molecular sequencing techniques. Environ. Microbiol. **4**, 262-276
100 Blakey, A. J., Colby, J., Williams, E. and O'Reilly, C. (1995) Regio-specific and stereo-specific nitrile hydrolysis by the nitrile hydratase from *Rhodococcus* AJ270. FEMS Microbiol. Lett. **129**, 57-61
101 Scholtz, R., Schmuckle, A., Cook, A. M. and Leisinger, T. (1987) Degradation of eighteen 1-monohaloalkanes by *Arthrobacter* sp. strain HA1. J. Gen. Microbiol. **133**, 267-274

102 Cowan, D., Cramp, R., Pereira, R., Graham, D. and Almatawah, Q. (1998) Biochemistry and biotechnology of mesophilic and thermophilic nitrile metabolizing enzymes. Extremophiles **2**, 207-16
103 Cramp, R. A. and Cowan, D. A. (1999) Molecular characterisation of a novel thermophilic nitrile hydratase. Biochim. Biophys. Acta **1431**, 249-260
104 Kato, Y., Tsuda, T. and Asano, Y. (1999) Nitrile hydratase involved in aldoxime metabolism from *Rhodococcus* sp. strain YH3-3: Purification and characterization. Eur. J. Biochem. **263**, 662-670
105 Kashiwagi, M., Fuhshuku, K.-I. and Sugai, T. (2004) Control of the nitrile-hydrolyzing enzyme activity in *Rhodococcus rhodochrous* IFO 15564: preferential action of nitrile hydratase and amidase depending on the reaction condition factors and its application to the one-pot preparation of amides from aldehydes. J. Mol. Biocat. B: Enz **29**, 249-258
106 Brady, D., Beeton, A., Zeevaart, J., Kgaje, C., van Rantwijk, F. and Sheldon, R. A. (2004) Characterisation of nitrilase and nitrile hydratase biocatalytic systems. Appl. Microbiol. Biotechnol. **64**, 76-85
107 Laemmli, U. K. (1970) Cleavage of Structural Proteins during the Assembly of the Head of Bacteriophage T4. Nature (London) **227**, 680-685
108 Brady, D., Dube, N. and Peterson, R. (2006) Green Chemistry: Highly Selective Biocatalytic Hydrolysis of Nitrile Compounds. S. Afr. J. Sci. in print
109 Komeda, H., Hori, Y., Kobayashi, M. and Shimizu, S. (1996) Transcriptional regulation of the *Rhodococcus rhodochrous* J1 *nitA* gene encoding a nitrilase. Proc. Natl. Acad. Sci. USA **93**, 10572-10577
110 Wang, M.-X., Feng, G.-Q. and Zheng, Q.-Y. (2004) Synthesis of high enantiomeric purity gem-dihalocyclopropane derivatives from biotransformations of nitriles and amides. Tetrahedron: Asymmetry **15**, 347-354
111 Effenberger, F. and Bohme, J. (1994) Enzyme-catalysed enantioselective hydrolysis of racemic naproxen nitrile. Bioorg. Med. Chem. **2**, 715-721
112 Beard, T. M. and Page, M. I. (1998) Enantioselective biotransformations using rhodococci. Antonie Van Leeuwenhoek **74**, 99-106
113 Nagasawa, T., Takeuchi, K. and Yamada, H. (1991) Characterization of a new cobalt-containing nitrile hydratase purified from urea-induced cells of *Rhodococcus rhodochrous* J1. Eur. J. Biochem. **196**, 581-589
114 Mizunashi, W., Nishiyama, M., Horinouchi, S. and Beppu, T. (1998) Overexpression of high-molecular-mass nitrile hydratase from *Rhodococcus rhodochrous* J1 in recombinant *Rhodococcus* cells. Appl. Microbiol. Biotechnol. **49**, 568-572
115 Kobayashi, M., Nagasawa, T. and Yamada, H. (1989) Nitrilase of *Rhodococcus rhodochrous* J1: Purification and characterization. Eur. J. Biochem. **182**, 349-356
116 Banerjee, A., Kaul, P., Sharma, R. and Banerjee, U. C. (2003) A High-Throughput Amenable Colorimetric Assay for Enantioselective Screening of Nitrilase-Producing Microorganisms Using pH Sensitive Indicators. J. Biomolecular Screening **8**, 559-565
117 Harper, D. B. (1977) Microbial metabolism of aromatic nitriles: Enzymology of C-N cleavage by *Nocardia* sp. NCIB 11216. Biochem. J. **165**, 309-319
118 Harper, D. B. (1985) Characterization of a nitrilase from *Nocardia* sp. NCIB 11215, using p-hydroxybenzonitrile as sole carbon source. Int. J. Biochem. **17**, 677-683
119 Harper, D. B. (1977) Fungal degradation of aromatic nitriles. Enzymology of C-N cleavage by *Fusarium solani*. Biochem. J. **165**, 685-692

120 Nagasawa, T., Nanba, H., Ryuno, K., Takeuchi, K. and Yamada, H. (1987) Nitrile hydratase of *Pseudomonas chlororaphis* B23. Purification and characterization. Eur. J. Biochem. **162**, 691-698
121 Honda, J., Teratani, Y., Kobayashi, M., Nagamune, T., Sasabe, H., Hirata, A., Ambe, F. and Endo, I. (1992) Light-induced oxidation of iron atoms in a photosensitive nitrile hydratase. FEBS Lett. **301**, 177-180
122 Nagasawa, T., Ryuno, K. and Yamada, H. (1986) Nitrile hydratase of *Brevibacterium* sp. R312. Purification and characterization. Biochem. Biophys. Res. Commun. **139**, 1305-1312
123 Nagasawa, T., Takeuchi, K. and Yamada, H. (1988) Occurrence of a cobalt-induced and cobalt-containing nitrile hydratase in *Rhodococcus rhodochrous* J1. Biochem. Biophys. Res. Comm. **155**, 1008-1016
124 Hook, R. H. and Robinson, W. G. (1964) Ricinine nitrilase II. Purification and properties. J. Biol. Chem. **239**, 4263-4267
125 Duran, R., Nishiyama, M., Horinouchi, S. and Beppu, T. (1993) Characterization of nitrile hydratase genes cloned by DNA screening from *Rhodococcus erythropolis*. Biosci. Biotech. Biochem. **57**, 1323-1328
126 Gasteiger, E., Hoogland, C., Gattiker, A., Duvaud, S., Wilkins, M. R., Appel, R. D. and Bairoch, A. (2005) Protein Identification and Analysis Tools on the ExPASy Server. In The Proteomics Protocols Handbook (Walker, J. M., ed.), pp. 571-607, Humana Press
127 Harper, D. B. (1976) Purification and properties of an unusual nitrilase from *Nocardia* NCIB 11216. Biochem. Soc. Trans. **4**, 502-594
128 Trott, S., Bauer, R., Knackmuss, H.-J. and Stolz, A. (2001) Genetic and biochemical characterization of an enantioselective amidase from *Agrobacterium tumefaciens* strain d3. Microbiology **147**, 1815-1824
129 Payne, M. S., Wu, S., Fallon, R. D., Tudor, G., Stieglitz, B., Turner, I. M., Jr. and Nelson, M. J. (1997) A stereoselective cobalt-containing nitrile hydratase. Biochemistry **36**, 5447-5454
130 Endo, T. and Watanabe, I. (1989) Nitrile hydratase of *Rhodococcus* sp. N-774 - purification and amino acid sequences. FEBS Lett. **243**, 61-64
131 Jandhyala, D., Berman, M., Meyers, P. R., Sewell, B. T., Willson, R. C. and Benedik, M. J. (2003) CynD, the Cyanide Dihydratase from *Bacillus pumilus*: Gene Cloning and Structural Studies. Appl. Environ. Microbiol. **69**, 4794-4805
132 Kobayashi, M. and Shimizu, S. (1999) Cobalt proteins. Eur. J. Biochem. 261, 1-9
133 Kato, Y., Yoshida, S., Xie, S. X. and Asano, Y. (2003) Aldoxime dehydratase co-existing with nitrile hydratase and amidase in the iron-type nitrile hydratase-producer *Rhodococcus* sp. N-771. J. Biosci. Bioeng. **97**, 250-259
134 Amarant, T., Vered, Y. and Bohak, Z. (1989) Substrates and inhibitors of the nitrile hydratase and amidase of *Corynebacterium nitrilophilus*. Biotechnol. Appl. Biochem. **11**, 49-59
135 Goldlust, A. and Bohak, Z. (1989) Induction, purification, and characterization of the nitrilase of *Fusarium oxysporum* f.sp. *melonis*. Biotech. Appl. Biochem. **11**, 581-601
136 Osswald, S., Wajant, H. and Effenberger, F. (2002) Characterization and synthetic applications of recombinant AtNIT1 from *Arabidopsis thaliana*. Eur. J. Biochem. **269**, 680-687